THE ROLE OF MITOCHONDRIAL DNA MUTATIONS IN SARCOPENIA: IMPLICATIONS FOR THE MITOCHONDRIAL "VICIOUS CYCLE" THEORY AND APOPTOSIS

By

ASIMINA HIONA

A DISSERTATION PRESENTED TO THE GRADUATE SCHOOL
OF THE UNIVERSITY OF FLORIDA IN PARTIAL FULFILLMENT
OF THE REQUIREMENTS FOR THE DEGREE OF
DOCTOR OF PHILOSOPHY

UNIVERSITY OF FLORIDA

2007

To my family – Thank you for your unwavering love and support.

In the memory of my deceased grandfather Lambros who I cherished so much – Thank you for the great childhood memories.

ACKNOWLEDGMENTS

This work would not have been possible without the support and guidance of several important people. First, I thank my family for their love and support during these difficult years. Their support has not been only moral but also financial. Without their help it would have been impossible for me to complete a Ph.D especially. I also thank my parents for teaching me some very important values in life: determination, persistence and how to always rely on my abilities and be an honest and fair person. Without their love and support I never could have come this far.

From my colleagues I first and foremost thank Dr. Barry Drew for his scientific guidance during my first years in the lab and his friendship. I appreciate everything that he taught me and more importantly, his ability to make the lab such an enjoyable environment to work in. He is a best friend of mine for life. I also thank Stephane Servais for his guidance and great mentorship regarding my project and my future career. I thank Alberto Sanz from Spain for all his contributions to my thesis and all the laughs we had during my thesis studies. I want to especially thank Rizwan Kalani, an outstanding undergraduate student in our lab and current medical student for always helping me during big studies, whenever I needed him. A special thanks to Alex Samhan Arias and Miguel Garcia from Spain that have been so helpful to me during their short stay in our lab. They made me laugh a lot and became great friends. Moreover, I thank Suma Kendhayia and Evelyn Kowenhoven for their help in the lab. I would also like to thank my advisor Christiaan Leeuwenburgh for all the opportunities I had in the lab during my Ph.D.

From University of Wisconsin, Madison, I especially thank Dr. Tomas Prolla. Without his help, guidance and mentoring I wouldn't have the thesis project I have, and great career opportunities. I also thank Dr. Greg Kujoth, a post-doc in Dr. Prolla's lab for constructing the

transgenic mice I used for my project, and for always being so helpful with providing me with transgenic mice for my studies and answering my multiple questions.

Importantly, I thank my committee members drs Meyer, Kilberg and Kaushal, for being such great, insightful, and helpful committee members. I would also like to thank them for their mentoring and for being so helpful to me during my applications for post-doc positions. They really made my journey to the final defense much easier. Individually, I thank first and foremost Dr. Meyer for tremendously helping me with my future career. I think that words do not do justice to how much I appreciate his help. I thank Dr. Kilberg for being so supportive of my transfer to the IDP, which I believe was one of the best things out of my Ph.D, since I enjoyed my classes so much and the extra knowledge, and for all his help regarding my job applications. Last, but not least, I thank Dr. Kaushal for all his help with my future career and for believing in me. If I had to choose anyone of the three to be my advisor I would do it in a heartbeat but it would be a very hard choice.

Finally, and most importantly, I want to thank two very important people I met while in Gainesville: Giorgos Leonis, who's been an amazing friend all these years and Joel French, for loving me and for being the most supportive boyfriend a girl could ever have.

TABLE OF CONTENTS

LIST OF FIGURES

Abstract of Dissertation Presented to the Graduate School
of the University of Florida in Partial Fulfillment of the
Requirements for the Degree of Doctor of Philosophy

ROLE OF MITOCHONDRIAL DNA MUTATIONS IN SARCOPENIA: IMPLICATIONS FOR THE MITOCHONDRIAL "VICIOUS CYCLE" THEORY AND APOPTOSIS

By

ASIMINA HIONA

August 2007

Chair: Christiaan Leeuwenburgh
Major: Medical Sciences--Biochemistry and Molecular Biology

Aging results in a progressive loss of skeletal muscle, a condition termed sarcopenia which can have significant effects on physical function and quality of life as aging commences. At the cellular level, the aging process can activate stress-associated signal transduction pathways that result in mitochondrial dysfunction and apoptosis. Because the mitochondrion contains its own DNA, a central role for mitochondrial DNA (mtDNA) mutations in mammalian aging has been postulated. In fact, mtDNA mutations have been shown to accumulate with aging in skeletal muscle fibers of various species. The purpose of my dissertation project was to determine whether mtDNA mutations are causal to sarcopenia. The central hypothesis tested was that mutations in mitochondrial DNA, known to be associated with aging in many post mitotic tissues, play a causal role in skeletal muscle loss, possibly by inducing mitochondrial dysfunction, leading to the activation of a mitochondrial-mediated apoptotic program. In order to demonstrate a causal relationship between mtDNA mutations and skeletal muscle loss with age, we used a transgenic mouse model that expresses a proofreading-deficient version of the mitochondrial DNA polymerase gamma (PolgD257A), resulting in increased spontaneous mutation rates in mtDNA. The causal role of mtDNA mutations in mammalian aging is supported in this mouse

model by the observation that mice with the PolgD257A (D257A) phenotype develop several aging phenotypes among which, is skeletal muscle loss.

We specifically hypothesized that the accumulation of mtDNA mutations in skeletal muscle will lead to compromised mitochondrial bioenergetics. We found that D257A mice have decreased protein content of complexes I, III and IV, all of which contain subunits encoded by mitochondrial DNA, compared to wild type (WT) mice at 11-mo of age. Mitochondrial dysfunction was also evident in D257A mice by decreased mitochondrial oxygen consumption, lower membrane potential during both state 3 (phosphorylative state) and state 4 (resting state), and lower ATP content. However, this dysfunction was not accompanied by an increase in mitochondrial reactive oxygen species (ROS) production or oxidative damage. In fact, we detected a decrease in the rate of H_2O_2 production by intact D257A mitochondria and no difference in mtDNA oxidative modification measured by 8-oxo-7,8-dihydro-2'-deoxyguanosine (8-oxodG), compared to WT. This is in contrast to the mitochondrial "Vicious Cycle" theory of aging which suggests that mtDNA mutations may lead to mitochondrial dysfunction via further increases in mitochondrial ROS production. We further hypothesized that mitochondrial dysfunction will result in mitochondrial-mediated apoptosis, which would be responsible for the loss of skeletal muscle mass we have observed in D257A mice. We detected DNA laddering and an increase in the amount of cytosolic mono- and oligo-nucleosomes in D257A mice compared to WT, indicative of apoptosis. Concurrently, we demonstrated increased activity of both, the initiator caspase-9, and the effector caspase-3, as well as an increase in cleaved (activated) caspase-3 content. This suggests that apoptosis in mutant mice is mitochondrial-mediated, and is conferred upon mitochondrial dysfunction. Thus, mutations in mtDNA play a causal role in sarcopenia, through enhancing apoptosis induced by mitochondrial dysfunction.

CHAPTER 1
INTRODUCTION AND HYPOTHESES

Aging individuals lose muscle mass at a rate of 1-2% per year past the age of 50 (1, 2). This age-related muscle atrophy, termed sarcopenia, is associated with muscle weakness and can have significant effects on an individual's health and quality of life. Sarcopenia affects a growing population, occurring in 10-25% of individuals under the age of 70 and in more than 40% of the elderly over the age of 80 (1, 2). The annual cost of treating sarcopenia is greater than the amount spent due to osteoporosis, yet little effort is made to increase public awareness to prevent sarcopenia (3). Thus, sarcopenia and the subsequent loss of physical function is a significant public health problem.

Mitochondria are the main source of cellular ATP and play a central role in a variety of cellular processes, including fatty acid β-oxidation, calcium signaling, reactive oxygen species (ROS) generation and apoptosis. The aging process can introduce a variety of stressors that result in the collapse of mitochondrial function, causing apoptotic cell death. Because the mitochondrion contains its own ~16-kilobase circular DNA, that is also intron-less and histone-less, and close to the main ROS generator in the cell: the electron transport chain (ETC), a central role for mitochondrial DNA (mtDNA) mutations in aging has been postulated (4-6). Indeed, mtDNA mutations have been shown to accumulate with aging in several tissues of various species (7-12), including skeletal muscle.

The central hypothesis tested in my research project is that mutations in mitochondrial DNA, known to be associated with aging in many post mitotic tissues, play a causal role in sarcopenia, possibly through enhancing apoptosis mediated by mitochondrial dysfunction.

Previous studies have provided strong experimental support for an association between mitochondrial DNA mutations and tissue dysfunction, particularly in long-lived post-mitotic

cells such as cardiomyocytes, skeletal muscle fibers and neurons (7, 9-12). However, such association studies can provide only correlative data. In order to determine whether mtDNA mutations underlie the aging process, we used a genetically engineered mouse model that expresses a proofreading-deficient version of the mitochondrial DNA polymerase gamma ($Polg^{D257A}$), resulting in increased spontaneous mutation rates in mitochondrial DNA. Previously (13), we have characterized accelerated aging in D257A mice and found that these mice exhibited various age-related phenotypes including thymic involution, loss of bone mass, cardiac dysfunction and skeletal muscle loss. In mitochondria from the tissues examined we showed that mtDNA mutations do not lead to increases in ROS production or oxidative stress, contrary to the "free radical theory of aging." Importantly, in most tissues examined, including skeletal muscle, we demonstrated increased levels of cleaved (activated) caspase-3, which is indicative of apoptosis (13). Hence, the accumulation of mtDNA mutations may be associated with the induction of apoptosis irrespective of elevations in ROS production and oxidative stress in mitochondria with age. The D257A mouse provides an *in vivo* model to study the mechanisms of apoptosis in skeletal muscle with age, specifically, the contribution of mtDNA mutations. Our hypotheses have implications for both the basic biology of aging and clinical approaches to age-related diseases of skeletal muscle, such as sarcopenia.

Specific Aim 1. Determine the Effect of mtDNA Mutations in Skeletal Muscle Mitochondrial Function

We, as well as, others have shown that mice with a mitochondrial mutator phenotype develop several aging phenotypes (13, 14). We found that D257A mice have significant skeletal muscle loss by 11-mo of age compared to WT, which is indicative of sarcopenia. However, our findings thus far, also indicate that despite increased mutational load, mitochondria from D257A mice do not show increased levels of oxidative stress in all currently examined tissues (13).

These observations do not support the idea that mtDNA mutations contribute to increased ROS production and oxidative stress in mitochondria with age, placing the mitochondrial "vicious cycle" theory of aging in question. In this aim we determined whether mtDNA mutations lead to mitochondrial dysfunction and further investigated the mechanism by which mutations induce mitochondrial dysfunction. Since these mice have elevated levels of mtDNA mutations, we expected that the structure and/or function of proteins encoded by mitochondrial DNA would be affected, ultimately affecting mitochondrial bioenergetics, and leading to mitochondrial dysfunction. The concentration, and enzymatic activity of respiratory complexes I, II, III, IV, and F_1F_0 ATPase, mitochondrial respiration, basal oxidant production, ATP content and production, mitochondrial membrane potential and oxidative damage to mtDNA were determined.

Hypothesis 1

We hypothesized that the accumulation of mtDNA mutations would lead to mitochondrial dysfunction, due to alterations in the content and/or activity of the respiratory complexes I, III, IV and F_1F_0 ATPase, which contain subunits encoded by mtDNA, leading to compromised ETC activity in skeletal muscle of 11-mo-old D257A mice compared to WT. Decrease in ETC activity would lead to a more extensive decrement in state 3 respiration, since this is the active state of the mitochondria when electron flux is highest. We expected that the decrease in state 3 respiration would be associated with reduced ATP content and production in skeletal muscle mitochondria, ultimately leading to mitochondrial dysfunction. We further hypothesized that mitochondrial dysfunction would not be associated with increases in basal ROS production in the D257A mice, compared to WT, and specifically, with increases in ROS production at the main ROS generators of the ETC, Complex I and Complex III. Rather, mitochondrial dysfunction would lead to loss of mitochondrial membrane potential and greater susceptibility of mitochondria to apoptosis.

Specific Aim 2. Determine Whether Increased Load of mtDNA Mutations Leads to Apoptosis in Skeletal Muscle

We have already demonstrated that D257A mice lose skeletal muscle and exhibit significantly greater content of cleaved (activated) caspase-3 in skeletal muscle by 11-mo of age, compared to WT mice (13). However, additional measures are needed in order to determine that apoptosis is indeed a central mechanism responsible for skeletal muscle loss associated with the accumulation of mtDNA mutations. In this aim, we wanted to corroborate and more extensively investigate apoptosis in skeletal muscle by performing specific apoptotic measures. We further measured caspase-3 activity, the content of mono- and oligonucleosomes released in the cytosol following apoptotic DNA fragmentation, and DNA laddering, evident on agarose gel during apoptotic nucleosomal fragmentation.

Hypothesis 2

We hypothesized that the levels of apoptosis would be elevated in skeletal muscle of D257A mice compared to WT by 11-mo of age, which may explain the decline in skeletal muscle mass we observed in D257A animals.

Specific Aim 3. Identify the Specific Apoptotic Signaling Pathway Responsible for Sarcopenia in D257A Mice

The significant skeletal muscle loss in conjunction with the elevated cleaved caspase-3 levels in the D257A animals suggest that loss of critical, irreplaceable cells through apoptosis may be a central mechanism of tissue dysfunction associated with the accumulation of mtDNA mutations. In this aim we determined the pathway of skeletal muscle apoptosis in the D257A mice. We speculated that the signaling pathway responsible for induction of apoptosis in D257A skeletal muscle has to be intrinsic to the mitochondria since loss of muscle mass in these animals is conferred upon accumulation of mtDNA mutations. Moreover, the mitochondrial pathway may encompass both caspase-dependent and –independent induction. Since the caspase-

independent path still remains to be elucidated, we assessed the activation of key proteins from the main mitochondrial-mediated, caspase-dependent pathway to evaluate whether this path is activated in response to the increase in mtDNA mutational load.

Hypothesis 3

We hypothesized that mitochondrial dysfunction in D257A mice would ultimately lead to mitochondrial outer membrane permeability and efflux of cytochrome c into the cytosol. Cytochrome c release would instigate formation of the apoptosome, leading to cleavage and activation of the initiator caspase-9. Caspase-9 would further cleave and activate the final effector caspase-3 which is responsible for carrying out the actual proteolytic events that result in cellular breakdown, leading to mitochondrial-mediated apoptosis.

CHAPTER 2
BACKGROUND AND SIGNIFICANCE

Introduction

Over the past two decades, increasing evidence suggests that mitochondrial dysfunction may play a causal role in the aging process. The essential role of mitochondria in cellular ATP production, the generation of reactive oxygen species (ROS), and the induction of apoptosis suggest a number of mechanisms for mitochondrial pathology. There is now strong evidence that age induces alterations in the mitochondrial genome that lead to defects in mitochondrial function, especially in tissues with high energy requirements such as the heart, liver, brain and skeletal muscle (15-18).

It was proposed that during an individual's life span, ROS, by-products of oxidative metabolism, accumulate and alter cell components (19). Mitochondria, one of the primary sources of ROS, are particularly affected, leading to changes in their structure as well as in the genetic information of mtDNA. The observed alterations of mtDNA include oxidative damage to DNA bases, point mutations and large scale deletions or duplications. MtDNA mutations are known to have deleterious effects on oxidative phosphorylation, especially in patients with mitochondrial diseases (20, 21), and tissues that rely heavily on oxidative phosphorylation are expected to be more affected. We chose skeletal muscle as the focus tissue in this project because this tissue is highly dependent on oxidative phosphorylation and suffers marked age-related degeneration (sarcopenia).

The background information presented in this section first focuses on the changes that are induced in mitochondrial function as a result of aging, and the cellular impact of mtDNA mutations, by providing direct evidence for a causal role of mtDNA mutations in the aging process. This is followed by an explanation of how mitochondrial dysfunction can lead to

apoptosis initiated by the mitochondria, and an examination of the specific pathways and functions of the molecules involved in mitochondrial-mediated apoptosis. Although much of the evidence suggests an important role for mtDNA mutations in aging, this evidence was largely correlative until 2004 when Trifunovic et al. published the first results on the POLG mouse model (14). We propose that this mouse model (also used in the present study), with altered mitochondrial mutation rates, represents a valuable tool to critically assess *in vivo* the role of mtDNA mutations on sarcopenia.

Age-Related Changes in Mitochondrial Function

The mitochondrial genome is a double-stranded, circular DNA molecule of 16,569 bp, lacking histones and compactly organized (i.e., no introns) that, apart from a 1.1 kbp non-coding D-loop, encodes for 13 protein components of the ETC (Fig 2-1), 22 tRNAs and 2 rRNAs. There are approximately 2 to 10 copies of the mitochondrial genome per mitochondrion (22) and 10's to 100's of mitochondria per cell, depending on the cell's energy requirements (23).

Biochemical analyses of ETC complex activities performed in tissue homogenates from humans, rhesus monkeys and rodents have, in general, identified age-associated decreases in the activities of complexes I and IV. Those tissues in which robust biochemical declines have been repeatedly detected are the highly oxidative, non-replicating tissues such as skeletal muscle, heart and brain (16, 24-31). Commonly used markers for mitochondrial ETC abnormalities include the loss of cytochrome c oxidase (COX) activity and the concomitant increase in succinate dehydrogenase (SDH) activity (SDH hyperreactive regions, also known as ragged red fibers (RRF)). *In situ* histochemical studies of human and monkey myocardial tissue have focused on detection of cells deficient in COX activity (32, 33); in these studies, the number of cardiomyocytes displaying defects in the ETC COX enzyme was found to increase with age in humans from 2-3 defects/cm^2 in the second and third decades, to 50 defects/cm^2 in the fifth to ninth

decades (32). Recent cytochemical-immunocytochemical studies of oxidative phosphorylation enzymes in monkeys (10-25 years of age) showed complex III, complex IV and complex V defects in skeletal muscles, diaphragm, myocardium and extraocular muscles of 25-year-old animals. These defects were randomly distributed and not associated with a loss of complex II, which is all nuclear encoded (33). Furthermore, in rats, aged mitochondria exhibit lower mitochondrial membrane potential (34), reduced cardiolipin levels (35-37), and a decrease in the activity of carnitine acetyltransferase, a key mitochondrial enzyme for fuel utilization (38). In general, the main feature of these age-related alterations in post-mitotic tissues is the development of a shift in activity ratios among different complexes, such that it would tend to hinder the ability of mitochondria to effectively transfer electrons down the respiratory chain and thus, adversely affect oxidative phosphorylation. In accordance with the above, energy depletion in the mitochondria during aging is also evident; Our laboratory recently found that mitochondrial ATP content and production in gastrocnemius muscle from aged rats significantly decreased, although H_2O_2 production and mtDNA 8-oxodGuo levels were unchanged compared to young animals (39). This decline observed in skeletal muscle may be a factor in the process of sarcopenia, which increases in incidence with advancing age (39). Consistent with our findings, a decline in human skeletal muscle mitochondrial ATP production with advancing age has recently been observed (40). Eventually, energy depletion could impair important cellular functions including damage repair/removal mechanisms, and also trigger apoptosis (41).

Electron Transport Chain Abnormalities and Mitochondrial DNA Mutations in Aging

There is growing evidence that the accumulation of mitochondrial mutations and deletions, associated with aging, result in tissue dysfunction. For example, in the rat, the levels of a particular deletion in mtDNA (4834 deletion) in the dorsal root ganglion were about 300-fold higher in old compared to young rats. The abundance of this particular mtDNA deletion in

dorsal root ganglia from individual rats correlated strongly with their decline in function (42). In normal aging, impaired respiratory function and oxidative phosphorylation in muscle fibers is becoming increasingly evident (39, 40), and point-mutations and deletions in mtDNA have been found to correlate with this reduced capacity (43-45). Cao et al., showed that fibers from the femoris muscle of 38- month-old rats, with electron transport system abnormalities, also had large mtDNA deletions (4.4–9.7 kb), whereas normal ETC fiber regions had wild-type mtDNA. Deletions occurred at the major arc of the mtDNA spanning the origin of replication, and were clonal within the fibers, with different deletions between the fibers (43). Similarly, Wanagat et al, have demonstrated an age-related increase in skeletal muscle fibers that display ETC abnormalities, and that, mtDNA deletion mutations, co-localize with segmental ETC abnormalities (7). Specifically, they showed that the proportion of ETC abnormal fibers that displayed the RRF phenotype (i.e., loss of COX activity with concomitant hyperactivation of SDH activity) increased significantly with age, and there were no ETC abnormal fibers with the RRF phenotype observed in the 5-month-old muscles, whereas 42% of the total ETS abnormal fibers in the 38-month-old animals displayed the RRF phenotype. They further detected shorter than wild type genomes in all of the RRFs, while mtDNA deletion mutations were not detected in ETS normal fibers from the same sections. Multiple microdissections along the same RRF amplified identically sized products, supporting the clonal nature of the mtDNA deletion (7).

Moreover, human studies also provide evidence for an increase in mtDNA mutations with aging, and a correlation between mtDNA mutations and the occurrence of skeletal muscle abnormalities with advancing age (44-46). Michikawa et al., showed that human fibroblast mtDNA from normal old individuals, revealed high copy point mutations at specific positions in the control region for replication, which was not evident in young subjects (47). Furthermore, in

longitudinal studies, one or more mutations appeared in an individual only at an advanced age. Most strikingly, a T414G transversion was found, in a generally high proportion (up to 50%) of mtDNA molecules, in 8 of 14 individuals above 65 years of age (57 percent) but was absent in 13 younger individuals (47). Wang et al., showed that muscle-specific mutations accumulate with aging in critical human mtDNA control sites for replication; specifically, they demonstrated that most of 26 individuals 53 to 92 years old, without a known history of neuromuscular disease, exhibited an accumulation of two new point mutations, i.e., A189G and T408A, at mtDNA replication control sites in muscle which were absent or marginally present in 19 young individuals. These two mutations were not found in fibroblasts from 22 subjects 64 to 101 years of age (T408A), or were present only in three subjects in very low amounts (A189G)(12). The investigators suggested that the striking tissue specificity of the muscle mtDNA mutations detected, and their mapping at critical sites for mtDNA replication, strongly point to the involvement of a specific mutagenic machinery and to the functional relevance of these mutations.

Latest experimental evidence also suggests that randomly deleted mtDNA appears mainly in skeletal muscle of healthy old subjects (beyond 80 years old), affecting up to 70% of mtDNA molecules, and coincides with a decrease in the activities of complexes III and IV of the ETC, which contain subunits encoded by mtDNA (Fig 2-1) (48). Most importantly, high levels of clonally expanded mtDNA point mutations were identified in cytochrome c oxidase deficient muscle fibers, from old individuals without muscle disease, but in none of the normal fibers (49). Immunohistochemical experiments showed that the majority of the cytochrome c oxidase deficient muscle fibers expressed reduced levels of subunit II of cytochrome c oxidase, which is encoded by mitochondrial DNA, whereas there was normal or increased expression of subunit IV

of cytochrome c oxidase, which is encoded by nuclear DNA (49). The authors concluded that mtDNA point mutations are associated with cytochrome c oxidase deficient muscle fiber segments in aging, the focal accumulation of which may cause significant impairment of mitochondrial function in individual cells in spite of low overall levels of mitochondrial DNA mutations in muscle (49). Indeed, although only a few cells develop COX deficiency, the resultant cellular dysfunction might have substantial effects, especially if the cell is part of a complex network—e.g., the central nervous system (50). It is therefore, likely that, in skeletal muscle of aged individuals, normal mtDNA devoid of deletions or point mutations may represent a minority of the total mtDNA pool. There is also evidence that the rate of mitochondrial mutagenesis is faster in mice than humans per unit time (51), a necessary condition if mitochondrial mutations are causally linked to aging. When taken as a whole, these studies provide compelling evidence for an important role of mitochondrial DNA mutations in aging.

Suggested Molecular Mechanisms for the Propagation of mtDNA Mutations, and Potential Reasons for the Greater Occurrence of mtDNA Mutations Compared to Nuclear DNA, with Age

The cellular and physiological ramifications of mtDNA disruption have been first made clear from studies of a broad class of neuromuscular disorders known as mitochondrial myopathies and encephalomyopathies (reviewed by Wallace, 1999; DiMauro, 1993) (52, 53). These diseases are, clinically and biochemically, a diverse group of disorders affecting primarily those tissues having the highest energy demands: brain, skeletal muscle and heart. The mtDNA abnormalities associated with these disorders were shown to range from point mutations (21, 54) to large mtDNA deletions in the mitochondrial encephalomyopathies (53, 55). The mtDNA abnormalities found in mitochondrial myopathies have been linked to many oxidative defects in cells, with a very common defect being the RRF phenotype which is also common in skeletal muscle fibers of aged individuals.

Mathematical models suggest that the same basic cellular mechanisms are responsible for the amplification of mutant mtDNA in aging and in mtDNA diseases (50); Using an *in silico* model of mitochondrial genetic processes within individual non-dividing cells, which was based on a contemporary understanding of "relaxed replication" of mtDNA (unlike nuclear DNA, which replicates once during the cell cycle, mitochondrial DNA is degraded and replaced continuously, even in non-dividing cells such as skeletal muscle fibers and central neurons), Chinnery et al. introduced a copy-error (mutation) rate, and measured the proportion of individual simulated cells over time (50). With this approach they were able to show that, even for very rare somatic mutations, "relaxed replication" leads to random drift of the amount of mutant mtDNA within the cell. This powerful mechanism alone leads to the clonal expansion of mutant mtDNA during the lifetime of a person, and the accumulation of COX-negative cells at a similar rate to that seen in vivo (50). They further showed that random genetic drift was also the mechanism for the clonal expansion of mutant mtDNA in progressive mtDNA disease. The mechanism proposed in this study is interesting, yet the actual process of propagation of somatic mtDNA mutations remains to be determined.

Several other hypotheses regarding the propagation of mtDNA mutations and thus, of the mutant mitochondria, have also been suggested. De Grey suggested in 1997 that it is precisely the loss of superoxide production that gives mutant mitochondria and their DNA a selective advantage and drives their clonal expansion: in this "survival of the slowest" hypothesis, mitochondrial turnover by autophagy is driven by self-inflicted free radical damage to the mitochondrial membranes, so a mutant mitochondrion is "less suicidal" and is more often replicated simply because it is more long-lived (56). Another hypothesis, known as the "crippled

mitochondrion" hypothesis, states that, the internal biochemistry of mutant mitochondria somehow stimulates them to replicate (57).

Furthermore, the greater occurrence of point-mutations and deletions observed in mtDNA compared to nuclear DNA could be due to: a) a greater mtDNA exposure to reactants, b) the lack of protective histones, and c) to a less advanced DNA repair system (58-60). In fact, mitochondria are believed to entirely lack nucleotide excision repair (NER), which constitutes a major nuclear defense system acting on various nDNA lesions including pyrimidine dimmers (58, 59). Mitochondria also have other discrepancies and may also have less advanced mismatch repair (MMR) (59). Like crosslinks between DNA bases (such as thymine dimmers), DNA–protein crosslinks, or bulky DNA-adducts can cause a stall during mtDNA replication which can induce DNA double-strand brakes (61, 62), contributing to the occurrence of mtDNA deletions with aging, and as previous research suggests, it is likely for mtDNA containing deletions, to acquire a replicative advantage over longer wild type mtDNA (43).

Mitochondrial DNA Damage and the Mitochondrial 'Vicious Cycle' Theory of Aging

Despite the fact that in animal cells mtDNA comprises only 1–3% of genetic material, several lines of evidence suggest that its contribution to cellular physiology could be much greater than would be expected from its size alone (63). For instance, (i) it mutates at higher rates than nuclear DNA, which may be a consequence of its close proximity to the ETC (electron transfer chain); (ii) it encodes either polypeptides of ETC or components required for their synthesis and, therefore, any coding mutations in mtDNA will affect the ETC as a whole; this could affect both the assembly and function of the products of numerous nuclear genes in ETC complexes; (iii) defects in the ETC can have pleiotropic effects because they affect cellular energetics as a whole (63).

Mitochondria have been shown to accumulate high levels of lipophilic carcinogens such as polycyclic aromatic hydrocarbons (64, 65) which can preferentially damage mtDNA (66). Other mutagenic chemicals also have been shown to preferentially target mtDNA (64, 67-69). Therefore, it is conceivable that life-long exposure to certain environmental toxins could result in a preferential accumulation of mtDNA damage and accelerate aging. However, by far, the predominant kind of insult to which mtDNA is exposed is oxidative damage. The susceptibility of the mitochondrial genome to oxidative DNA damage may be due to a number of factors including: 1) its close proximity to the ETC, whose complexes I and III are believed to be the predominant sites of ROS production inside the cell, 2) lack of protective histones and, 3) the compactness of its genetic information is such that damage at any point in the genome will likely occur in a gene. The phenotypic implications of mtDNA mutations are dependent on which gene product is disrupted and one might predict that damage may occur in those complexes to which the mitochondrial genome makes the greatest contributions.

The free radical theory of aging first put forward by Harman (4, 5, 70, 71) states that it is the mitochondrial production of ROS, such as superoxide and H_2O_2, and the resulting accumulation of damage to macromolecules that causes aging. Cumulative damage to biological macromolecules was proposed to overwhelm the capacity of biological systems to repair themselves, resulting in an inevitable functional decline (63). The mitochondrial 'vicious cycle' theory of aging can be considered as an extension and refinement of the free radical theory (63). Its major premise is that mtDNA mutations accumulate progressively during life, as a side effect of respiration, and are directly responsible for a measurable deficiency in cellular oxidative phosphorylation activity, leading to an enhanced ROS production (63). In turn, increased ROS production results in an increased rate of mtDNA damage and mutagenesis, thus causing a

'vicious cycle' of exponentially increasing oxidative damage and dysfunction, which ultimately culminates in death (Fig 2-2) (63).

Challenging the Mitochondrial 'Vicious Cycle' Theory of Aging

Bandy and Davison were the first to put forward a mechanistic elaboration of what later became known as the mitochondrial 'vicious cycle' theory (72). While they showed that mtDNA mutations may have the same effect on the respiratory chain as small-molecule inhibitors of respiration, that is, to stimulate the one-electron reduction of molecular oxygen to superoxide (therefore, increasing ROS production), they also carefully noted that not all mutations stimulate superoxide production. Specifically, they pointed out that a mutation preventing the synthesis of cytochrome b would actually abolish any superoxide production at complex III that normal mitochondria might exhibit, because without cytochrome b in place, complex III cannot be assembled (72). Later studies reported that respiration-deficient cells of several tissues possessed mutations that would indisputably preclude assembly of both the enzyme complexes known to be responsible for mitochondrial ROS production, complexes I and III (73-76). These mutations were large deletions, which eliminated the genes for at least a couple of respiratory chain subunits, but also removed at least one tRNA gene. There is no redundancy of tRNA genes in the mtDNA, so the loss of any such gene abolishes the synthesis of all 13 mtDNA-encoded proteins (77, 78). These findings are highly relevant to the plausibility of the 'vicious cycle' theory in normal aging.

Recently, there is an increasing body of evidence challenging the vicious cycle theory of aging (63, 78-80), and our results provide direct proof against the theory (13) (Figs 4-11, 4-12, 4-14). In our specific aim #1 we tested the hypothesis that the accumulation of mtDNA mutations indeed leads to impaired synthesis of mtDNA-encoded ETC subunits and loss of activity of the mitochondrial complexes, which could explain the decrease in O_2 consumption in conjunction

with the decrease in H_2O_2 production we have shown in the D257A skeletal muscle mitochondria (Figs 4-2, 4-11, 4-12).

Direct Evidence for a Causal Role of mtDNA Mutations in Aging: D257A Mice

As already discussed, there is an ever growing body of research that supports an important role for mtDNA mutations in aging by providing experimental support for an association between mtDNA mutations, apoptosis and tissue dysfunction, particularly in long-lived post mitotic cells such as cardiomyocytes and skeletal muscle fibers (7, 81). However, most of the studies to date are correlative in nature. In particular, until recently, it has been unclear whether mtDNA mutations are simply associated with aging in various tissues, or if they actually cause alterations in tissue function. In 2004, Trifunovic et al. published the first experimental evidence providing a causative link between mtDNA mutations and mammalian aging (14). They showed that homozygous knock-in mice that express a proof-reading-deficient version of PolgA, the nucleus-encoded catalytic subunit of mtDNA polymerase, develop a mtDNA mutator phenotype with a threefold to fivefold increase in the levels of point mutations, as well as increased amounts of deleted mtDNA. This increase in somatic mtDNA mutations was associated with reduced lifespan and premature onset of aging-related phenotypes such as alopecia, kyphosis, osteoporosis, and heart enlargement. A year later we corroborated Trifunovic's findings regarding the impact of mtDNA mutations in aging, using mice with the same mutation, and we also showed that the accumulation of mtDNA mutations was not associated with increased levels of oxidative stress or a defect in cellular proliferation, but was correlated with the induction of apoptotic markers, suggesting that accumulation of mtDNA mutations that promote apoptosis may be a central mechanism driving mammalian aging (13).

Moreover, Zassenhaus and colleagues studied mice that express a proofreading-deficient POLγ specifically in the heart, and develop cardiac mtDNA mutations, in order to determine

whether low frequency mitochondrial mtDNA mutations are pathogenic. They found that sporadic myocytic death occurred in all regions of the heart, due to apoptosis as assessed by histological analysis and TUNEL staining (82). They also pointed out that cytochrome c was released from mitochondria and concluded that mtDNA mutations are pathogenic, and seem to trigger apoptosis through the mitochondrial pathway (82). The use of D257A mice in the present investigation allowed us to elucidate *in vivo,* the contribution of mtDNA mutations to the aging phenotype in skeletal muscle, and their role in apoptosis.

Mitochondrial Dysfunction, Apoptosis and Skeletal Muscle Aging/Sarcopenia

An age-related loss of muscle mass and function occurs in skeletal muscle of a variety of mammalian species; this process is referred to as sarcopenia, and is reflected by 25% to 35% decreases in the cross-sectional area of several limb muscles due to muscle fiber atrophy and loss (83). The public health ramifications of this large decline are evident in the clinical presentation, which includes decreased mobility and respiratory function. These declines have significant effects on individual health and quality of life, affecting the ability of elderly people to live independently.

In humans, specific skeletal muscles may undergo a ~40% decline in muscle mass between the ages of 20 and 80 years (84). What is more, a 25% decrease in cross-sectional area of vastus lateralis (VL) (the most studied muscle in the context of sarcopenia) is consistently seen in comparisons of 70- to 75-year-olds with 20- to 30-year-olds (85, 86). Large declines also occur in the number of fibers in the VL. Progressive muscle wasting has also been demonstrated in murine and nonhuman primates. These sarcopenic changes are evidenced by a significant reduction in muscle cross sectional area, muscle mass loss and fiber number loss over time. In the Fischer 344 x Brown Norway (FBN) hybrid rat, the difference between the rectus femoris muscles of 18- and 38-month-old animals is striking. Muscle cross sectional area is reduced by

30% in the older animals and the muscle composition is more heterogeneous including an increase in fibrotic tissue (87). A significant reduction in muscle mass (45%) is observed between 18- and 36/38-months of age, as well as, a significant (27%) loss of muscle fibers (87). Another study in male $FxBNF_1$ rats found that atrophy occurs from 9 to 31 months of age in the soleus (13%), EDL (15%), plantaris (22%), and gastrocnemius (25%) (88). In C57BL/6 mice (the same background strain used in this study) skeletal muscle mass also decreases with aging with percent atrophy reported ranging from 15% to more than 30% (89). When we compared aged WT C57BL/6 mice (30-mo) to young WT (5-mo old) animals we also found significant muscle atrophy (Fig 4-15).

Although the specific characteristics of sarcopenia in murine depend on the strain, gender, muscle and age groups studied, the relative magnitude of muscle atrophy in old animals resembles that of old persons (90). We have observed a similar degree of atrophy in the skeletal muscle of 11-mo-old D257A mice (24% atrophy in gastrocnemius and 19% atrophy in quadriceps) that very closely resembles sarcopenia during aging (Fig 4-15). Although the molecular events responsible for sarcopenia are unknown, the muscle mass loss is due to both fiber atrophy (84, 91, 92) and fiber loss (84, 93, 94), and proposed mechanisms for fiber loss include mtDNA mutations and altered apoptotic signaling (87). It is also important to point out that skeletal muscle does not possess the high repair capacities that occur in more mitotically active tissues, which makes it more susceptible to age-induced deterioration; although satellite cells are capable of replacing lost muscle fibers, both the percentage of satellite cells and their proliferative capacities decrease with aging (95). Therefore, skeletal muscle degenerates with aging in both humans and murine, and may represent an important target for age-related mitochondrial dysfunction.

The consequences on skeletal muscle of mtDNA disruption, ranging from point mutations to large deletions, are clear from neuromuscular disorders known as mitochondrial myopathies (96). The mtDNA abnormalities associated with these disorders cause ETC dysfunctions in muscle fibers (97). Moreover, mutations affecting the mitochondrial genome can increase the susceptibility of cells to apoptosis (98). Several prominent examples include Friedreich's Ataxia, a neurodegenerative disease in which mtDNA mutation sensitizes the cells to undergo apoptosis (99, 100) and Leigh syndrome, the most common neurodegenerative disorder affecting oxidative phosphorylation in children, in which mtDNA mutations also increase mitochondrial-mediated apoptosis (101). In the normally aged skeletal muscle of rats it was clearly shown that segmental mitochondrial abnormalities colocalize with mtDNA deletion mutations (7). Importantly, these muscle fibers harboring mitochondrial abnormalities displayed a striking decrease in cross sectional area indicative of atrophy, and fiber splitting, strongly suggesting a causal role for age-associated mitochondrial DNA deletion mutations and mitochondrial dysfunction in sarcopenia (7). The same group also showed that the vastus lateralis muscle, which undergoes a high degree of sarcopenia, exhibited more ETS abnormalities and associated fiber loss than the soleus and adductor longus muscles, which are more resistant to sarcopenia, suggesting a direct association between ETS abnormalities and fiber loss (102). Moreover, Prolla and co-workers have demonstrated that aging of specific organs, including skeletal muscle, is associated with specific patterns of transcriptional alterations that serve as molecular biomarkers to indicate mitochondrial dysfunction in the aging process (103).

There is evidence indicating that deregulation of apoptosis plays a key role in the pathophysiology of skeletal muscle cell loss. Indeed, accelerated skeletal muscle apoptosis has been documented to occur with aging (104, 105). Our laboratory has previously shown that in

the gastrocnemius muscle of old Fischer-344 rats, apoptosis is significantly elevated compared to young rats and this also coincided with a significant increase in the levels of cleaved caspase-3 (105). These findings also agree with the elevated caspase-3 levels we have detected in the gastrocnemius of aged, 30-mo old WT mice, and in the gastrocnemius of 11-mo old D257A mice, a time-point when the sarcopenic phenotype is evident in these mice (13) (Fig 4-18).

Despite a very likely role of apoptosis in sarcopenia, there are only sparse reports on the occurrence of skeletal muscle cell apoptosis in humans with normal aging. In 1999, Strasser et al. showed that, in humans, an age-dependent increase in apoptosis of the striated muscle fibers of the rhabdosphincter led to a dramatic decrease in the number of striated muscle cells (106); in a 5-week-old neonate, 87.6% of the rhabdosphincter consisted of striated muscle cells, in striking contrast with only 34.2% in a 91-year-old subject. To our knowledge this was the first report on the role of apoptosis in human skeletal muscle atrophy with age. Results from a very recent study in humans indicate that apoptosis appears to be a contributing pathway to skeletal muscle wasting in healthy older adults compared to healthy young adults (107). This was marked by significant increases in TUNEL positive cells stained for DNA fragmentation (older adults showing an increase of 87% over young adults) in the vastus lateralis (107).

Several investigations have implicated the mitochondria as key mediators involved in sarcopenia. Cortopassi and others (100, 108, 109) suggested that mitochondrial dysfunction could induce the mitochondrial permeability transition pore (PTP), the release of cytochrome *c*, and eventually initiation of apoptosis. Furthermore, Fitts *et al* (110) showed increases in glycolysis and glycogen utilization during contractile activity in aged rats, suggesting an increased reliance on energy production from glycolytic processes possibly as a consequence of an age-related mitochondrial dysfunction. Importantly, in the white gastrocnemius of Fischer-

344 rats, it was recently demonstrated that aging significantly increased DNA fragmentation and cleaved caspase-3 content and this also coincided with a 35.4% lower mean fiber cross- sectional area in the old sedentary rats versus the young sedentary controls (111). Additionally, pro-apoptotic Bax was increased in the old rats compared to young, while anti-apoptotic Bcl-2 protein expression declined in both white gastrocnemius and soleus muscles (111), suggesting that mitochondria may be a target for skeletal muscle aging and alterations in mitochondrial apoptotic regulatory proteins may be responsible for the observed age-induced muscle fiber atrophy. Moreover, Leeuwenburgh et al., showed that the soleus muscle weight and cross sectional area from 32-mo-old rats were 24% and 26% lower, respectively, compared to 6-mo-old animals, and in the old rats there was a six-fold higher incidence of total TUNEL-positive nuclei compared to young rats (112). Interestingly, Endonuclease G translocation from the mitochondria to the nucleus also occurred in old, but not in young animals, implicating the mitochondrial mediated apoptosis in the loss of skeletal muscle mass with age.

In summary, our review of the literature suggests that: a) aging is undoubtedly associated with loss of skeletal muscle mass, b) aging is associated with mitochondrial abnormalities in skeletal muscle of several species, including humans, and c) age-associated mtDNA mutations, leading to mitochondrial dysfunction, may be important contributors to sarcopenia. Furthermore, mitochondrial-mediated apoptosis appears to be a likely mechanism for sarcopenia, but this still remains to be substantiated.

Mitochondrial-Mediated Pathways of Apoptosis.

Apoptosis is a cell suicide program that is highly conserved among species. Under physiological conditions, apoptosis is essential for embryonic development, tissue homeostasis and removal of cells whose persistence would be detrimental to the organism (e.g. self-reactive immune cells, neoplastic cells, virus-infected cells) (113). Apoptosis is up-regulated in many

tissues with age. Accelerated apoptosis in mitotic tissues during aging, such as liver and white blood cells, is most likely beneficial as it may serve, respectively, to prevent age-associated tumorigenesis and to maintain overall control of immunocompetent cells. However, excessive apoptosis in post mitotic cells, such as skeletal muscle fibers and cardiomyocytes may lead to a decline in function and the development of pathological conditions, such as sarcopenia and cardiac dysfunction, since these types of cells have a limited ability to regenerate.

Apoptosis is executed via activation of specific signaling pathways which are tightly regulated. Hence, particular morphological, biochemical, and molecular events occur, such as DNA fragmentation, nuclear condensation, and formation of apoptotic bodies, which are then engulfed by macrophages or neighboring cells without initiating an inflammatory response (60).

Recent evidence has implicated mitochondria as key regulators of apoptosis (114-116). Although other apoptotic pathways exist, this proposal focuses exclusively on the main mitochondrial-mediated pathway, since mtDNA mutations are expected to affect mitochondrial function and possibly mitochondrial outer membrane permeability (MOMP). MOMP can lead to 1) release of molecules implicated in the activation of caspases that orchestrate downstream events associated with apoptosis, 2) release of molecules involved in caspase-independent cell death, and 3) loss of mitochondrial functions essential for cell survival. The key step in the initiation of mitochondrial-mediated apoptosis is the release of pro-apoptotic proteins from the mitochondrial inter-membrane space into the cytosol.

Mitochondrial-mediated apoptosis entails both caspase-dependent and caspase-independent modes (Fig 2-3). Caspases normally exist in an inactivated state, called procaspases, in the cytoplasm but can be activated by dimerization or proteolytic cleavage. Cytochrome c release from the mitochondrial intermembrane space, in the caspase-dependent pathway, is one of the

most intensively studied pathways of apoptosis. Upon receiving a death-inducing signal, there is a disruption of the mitochondrial inner transmembrane potential, which results in the opening of the mitochondrial permeability transition pore (PTP), that involves components of the outer mitochondrial membrane (VDAC, Bax and Bcl-2), inner mitochondrial membrane (ANT-adenine nucleotide translocase), and matrix (cyclophilin D). PTP opening results in loss of membrane potential, osmotic swelling of the mitochondrial matrix, rupture of the outer membrane, and the release of cytochrome *c* and other apoptogenic factors from the inter-membrane space (117, 118).

A second model proposes that at least some of the pro-apoptotic Bcl-2 proteins (e.g Bax and Bak) are able to form tetrameric outer membrane channels that could also mediate the release of apoptogenic factors from the inter-membrane space, without the involvement of inner mitochondrial membrane components (119).

Cytochrome c in the cytosol combines with procaspase-9 and (Apoptotic Protease Activating Factor 1) Apaf-1, which is constitutively expressed in the cytoplasm, and in the presence of ATP (which is required for the induction of apoptosis) forms the “apoptosome”. This complex cleaves off the pro-enzyme of caspase-9 into the active form. This allows the molecule to change conformation, and bind to another cleaved caspase-9 precursor, forming a homodimer. Caspase-9 is autocatalytic, thus it activates other caspase-9 molecules by cleaving off their N-terminal prodomain. This is known as the "Caspase Cascade." Caspase-9 also activates caspase-3, which is not autocatalytic, by cleavage at the C-terminal side of a specific aspartate residue. Activation of the final apoptosis-effector, caspase-3, which carries out the actual proteolytic events that result in cellular breakdown will irreversibly commit the cell to suicide (120) (Fig 2-3).

Alternatively, mitochondria can release apoptosis inducing factor (AIF) and endonuclease G (EndoG), which have been suggested to function in a caspase-independent fashion (121-124), as both AIF and EndoG induce apoptotic changes in purified nuclei, even in the presence of caspase inhibitors (125, 126). Upon release from the mitochondria, both mediators translocate to the nucleus and may lead to large-scale DNA fragmentation and peripheral chromatin condensation (Fig 2-3), but not oligonucleosomal DNA laddering. In vitro, AIF appears to be an essential mitochondrial pathway for cell death since caspase inhibitors block only 40-50% of cell death (127). Moreover, genetic analyses in C. elegans indicate that AIF cooperates with EndoG to participate in the regulation of cell death (128), however, it is unclear whether the same occurs in mammalian cells. Recent data also reveal an important contradiction to the idea that AIF functions in a strictly caspase-independent manner (128, 129). Arnoult et al. showed that the mitochondrial release of AIF, occurring in HeLa and Jurkat cell lines treated with general apoptosis inducers, such as staurosporine or actinomycin D, is suppressed (or at least delayed) by caspase inhibitors. The authors suggested that AIF would be released only after cytochrome *c* release, subsequent to apoptosome-mediated caspase activation (129). However, it has not been elucidated whether and how AIF can induce DNA fragmentation since it has no reported intrinsic DNAse activity.

Since all mammalian nucleated cells have the ability to undergo apoptosis (130), several apoptotic regulatory mechanisms have evolved, some inhibiting mitochondrial release of pro-apoptotic proteins and others preventing caspase activation in the cytosol (131). One of these, the Bcl-2 family of proteins consists of both pro- (Bax) and anti-apoptotic (Bcl-2) proteins that are structurally related, and act to either prevent or promote the release of cytochrome *c* in the cytosol (132). It appears that the relative ratios of these proteins influences whether a cell lives or

dies. In the aged rat heart, the Bcl-2/Bax ratio has been shown to decrease while cytosolic cytochrome *c* rises, indicating that the heart becomes more sensitive to apoptotic stimuli (133). A very recent study showed that in the white gastrocnemius, the Bax/Bcl-2 ratio increased by 98% with age and this increase was associated with a dramatic increase in cleaved caspase-3 and in histone-associated DNA fragmentation (111).

Furthermore, endogenous inhibitors of apoptosis proteins (IAP's), initially discovered in baculoviruses, also exist in mammalian cells (134-136). Amongst them, the X-linked IAP (XIAP) is regarded as the most potent suppressor of mammalian cell death. At least one explanation for the versatile suppression of cell death exhibited by this protein resides in its ability to bind directly to, and inhibit, caspases in the cytosol (137). Specifically, the BIR2 region of XIAP is a potent and specific inhibitor of caspase-3, whereas the BIR3 domain is specific for caspase-9 (137).

Apoptosis mediated by the mitochondria appears to be the most likely pathway responsible for skeletal muscle loss in the D257A mice, since the observed mitochondrial dysfunction (Figs 4-2, 4-9) can be a trigger for apoptosis. In our specific aim # 3 we investigated the impact of mtDNA mutations in the induction of the main caspase-dependent mitochondrial-mediated pathway of apoptosis.

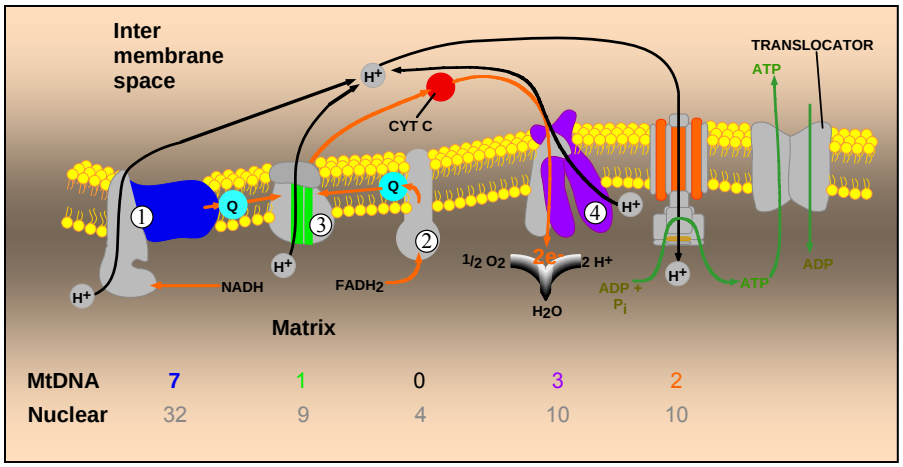

Figure 2-1. Contributions of the mitochondrial and nuclear DNA to protein subunits of the complexes of the ETC. Depicted are the 5 enzymatic complexes of the mitochondrial ETC embedded in the inner mitochondrial membrane. The number of subunits from each complex encoded from mtDNA and nuclear DNA are also shown. Note that complex II is all nuclear encoded while complex IV has the greatest contribution of mtDNA-encoded subunits. Adapted from Wallace, 1997.

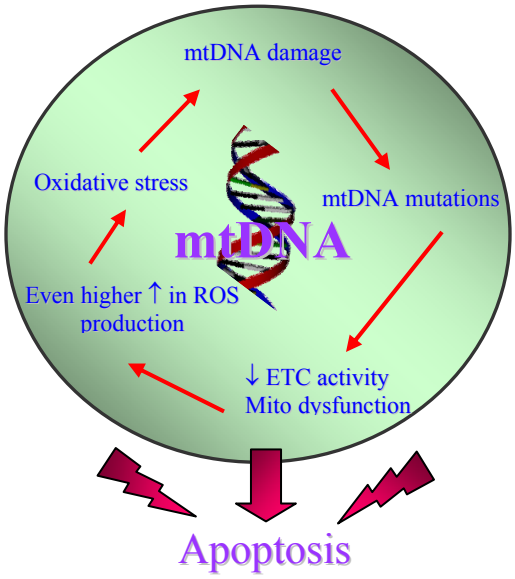

Figure 2-2. The mitochondrial 'vicious cycle' theory.

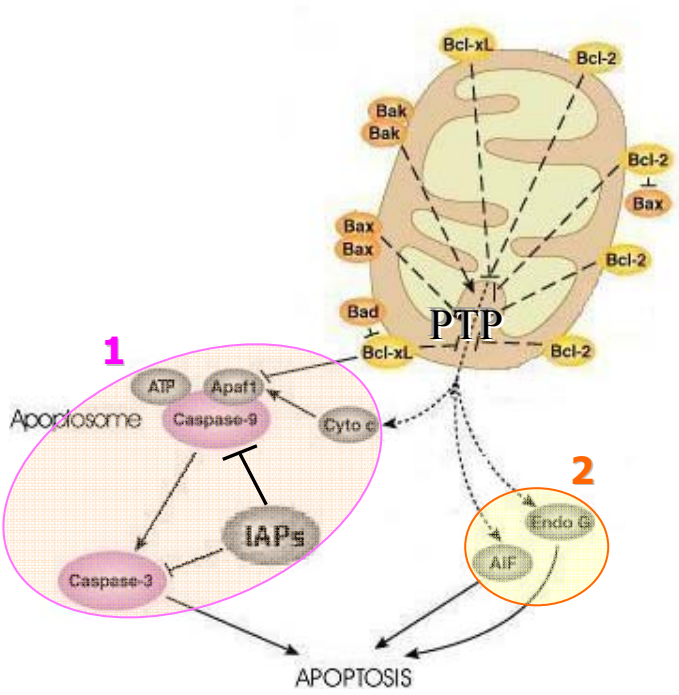

Figure 2-3. Mitochondrial-mediated apoptosis. Scheme was adapted from Cell Signaling Technology Inc. and modified.

CHAPTER 3
MATERIALS AND METHODS

Experimental Design

In recent published results we performed experiments at different time points of the D257A animals' lifespan in order to determine the point at which the D257A phenotype deviates significantly from the WT phenotype (13). For post mitotic tissues, such as skeletal muscle and heart, we detected a phenotype that resembles normal aging at ~ 9-10 mo of age in D257A mice, while at 3-mo of age there was no difference in phenotype between WT and D257A for the parameters measured, which indicates that the phenotype is age-related and is not due to developmental defects. To ensure the selection of an ideal time-point for the present dissertation project, in our pilot study we performed the same experiments at two different time points: 3 months and 11 months, and our results corroborated our previous findings regarding the change in the phenotype. Indeed, we did not detect any differences in skeletal muscle mass, oxygen consumption, ROS production, free radical leak or caspase-3 levels, between WT and D257A mice at 3 months of age (Appendix-a, Figs A-1, A-2, A-3, A-4). Therefore, in our design, we selected a time point between 11-13-mo old for our experiments in order to ensure that we will get the age-related phenotype. For all three specific aims the experimental groups are identical. We used and compared two groups: 11-13 mo-old WT (n = 11) versus 11-13 mo-old D257A (n = 11) mice (Fig 3-1).

General Procedures

Animals

C57BL/6 strain WT and D257A male and female mice were obtained at ~11 months of age from University of Wisconsin, Madison, from the lab of our collaborator Dr. Tom Prolla. The animals were housed in quarantines, in the animal care facility located at the Progress Park

(Specific-pathogen free and accredited facility). The facility is climate- and light-controlled. After one week of acclimation in the facility the animals were sacrificed by rapid cervical dislocation followed by extraction of the gastrocnemious and quadriceps muscles and immediate isolation of mitochondria for the measurements of mitochondrial respiratory and functional parameters. Cervical dislocation was chosen in order to avoid the influence of other anesthetics (e.g. volatile gases) on some of the parameters to be measured, primarily mitochondrial functional parameters (basal mitochondrial respiration, and ROS production) (138, 139). Four animals a day were sacrificed. The number of animals used per group is n ≈11 (Fig 3-1). This number was determined via a power analysis based on detecting a 50% difference, using previous data from our laboratory. The power was set at 0.90 and alpha level at $p<0.05$.

Mitochondrial and Cytosolic Isolation

Mitochondrial and cytosolic protein fractions were isolated using differential centrifugation. Immediately after sacrifice, skeletal muscle (both gastrocnemious and quadriceps muscles were mixed) was removed, cleaned, and weighed. Skeletal muscle was finely minced into small pieces and homogenized in (1:5 wt/vol) ice-cold isolation buffer containing 0.21 M mannitol, 0.07 M sucrose, 0.005 Hepes, 0.001 M EDTA, 0.2% fatty acid free BSA, pH 7.4, using a Potter-Elvehjem glass homogenizer. The homogenate was centrifuged at 1,000 g for 10 min. After the first spin, the pellets containing nuclei were frozen for future analysis. The supernatant was then centrifuged at 14,000 g for 20 min. The supernatant (crude cytosol) was stored at -80°C and the mitochondrial pellet was re-suspended in isolation buffer without BSA and was centrifuged again at 14,000 g for 10 min. The final mitochondrial pellet was re-suspended in 350 µl of isolation buffer without BSA, and was used immediately for the measurements of mitochondrial H_2O_2 production, oxygen consumption and ATP content and production. All

centrifugation steps were carried out at 4°C. Protein concentrations were determined using the Bradford method (140).

Specific Methods

Specific Aim 1. Effect of mtDNA Mutations on Skeletal Muscle Mitochondrial Function

In this specific aim we investigated the impact of the accumulation of mtDNA mutations on mitochondrial bioenergetics, specifically, on O_2 consumption, ATP content and production, and ROS generation. Using specific complex inhibitors we also determined maximum ROS production at the main ROS-generating sites within the ETC, complex I and complex III. In our preliminary studies we had measured mitochondrial oxygen consumption and our results match our hypothesis: D257A mitochondria show compromised respiration during state 3, and uncoupling between oxidation and phosphorylation (Fig 4-2). Interestingly, H_2O_2 production and free radical leak from mutant mitochondria was lower compared to that of WT (Fig 4-11, 4-12). As previously mentioned, this finding doesn't support the mitochondrial "vicious cycle" theory of aging, suggesting that mtDNA mutations may lead to mitochondrial dysfunction without increases in ROS production.

In this aim we are providing additional evidence that oxidative stress levels are not elevated in response to high mtDNA mutational rate, by demonstrating that 8-oxodGuo levels in skeletal muscle mtDNA were not significantly different between WT and D257A mice (Fig 4-14). In this aim we further determined whether the mitochondrial dysfunction we have observed in the mutant mice leads to loss of membrane potential thus making the mutant mitochondria more susceptible to apoptosis. We examined the possible mechanism by which this dysfunction is induced by assessing the content and activity of ETC respiratory complexes I, III, IV and F_1F_0 ATPase, which contain subunits encoded by the mitochondrial genome, and compare them to complex II which is all nuclear-encoded.

Rationale

Part of the focus in this aim was to determine whether mtDNA mutations induce mitochondrial dysfunction. We have evaluated several mitochondrial functional parameters and we determined that indeed mitochondrial dysfunction is evident by the reduction in mitochondrial respiration at state 3, and the higher degree of uncoupling we have observed in the D257A mice.

As previously mentioned, D257A mice accumulate mutations due to the mutated exonuclease domain of POLγ, which is devoid of proof-reading activity. We expected that mutated gene-encoding areas of the mitochondrial genome will have a direct effect on protein transcription and/or translation. Therefore, we anticipated that the proteins encoded by the mitochondrial genome will be directly affected. Depending on the type of mutations introduced and the location at which they occur, the proteins encoded by mtDNA may be truncated, or completely absent, may partially or totally lose activity. We hypothesized that the end result would be that the content and/or activity of the proteins encoded by mtDNA would be compromised in the mutant mice. Since the proteins encoded by the mitochondria (total of 13 proteins) are all proteins of the electron transport chain (ETC), we expected that the mtDNA mutations would have a direct impact on mitochondrial ETC activity and hence, on mitochondrial function. Differently stated, we hypothesized that the reduction in the content and/or activity of ETC proteins would be the primary mechanism of the observed mitochondrial dysfunction associated with mtDNA mutations. We evaluated the total concentration and maximum activity of the respiratory complexes I, III, IV and F_1F_0 ATPase. These are the ETC complexes that contain subunits encoded by mtDNA. We also evaluated the content of selected individual subunits from these complexes that are either nuclear- or mitochondrial-encoded.

These measures helped us understand and explain how the mitochondrial dysfunction we have observed in the D257A mice is induced.

Furthermore, the measurement of mitochondrial membrane potential was critical to help us understand why mutant mitochondria produce less ROS (evident by the decrease in H_2O_2 generation), and explain the induction of apoptosis in the mutant mice. Importantly, loss of membrane potential represents a link between mitochondrial dysfunction and apoptosis and hence, a link between aim #1 and aims #2, #3 (see also Fig 3-1).

Experimental approach

Mitochondrial H_2O_2 generation

The rate of mitochondrial H_2O_2 production was assayed in freshly isolated mitochondria by a highly sensitive fluorometric method according to Barja (141), and adapted to a microplate reader. H_2O_2 generation was monitored by measuring the increase in fluorescence (excitation at 312 nm, emission at 420 nm) due to the oxidation of homovanillic acid by H_2O_2 in the presence of horseradish peroxidase like it is shown in the reaction below:

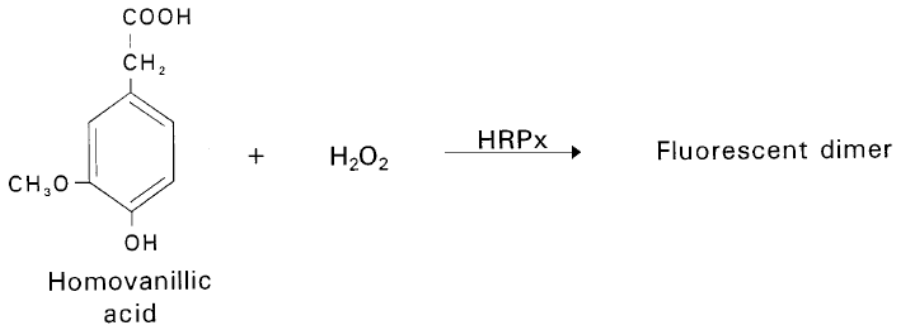

The assay was performed in incubation buffer (145-mM KCl, 30-m Hepes, 5-mM KH2PO4, 3-mM MgCl2, 0.1-mM EGTA, 0.1% BSA, pH 7.4) at 37◦C, and the reaction conditions were: 0.25 mg of mitochondrial protein per mL, 6 U/mL of horseradish peroxidase, 0.1-mM homovanillic acid and 50-U/mL of superoxide dismutase (SOD). The reaction was started by the addition of 2.5 mM pyruvate/2.5 mM malate or 5 mM succinate as substrates.

Pyruvate/malate was used to study complex I ROS production, and succinate was used to study complex III ROS production (for details also see Barja, 1999) (142). We also used inhibitors of the ETC in order to study maximum rates of H_2O_2 production from complexes I and III, since they represent the main sites of ROS generation (especially complex I) within the mitochondria. For complex I maximum rate we used 2 μM rotenone added to pyruvate/malate supplemented mitochondria. For complex III maximum rate we used 2 μM antimycin A plus 2 μM rotenone, added to succinate supplemented mitochondria. In addition, some of the assays with succinate as substrate were performed in the presence of 2 μM rotenone alone, in order to avoid the backwards flow of electrons to Complex I. After 15 min of incubation at 37 °C, the reaction was stopped and the samples were transferred on ice and a stop solution (0.1-M glycine, 25-mM EDTA, pH 12) was added. Known amounts of H_2O_2 generated in parallel by glucose oxidase, with glucose as substrate, were used as standards. Since the SOD added in excess converts all the $O_2^{\cdot -}$ produced (if any) to H_2O_2, the measurement represents the total ($O_2^{\bullet -}$ plus H_2O_2) rate of mitochondrial ROS production. All samples were run in duplicate. H_2O_2 production and O_2 consumption were measured in parallel in the same muscle mitochondria under similar experimental conditions. This allowed the calculation of the fraction of electrons out of sequence which reduce O_2 to ROS at the respiratory chain (the percent free radical leak or FRL%) instead of reaching cytochrome oxidase to reduce O_2 to water. Since two electrons are needed to reduce 1 mole of O_2 to H_2O_2 whereas four electrons are transferred in the reduction of 1 mole of O_2 to water, the percent free radical leak can be calculated as the rate of H_2O_2 production divided by two times the rate of O_2 consumption, and the result is multiplied by 100.

Mitochondrial respiration

Mitochondrial oxygen consumption was measured at 37°C by polarography, with a Clark-type oxygen electrode (Oxytherm, Hansatech, Norfolk, UK) under the same conditions used (same mitochondria, buffer composition and substrate concentrations) for H_2O_2 production measurements: incubation buffer (145 mM KCl, 30 mM Hepes, 5 mM KH2PO4, 3 mM MgCl2, 0.1 mM EGTA, pH 7.4) with 0.25 mg of mitochondrial protein per ml and 2.5 mM pyruvate/2.5 mM malate as substrates. The assay was performed in the absence (State 4-resting state) and in the presence (State 3-phosphorylating state) of 500 μM ADP. Clark-type electrode without (State 4) and with (State 3) saturant ADP allows calculation of the respiratory control ratio (RCR) (State 3/State 4 oxygen consumption) as an indicator of the degree of coupling and metabolic activity of the mitochondrial preparations.

ATP content and production

Mitochondria isolated from skeletal muscle were used immediately after isolation to determine mitochondrial ATP content and production, following the method of Drew (143). This bioluminescence assay is based on the reaction of ATP with recombinant firefly luciferase and its substrate luciferin. Upon addition, ATP combines with luciferin to form luciferyl adenylate and inorganic pyrophosphate (PPi) on the surface of the luciferase enzyme as shown in *reaction 1* below:

Reaction 1 Luciferin + ATP $\xrightarrow{\text{Luciferase}}$ Luciferyl Adenylate + PPi

While bound to the enzyme, luciferyl adenylate combines with O_2 to form oxyluciferin and AMP through a series of enzymatic redox reactions. As oxyluciferin and AMP are released from the enzyme's surface, a quantum yield of light is emitted in proportion to the ATP concentration as shown in *reaction 2*:

Reaction 2 Luciferyl Adenylate + O_2 $\longrightarrow$ Oxyluciferin + AMP + *hv*

The light emission (*h*v) can then be recorded and quantified using a chemiluminometer. ATP content methodology was modified from a method of Molecular Probes (A-22066, Eugene, OR). Chemicals used are *D*-luciferin, luciferase (40 μL of a 5 mg/mL solution in 25 mM Tris-acetase, pH 7.8, 0.2 M ammonium sulfate, 15% (v/v) glycerol and 30% (v/v) ethylene glycol), dithiothreitol (DTT), adenosine 5′-triphosphate (ATP), and a Reaction Buffer (10 mL of 500 mM Tricine buffer, pH 7.8, 100 mM $MgSO_4$, 2mM EDTA and 2 mM sodium azide). The reagents and reaction mixture were combined according to the protocol by Molecular Probes. In order to determine ATP content, freshly isolated mitochondria were added to a cuvette containing reaction buffer, *D*-luciferin, luciferase and DTT. In addition, 2.5 mM pyruvate and 2.5 mM malate were added to the reaction mixture, as substrates for oxidative phosphorylation. Immediately after the ATP content measurements, 2.5 mM ADP was added to the cuvette containing the reaction mixture and mitochondria in order to determine the rate of ATP production. A blank cuvette containing no sample, only reaction mixture, was assayed to account for background luminescence, and known concentrations of ATP standards were used to establish a standard curve. The values for ATP content and rate of production were normalized to total mitochondrial protein concentration. All mitochondrial samples were assayed in duplicate, and an average of these results was used to calculate final ATP content and rate of production.

Mitochondrial membrane potential

Mitochondrial membrane potential changes in isolated skeletal muscle mitochondria were followed qualitatively by monitoring the fluorescence of tetramethyl rhodamine methyl ester (TMRM, Molecular Probes, Eugene, OR), a cationic lipid-soluble probe that accumulates in energized mitochondria. The method of Scaduto (144) was followed without modification. Briefly, mitochondria (0.25 mg/ml) were incubated at 37°C in a medium composed of 135 mM

KCl, 20 mM MOPS, 5 mM K2HPO4, and 5 mM MgCl2 at pH 7.00. The experiment was initiated by the addition of mitochondria to the medium, also containing 0.33 mM TMRM and either 5mM succinate or 5mM glutamate + 2.5mM malate in order to record membrane potential during state 4. Fluorescence at 546 and 573 nm excitation was monitored using an emission wavelength of 590 nm. This was followed by the addition of ADP (0.17 mM) to record membrane potential during state 3. Addition of 0.5 mM CCCP followed to serve as a control for TMRM binding. An increase in fluorescence represents de-quenching of TMRM when the probe is released into the medium upon mitochondrial depolarization.

Blue native page (BN-page) for determination of content and enzymatic activity of respiratory complexes

For determination of the content of the ETC complexes we followed the protocol as described by Schagger *et* al. with some modification (145). Skeletal muscle was homogenized in buffer 1 containing 20 mM MOPS, 440 mM saccharose, 1 mM EDTA and 0.5 mM PMSF, pH 7.2 at 4°C. The homogenates were centrifuged at 20,000 g for 20 min. The pellet was re-suspended in 80 µl of buffer containing 1 M aminocaproic acid, 50 mM Bis-tris and 0.5 mM PMSF, pH 7.0. The membranes were then solubilized by the addiction of 30 µl n-dodecylmaltoside (10 %, prepared fresh). Mitochondrial suspensions were incubated on ice for 30 minutes with vortex mixing every 5 min, followed by ultracentrifugation for 25 min at 100,000 g (Beckman, Optima LE-80K). The supernatant, containing all the solubilized mitochondrial membrane proteins was used for the BN-page. 7 µl of 5% w/v coomassie brilliant blue G-250 in aminocaproic acid (1M) were added to 100 µl of supernatant. Samples were then stored on ice for no more than 30 min prior to gel loading. For electrophoresis, a 3-12 % gradient gel with 4% of stacker was used. The anode buffer was comprised of 50 mM Bis-Tris, pH 7.0. The cathode buffer was comprised of 50 mM tricine, 15 mM Bis tris, and coomassie brilliant

blue G-250 (0.02% w/v), pH 7.0. Samples were electrophoresed at 90 V for 20 min, and thereafter at 170 V for 2 h, at 4°C. Immediately after electrophoresis gels were incubated in coomassie brilliant blue G-250 solution (0.1% coomassie in 10% acetic acid and 40% methanol) for 1h, followed by incubation in de-staining solution (10% acetic acid, 40% methanol) for 2h. After de-staining gels were photographed and analyzed using the Alpha Innotech FluorChem SP imaging system. Densitometry values were normalized to total protein loaded per well, measured by the Bradford assay.

For determination of enzymatic activity, enzymatic colorimetric reactions were performed on the BN-PAGE. Gels were incubated overnight at room temperature with the following solutions: Complex I: 2mM Tris–HCl, pH 7.4, 0.1 mg/ml NADH, and 2.5 mg/ml NTB (nitrotetrazolium blue). Complex II: 4.5mM EDTA, 10mM KCN, 0.2mM phenazine methasulfate, 84mM succinic acid and 50mM NTB in 1.5mM phosphate buffer, pH 7.4. Complex IV: 5 mg 3:30-Diamidobenzidine tetrahydrochloride (DAB) dissolved in 9ml phosphate buffer (0.05 M, pH 7.4), 1ml catalase (20μg/ml), 10 mg cytochrome c, and 750 mg sucrose. Complex V: 35mM Tris, 270mM glycine, 14mM $MgSO_4$, 0.2% $Pb(NO_3)_2$, and 8mM ATP, pH 7.8. Gels were then washed in distilled water and photographed immediately. Densitometry values for activity were normalized to respective content densitometry values.

Determination of protein content of selected mitochondrial- and nuclear-encoded subunits from ETC complexes I, II, III and IV

Skeletal muscle tissue was immersed and rinsed in cold homogenization buffer: 50mN Tris-HCl pH 7.4, 1% Tween 20 (Amersham Biosciences), 0.25% sodium deoxycholate, 150 mM NaCl, 1mM disodium ethylenediaminetetraacetate dehydrate (EDTA), 1mM Diethylenetriaminepenta-acetic acid (DTPAC), 1μM 2,6-di-tert-butyl-4-methylphenol (BHT), and 1.5% Protease Inhibitor Mix (Amersham Biosciences). This was followed by homogenization in

25 ml homogenization buffer/g of skeletal muscle with a Potter-Elvehjem type homogenizer system (Glas-Col, Terre Haute, IN). The homogenate was then centrifuged at 500 x g for 5 min at 4°C yielding a pellet corresponding to crude nuclear fraction. Protein concentration was determined by the Bradford method using BioRad reagent and BSA as standard. Homogenates were immediately frozen at –80°C until further analysis. The protein content of skeletal muscle mitochondrial respiratory chain complexes was estimated using western blot analysis. Immunodetection was performed using specific antibodies for the 39KDa (NDUFA9) and 30KDa (NDUFS3) subunit of complex I (1:1000 and 1:1000, respectively), 70KDa subunit (Flavoprotein) of complex II (1:500), 48KDa (CORE 2) and 29KDa (Rieske iron-sulfur protein) subunits of complex III (1:1000 and 1:1000, respectively), and COXI subunit of complex IV (1:1000) (ref. A21344, A21343, A11142, A11143, A21346 and A6403, respectively; Molecular Probes). An antibody to porin (1:5000, A31855, Molecular Probes) or beta-actin (1:5000, AB20272, Abcam), as a loading control for total mitochondrial mass or total protein content, was also used. Appropriate peroxidase-coupled secondary antibodies and chemiluminescence HRP substrate (Millipore, MA, USA) were used for primary antibody detection. Signal quantification and recording was performed with a ChemiDoc equipment (Bio-Rad Laboratories, Inc., Barcelona, Spain). Protein concentration was determined by the Bradford method. Data were expressed as Arbitrary Units.

Determination of mitochondrial protein yield

In order to determine mitochondrial yield, we first determined the total protein concentration in each mitochondrial extract by the Bradford assay. We then multiplied each concentration value by the total volume of each mitochondrial extract. Last, we divided this product by the skeletal muscle weight used each time to obtain the respective mitochondrial extract. In this way we were able to normalize and express the total mitochondrial content per gram of skeletal muscle tissue.

Determination of MnSOD and Catalase mRNA expression by RT-PCR

To extract RNA skeletal muscles (1/10 weight/reagent volume) were homogenized in 1mL of Trizol reagent and the Trizol protocol for RNA isolation was followed. Briefly, after homogenization samples were centrifuged at 12,000 x g for 10 min in order to remove insoluble material. To the clear supernatant, 0.2mL of chloroform was added and the supernatant was centrifuged at 12,000 x g for 15 min. This separates the mixture into 3 phases: a red organic phase, an interphase and a colorless upper aqueous phase containing RNA. To the aqueous phase 0.6 mL of isopropanol was added and the mixture was centrifuged again at 12,000 x g for 10 min. The precipitated RNA was washed with 75% ethanol, centrifuged again at 7,500 x g for 5 min and the resulting RNA pellets were dried for 5-10 minutes under a vacuum. 1 μg of isolated RNA was reverse transcribed (Eppendorf RT plus PCR kit) using oligo (dT) primer, as described by the manufacturer's instructions. PCR was performed on 3-μl aliquots from each cDNA reaction, using primer sets for detecting MnSOD (5′-GGTGGCCTTGAGCGGGGACTTG-3′, 5′-GGTGGGTGGGGAGGTAGGGAGGAT-3′, sense and antisense, respectively) and Catalase (5′-ATGGCCTCCGAGATCTTTTCAATG-3′, 5′-GAGCGCGGTAGGGACAGTTCAC-3′, sense and antisense, respectively). The sizes of the amplification products were 611 bp for MnSOD and 366 bp for Catalase. Conditions for PCR reactions were for MnSOD: 94 °C for 30 sec, 58 °C for 30 sec, and 72 °C for 30 sec and for Catalase: 94 °C for 30 sec, 57.7 °C for 30 sec, and 72 °C for 30 sec. PCR amplification was conducted for 29 cycles for both MnSOD and Catalase. RT-PCR products were analyzed by agarose gel electrophoresis and digital imaging of the ethidium bromide-stained gel, using the Alpha Innotech FluorChem SP imaging system.

Oxidative damage to mtDNA

Mitochondrial DNA oxidation was measured according to Sanz et al.(146), with modification. Briefly, mitochondrial DNA, free of nDNA, were isolated by the method of

Latorre et al. (1986), adapted to mammals (Asuncion et al., 1996). After isolation mtDNA was completely dissolved in 85 μL of 30 μM DFOM, DNA was digested with 4 U of Nuclease P1 (dissolved in 300 mM sodium acetate, 0.2 mM ZnCl2, pH 5.3), and 5 U of alkaline phosphatase during 60 min at 50ºC. After filtering, samples were put into an autosampler vial for HPLC-EC-UV analysis. 8-oxodG and dG were measured by HPLC with online electrochemical and ultraviolet detection respectively. For analysis, the nucleoside mixture was injected into two Delta-Pak (150x3.9mm id, 5 μm) C-18 reversed-phase columns (Waters, Milford, MA). 8-oxodG was detected with an electrochemical detector (Coulochem III, ESA Inc, Chelmsford, MA, USA) with a PEEK filter protected 5011A analytical cell (ESA, 5 nA, screen electrode: +205 mV analytical electrode: +275), and dG was measured with a Spectra SYSTEM UV1000 detector (Thermo Electron Corp., San Jose, CA, USA) set at 290 nm. Chromatograms were recorded using EZChrome Elite (Scientific Software INC., Pleasanton, CA, USA). Calibration curves for dG and 8-oxodG were constructed by injection of each standard 3-4 times. The HPLC buffer consisted of 9% v/v methanol and 50 mM sodium acetate, set to pH 5.3, with acetic acid filtered through a CN 0.2 μm filter from Nalgene Nunc (Rochester, NY, USA).

Specific Aim 2. mtDNA Mutations and Apoptosis in Skeletal Muscle

In out pilot study we had already measured cleaved (activated) caspase-3 content in skeletal muscle of 3-mo and 11-mo old WT and D257A mice. Proteolytic activation of caspase-3 is a key event in the execution of apoptosis, marking the point at which the cell is committed to die. We have shown significant elevation in cleaved caspase-3 levels by 11-mo of age in skeletal muscle of D257A mice compared to WT, which was not evident in D257A mice at 3-mo-of age, a time-point when the D257A phenotype is also not evident (Figs 4-18, A-2). We also have found that 30-mo-old WT mice have significant muscle atrophy in concert with elevated

caspase-3 levels compared to young, 5-mo-old mice (Figs 4-15, 4-18) (13). Therefore, the elevation in cleaved caspase-3 levels, coupled to a significant skeletal muscle loss at 11-mo of age (Figs 4-15, 4-18), suggests that D257A muscle becomes sarcopenic (13). Together, these findings suggest that caspase-3-mediated apoptosis may be one of the main pathways responsible for the decline in skeletal muscle loss associated with mtDNA mutations in the accelerated aging D257A mice and the same mechanism may also be responsible during normal aging.

Rationale

Although we showed increased levels of one marker of apoptosis (caspase-3), additional measures are needed in order to corroborate that apoptosis is indeed a central mechanism responsible for skeletal muscle loss in the D257A mice. Therefore, in this aim, we wanted to further investigate apoptosis in skeletal muscle, by conducting specific apoptotic measures. Besides the content of cleaved caspase-3 we further evaluated caspase-3 activity. Furthermore, we used a quantitative ELISA to measure the amount of mono- and oligo-nucleosomes released in the cytosol after apoptotic DNA fragmentation. Last, we isolated DNA from skeletal muscle, performed a DNA laddering-specific ligation PCR in order to amplify apoptotic fragments, and subjected PCR products to electrophoresis through agarose gel in order to detect oligonucleosomal fragmentation evident by the formation of specific ladders of ~180-200 bps or multiples in the gel.

Experimental approach

Determination of cleaved caspase-3 content

The active form of caspase-3, cleaved caspase-3, was quantified by Western blotting. Activation of caspase-3 requires proteolytic processing of its inactive zymogen into activated fragments. The specific antibody used detects endogenous levels of the large fragment (17/19 kDa) of activated caspase-3 resulting from cleavage adjacent to Asp175. Proteins were separated

using 15% PAGEr® Gold pre-cast Tris-glycine gels (Cambrex, USA) under denaturing conditions, and then transferred to PVDF membranes (0.2 µm, Trans-Blot® Transfer Medium, Bio-Rad Laboratories, CA USA). Protein concentration was determined using the Bradford assay, and samples were subsequently normalized so that the protein content among samples is identical. Subsequently, 20 µl of sample were loaded to each well. HL-60 cells induced with etoposide were also loaded in a well as an appropriate positive control. Membranes were blocked for 1.5 hrs using a blocking solution containing TBS and 5% milk. Membranes were then incubated overnight in the 5% blocking solution containing the monoclonal primary antibody caspase-3 (Cell Signaling, Beverly, MA, USA) in a dilution of 1:500. The following day membranes were incubated for 1 h at room temperature with IgG horseradish peroxidase-linked whole secondary antibody (1:1000, Amersham Biosciences UK Ltd, Amersham, UK). Specific protein bands were visualized using ECL reagent (Amersham, UK). The resulting Western blots were analyzed using the Alpha Innotech FluorChem SP imaging system. Specific protein bands were further normalized to b-actin bands. Values were expressed as arbitrary units after normalizing and expressing samples as % of a control sample that was included in all membranes.

Enzymatic measurement of caspase 3 activity

Caspase-3 activity was measured using a fluorometric protease assay kit: (Caspase-3/CPP32, Biovision, Mountain View, CA, USA) according to manufacturer's instructions. Briefly, the assay is based on detection of cleavage of the substrate DEVD-AFC (AFC: 7-amino-4-trifluoromethyl coumarin) by caspase-3. DEVD-AFC emits blue light (λmax = 400 nm); upon cleavage of the substrate by caspase-3, free AFC emits a yellow-green fluorescence (λmax = 505

nm), which can be quantified using a fluorescence microplate reader. Samples were run in triplicate and values were expressed as raw fluorescence units per mg of cytosolic protein.

Determination of cytosolic mono- and oligonucleosomes

Endogenous endonucleases activated during apoptosis cleave double-stranded DNA in the linker region between nucleosomes to generate mono- and oligonucleosomes of ~180 bp or multiples. Apoptotic DNA fragmentation was quantified in skeletal muscle by measuring the amount of cytosolic mono- and oligonucleosomes using a Cell Death detection ELISA (Roche Molecular Biochemicals, Germany). The assay is based on the quantitative sandwich-enzyme-immunoassay-principle. Briefly, wells were coated with a monoclonal anti-histone antibody. Nucleosomes in the sample bound to the antibody followed by the addition of anti-DNA-peroxidase, which reacted with the DNA associated with the histones. The amount of peroxidase retained in the immunocomplex was determined spectrophotometrically with ABTS (2.2'-azino-di-[3-ethylbenzthiazoline sulfonate]) as a substrate. All samples were run in triplicate and the means were expressed as arbitrary OD units normalized to milligrams of cytosolic protein, with sample protein concentrations determined by the Bradford method.

DNA laddering

To enable detection of nucleosomal ladders in apoptotic cells, the DNA ladder assay was performed. Skeletal muscle was homogenized in 1 mL DNAzol (Molecular Research Center Inc., Cincinnati, OH). Proteinase K (Qiagen, Valencia, CA) was added to the homogenates, which, after a 3 h incubation period, were centrifuged (10,000 × g for 10 min at 4°C) and the supernatants were precipitated and washed with 100% and 75% ethanol, respectively. After digestion with RNase A, DNA samples were subjected to a DNA ladder-specific ligation PCR, following the manufacturer's protocol (Maxim Biotech, CA). Briefly, isolated DNA is subjected to an overnight ligation reaction using de-phosphorylated adaptors (12-mer: 5'-

AGTCGACACGTG-3', 27-mer: 5'-GACGTCGACGTCGTACACGTGTCGACT-3') that are ligated to the ends of DNA fragments generated during apoptosis, using T4 DNA ligase. In mammalian cells, such fragments generally have 5'-phosphorylated blunt ends and 3'-OH ends, thus only the 27-mer is ligated to the DNA fragments. When the mixture is heated to 55 °C, the 12-mer is released. Next, the 5' protruding ends of the molecules are filled by Taq polymerase. The 27-mer then serves as a primer for PCR in which the fragments with adaptors on both ends are amplified. Conditions for PCR reactions were 72 °C for 10 min, 94 °C for 1min, 94 °C for 1 min, and 70 °C for 2 min. PCR amplification was conducted for 30 cycles. PCR products were electrophoresed through 1% agarose gels containing 0.5 μg/mL ethidium bromide at 80 V for 1 h, and were examined under UV light for the presence of apoptosis-specific nucleosomal ladders.

Specific Aim 3. Identification of the Specific Apoptotic Signaling Pathway Responsible for Skeletal Muscle Loss in D257A Mice

In this aim we hypothesized that mitochondrial dysfunction in D257A mutator mice would lead to mitochondrial outer membrane permeability and leakage of cytochrome *c* and other pro-apoptotic factors into the cytosol. Cytochrome *c* release from the mitochondria may subsequently activate the caspase-dependent mitochondrial-mediated pathway of apoptosis, leading to the activation of caspase-9 and downstream cleavage and activation of caspase-3 that we have observed in these mice (Figs 4-18, 4-20).

Rationale

The demonstration that the effector caspase-3 is cleaved and thus, activated, in D257A mice does not provide proof of activation of a mitochondrial-mediated pathway of apoptosis, since other apoptotic pathways, such as, receptor-mediated (extrinsic pathway), and ER-stress-mediated pathways may also lead to the activation of the final effector caspase-3. Since the accumulation of mtDNA mutations was expected to cause changes in mitochondrial

bioenergetics, ultimately leading to mitochondrial dysfunction, we hypothesized that the pathway of apoptosis would be intrinsic to the mitochondria. The D257A mouse model allowed us to elucidate the relevant mitochondrial pro-apoptotic proteins that are activated in response to mtDNA mutations. Apoptosis originating from these pathways has been strongly implicated to be causal in the aging process and is also highly relevant to many clinical conditions in humans that are associated with mtDNA mutations (147). Since the specific functions of AIF and EndoG (caspase-independent pathway) in mitochondrial function, as well as, in apoptosis-initiated by the mitochondria remain to be substantiated, we evaluated the levels of key regulators of the main caspase-dependent, mitochondrial-mediated pathway of apoptosis: Cytochrome c and the initiator caspase-9. We further correlated caspase-9 activity levels with caspase-3 activity levels (Fig 4-21) in order to demonstrate that activation of caspase-9 indeed leads to downstream activation of caspase-3 and apoptosis.

Experimental approach

Determination of cytochrome c content by Western Blotting

For quantification of cytochrome c content by Western blot analysis, proteins were separated using 15% PAGEr® Gold pre-cast Tris-glycine gels (Cambrex, USA) under denaturing conditions, and then transferred to PVDF membranes (0.2 μm, Trans-Blot® Transfer Medium, Bio-Rad Laboratories, CA USA). Protein concentration was determined using the Bradford assay, and was subsequently normalized so that the protein content among samples is identical. Subsequently, 20 μl of sample were loaded to each well. 5 μl of purified human heart mitochondria were also loaded in a well as an appropriate positive control. Membranes were blocked for 1.5 hrs using a blocking solution containing TBS and 5% milk. Membranes were then incubated overnight in the 5% blocking solution containing the cytochrome c monoclonal

primary antibody at a dilution of 1:1000. The following day membranes were incubated for 1 h at room temperature with IgG horseradish peroxidase-linked whole secondary antibody (1:1000, Amersham Biosciences UK Ltd, Amersham, UK). Specific protein bands were visualized using ECL plus reagent (Amersham Pharmacia Biotech, UK). The resulting Western blots were analyzed using the Alpha Innotech FluorChem SP imaging system. Specific protein bands were further normalized to tubulin. Values were expressed as arbitrary units after normalizing and expressing samples as % of a control sample that was included in all membranes.

Enzymatic measurement of caspase-9 activity

Caspase -9 activity was measured using a fluorometric protease assay kit: (Caspase-9/Mch6, Biovision, Mountain View, CA, USA) according to manufacturer's instructions. Briefly, the assay is based on detection of cleavage of the substrate LEHD-AFC (AFC: 7-amino-4-trifluoromethyl Coumarin) by caspase-9. LEHD-AFC emits blue light (λmax = 400 nm); upon cleavage of the substrate by caspase-9, free AFC emits a yellow-green fluorescence (λmax = 505 nm), which can be quantified using a fluorescence microtiter plate reader. Samples were run in triplicate and values were expressed as raw fluorescence units per mg of cytosolic protein.

Statistical Analyses

All results are expressed as means ± SEM and the means obtained were used for independent t tests. Statistical analyses were carried out using the Graph-Pad Prism 4.0 statistical analysis program (San Diego, CA, USA). Statistical significance was set at $P<0.05$.

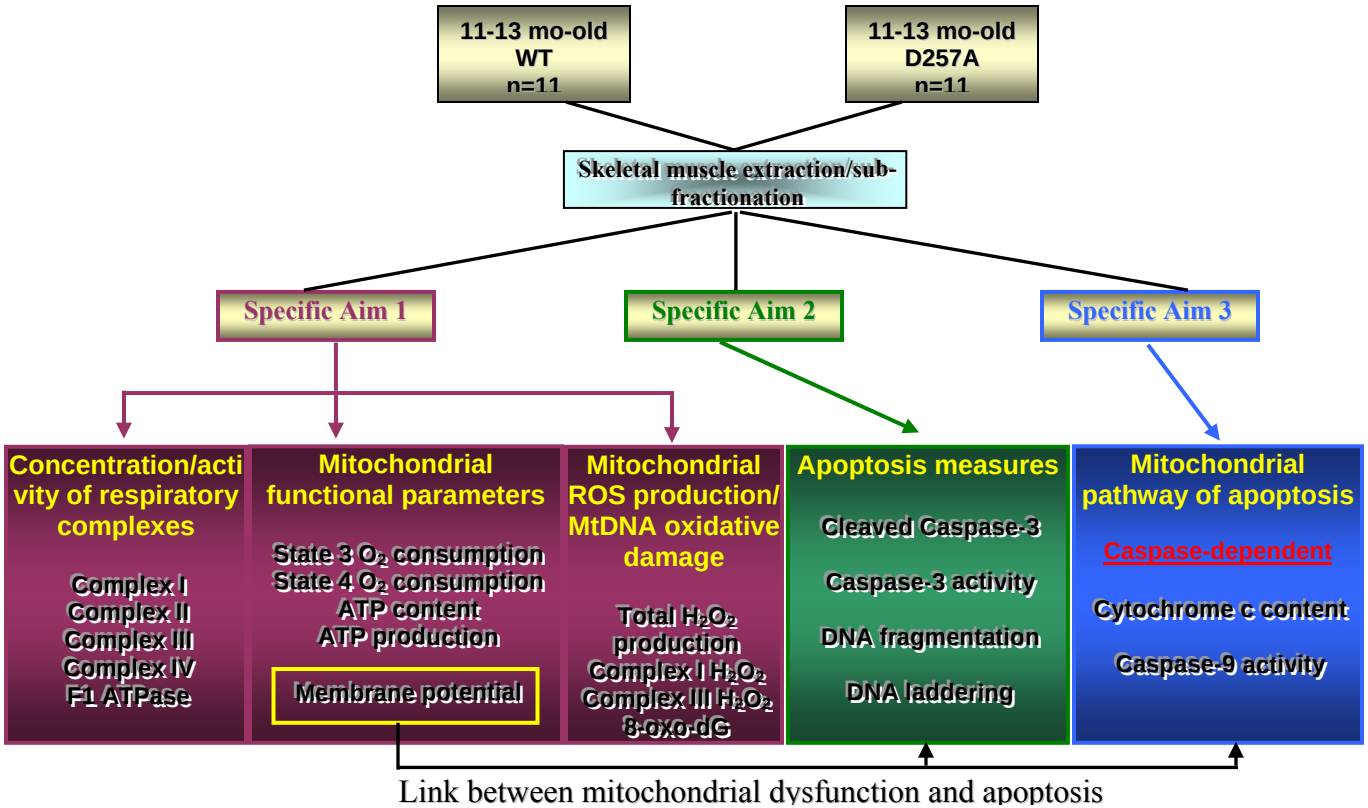

Figure 3-1. Experimental design and summary of the parameters measured in specific aims 1, 2 and 3.

CHAPTER 4
RESULTS

Mouse Characterization Data from Dr. Prolla's Lab: Generation and Phenotype of D257A Mice

In order to elucidate the role of mtDNA mutations in skeletal muscle loss, observed with age, we will use a "knock in" mouse model ($Polg^{D257A}$) with increased spontaneous mutation rates in mtDNA. In brief, these mice contain a mutation that results in a functional disruption of the exonuclease domain of mouse mitochondrial DNA polymerase γ, POLG.

Based on yeast, site directed mutagenesis studies, our collaborators constructed a mutation that corresponds to the D230 substitution in yeast (D257 in mice), which was the substitution that elicited the strongest mutator phenotype *in vivo* among the substitutions tested (148). This residue, D257, is conserved in all POLG proteins identified to date and is involved in dNMP and divalent ion binding, playing an essential role in the catalytic activity of the 3'-5' exonuclease (149, 150). This mutation completely abolishes POLG exonuclease activity in yeast and mice, but has no significant effect on polymerase activity (148).

The mouse POLG locus, PolgA, was cloned and gene targeting in embryonic stem (ES) cells was used to introduce an AC → CT two-base substitution that corresponds to positions 1054 and 1055 of the exonuclease-encoding domain (see supporting data on *Science* online). This mutation results in a critical residue substitution in the conserved exonuclease domain of POLG, impairing its proofreading ability (14). Seven correctly targeted ES cell clones were expanded and the cells were injected into blastocysts derived from B6 female mice. Injected blastocysts were implanted in pseudo-pregnant females for generation of chimeric mice. Several chimeric mice were identified as determined by coat color. Of these, six chimeras, representing four different ES cell clone lines, resulted in germline transmission of the $Polg^{D257A}$ allele when

mated to B6 females. Germline transmission of the mutation produced PolgA$^{D257A/+}$ mice, which were then intercrossed to generate homozygous PolgA$^{D257A/D257A}$ mice. Mice carrying one copy of the Polg^{D257A} allele are healthy and fertile, and are continuously used to generate homozygote Polg^{D257A} mice. Young homozygous Polg^{D257A} mice, which are devoid of WT Polg protein, were indistinguishable from wild-type littermates, however, long-term follow-up revealed a striking premature aging phenotype beginning at ~ 9 months of age (13). Phenotypes are age-related and consisted of: hair loss, loss of bone mass, hearing loss, kyphosis, skeletal muscle loss, and cardiac dysfunction (Fig 4-1). The mutant mice have a significantly reduced life span (for D257A mice, maximum survival 460 days, median survival 416 days; for wild-type littermates, maximum and median survival >850 days (Fig 4-1) (13).

Data from Our Lab

In our pilot study we had obtained data on both 3-mo and 11-mo old WT and D257A animals in several parameters, therefore, we occasionally report results obtained at both time points.

Results for Specific Aim 1

Impaired mitochondrial bioenergetics in 11-month-old D257A mice

We have evaluated mitochondrial respiration in 3-month old and 11-month old WT and D257A mice. O_2 consumption by skeletal muscle mitochondria was almost identical between WT and D257A mice at 3-mo of age for both state 4 (WT: 8.4 ± 0.7 nmol/min/mg protein vs. D257A: 8.2 ± 1.2, p=0.9) and state 3 respiration (WT: 41.1 ± 3.3 vs. D257A: 38.4 ± 4.7, p=0.64) (Fig A-3). This suggests that mtDNA mutations do not affect mitochondrial bioenergetics early on in the D257A animal's life, and that the D257A phenotype is age-induced. At 11-months, O_2 consumption during state 4, the resting state of the mitochondria, did not differ between genotypes (WT: 12.7 ± 1.3 vs. D257A:11.9 ± 0.95, p=0.31), which was not unexpected since O_2

consumption during this state is usually minimal. However, at 11 months of age mutant mitochondria displayed a marked decrease in oxygen consumption (-43 %) during state 3 (WT: 68.4 ± 5.1 vs. D257A: 39 ± 5.8, p=0.0006) (Fig 4-2), the phosphorylative state of the mitochondria, which also led to a significantly lower respiratory control ratio (RCR: -43 %) for the mutant mitochondria (WT: 5.7 ± 0.49 vs. D257A: 3.27 ± 0.39, p=0.0005). RCR is used as an index of mitochondrial coupling and the significant decrease in the D257A mitochondria suggests that there is significant uncoupling between oxidation and phosphorylation (Fig 4-2). It is therefore evident that accumulation of mtDNA mutations may lead to mitochondrial dysfunction associated with compromised state 3 respiration.

D257A mice display decreased content of ETC Complexes I, III, and IV that contain mtDNA-encoded subunits

We measured the content of ETC complexes I, II, III, IV and F1 domain of ATPase in 11-mo old WT and D257A skeletal muscle using blue native page. We found that the total contents of complexes I (WT: 40050 ± 2281 arbitrary units vs. D257A: 26100 ± 2724, p=0.002), III (WT: 50970 ± 3673 vs. D257A: 31960 ± 4925, p=0.0093), and IV (WT: 50900 ± 4782 vs. D257A: 25460 ± 5532, p=0.0046), all of which contain subunits encoded by mtDNA, were significantly reduced in D257A mice (Figs 4-3, 4-4), suggesting that complex formation in D257A mice - specifically those containing subunits encoded by mtDNA - is abolished. In contrast, the content of complex II (WT: 20710 ± 4079 vs. D257A: 28610 ± 7051, p=0.3513) and F1 (WT: 19760 ± 2831 vs. D257A: 18330 ± 747.9, p=0.64), both of which contain only nuclear-encoded subunits, was not different between genotypes (Figs 4-3, 4-4). The latter reinforces the idea that the accumulation of mtDNA mutations directly impacts assembly of complexes that are partly mitochondrial-encoded, while all nuclear-encoded complexes appear unaffected.

Electron transport chain complex specific activity remains unaffected by mtDNA mutations in D257A mice

The activities of complex I and IV (partly mtDNA-encoded) appear greatly reduced in the mutant mice (Fig 4-5) while for the all-nuclear-encoded complexes II, and F1 domain there are no apparent differences between genotypes (Fig 4-5). However, when we normalized the activity for each sample to the respective complex content we saw no differences between WT and D257A mice for all complexes evaluated (Fig 4-6): Complex I (WT: 314.5 ± 13.56 arbitrary units vs. D257A: 349.1 ± 28.8, p=0.29), complex II (WT: 313 ± 118.9 vs. D257A: 163.8 ± 26.3, p=0.26), complex IV (WT: 364.7 ± 19.6 vs. D257A: 440 ± 100.5, p=0.49), F1 domain of ATPase (WT: 435.1 ± 96.5 vs. D257A: 384.3 ± 18, p=0.62).When we take into account the complex content and activity results (Figs 4-3, 4-4, 4-5, 4-6) as well, as the O_2 consumption (Fig 4-2) and the ATP content data (Fig 4-8), we can conclude that although the content of ETC complexes per mitochondrion, or per amount of total mitochondrial protein is reduced, the activity of the remaining complexes remains unaffected, at least at the time of the measurement which represents a "snap shot" in the continuum of time. However, this still leaves mitochondria with energy deficits which are well demonstrated in our experiments by greatly compromised mitochondrial respiration and reductions in ATP content.

D257A mice show decreased content of both nuclear-encoded and mitochondrial-encoded ETC subunits

Besides measuring the content of fully assembled and enzymatically active ETC complexes, we further determined the content of selected individual subunits from each complex. We evaluated the subunit NDUFA9 from complex I, which is nuclear-encoded, as well as the subunit NDUFS3 from complex I which is mitochondrial-encoded. We also evaluated one subunit from complex II (70 kDa) and 2 selected subunits from complex III, 29 kDa and 48 kDa, all of which are nuclear-encoded. Last, we evaluated the COX1 subunit from complex IV which

is mitochondrial-encoded and is a part of the active redox center of this complex, and is thus, essential for catalysis. We observed a significant down-regulation of protein expression in the D257A mice compared to WT, for all subunits evaluated either nuclear- or mitochondrial-encoded (NDUFA9-WT: 1.47 ± 0.14 arbitrary units vs. D257A: 0.36 ± 0.024, p<0.0001) (NDUFS3-WT: 3.8 ± 0.2 vs. D257A: 3.1 ± 0.2, p=0.03) (Complex II 70kDa-WT: 0.8 ± 0.025 vs. D257A: 0.53 ± 0.034, p<0.0001) (Complex III 48kDa-WT: 2.05 ± 0.13 vs. D257A: 1.2 ± 0.07, p<0.0001) (COX1-WT: 1.44 ± 0.12 vs. D257A: 0.53 ± 0.05, p<0.0001) (Fig 4-7), with the exception of the 29kDa subunit of complex III which was almost significantly affected in the mutant mice (WT: 0.6 ± 0.055 vs. D257A: 0.47 ± 0.04, p=0.07) (Fig 4-7).

D257A mice display decreased ATP content

ATP content, determined at 11-mo of age was significantly lower in D257A mice compared to WT (WT: 0.29 ± 0.08 nmol/mg protein vs. D257A: 0.11 ± 0.04, p=0.046) (Fig 4-8). It is apparent that loss of ETC complex content (see Figs 4-3, 4-4) can have an impact on ATP content. Therefore, if ETC complex content is reduced in D257A muscle per amount of total mitochondrial protein, as we have observed (Figs 4-3, 4-4), it is only expected that ATP content per amount of total mitochondrial protein would be reduced, as we also show, because there are probably less ETC complexes per mitochondrion. ATP production at the same time point remained unaffected by the accumulation of mtDNA mutations (WT: 142.3 ± 19.65 nmol/mg protein/min vs. D257A: 124.7 ± 21.7, p=0.28) (Fig 4-8).

Mitochondrial membrane potential is significantly lower in D257A mice

We determined the effect of increased mtDNA mutational load on mitochondrial membrane potential ($\Delta\psi$) in 13-mo old WT and D257A skeletal muscle. Membrane potential was significantly lower in D257A mice during both state-4 (WT: 195.2 ± 1.4 mV vs. D257A: 187.9 ± 2.15 mV, p=0.017) (Fig 4-9) and state 3 (WT: 177.7 ± 2.5 vs. D257A: 167.3 ± 2.25,

p=0.01) (Fig 4-9). This drop in $\Delta\psi$ is possibly conferred upon energy deficits in the mitochondria due to the dysfunction of ETC complexes (see Figs 4-2, 4-3, 4-4, 4-7 and 4-8) and can be the trigger for the mitochondrial-mediated apoptosis we detected in the mutant mice (see Figs 4-16, 4-17, 4-18, 4-20).

Mitochondrial protein yield is reduced in skeletal muscle of D257A mice

We measured total mitochondrial protein yield in 13-mo old WT and D257A skeletal muscle and found that mitochondrial yield is drastically reduced in D257A mice by 13-mo of age (45.9% reduction compared to WT) compared to WT (WT: 4.3 ± 0.14 mg of mitochondrial protein/gram of muscle tissue vs. D257A: 2.35 ± 0.2, $p<0.0001$) (Fig 4-10). Interestingly, this may suggest that mitochondria are getting eliminated in D257A mice. We also compared this content with a group of ~10-11 mo old animals in order to observe whether it gets continuously reduced as the D257A animals get older and closer to their mean lifespan. Indeed, at 11 months we also observed a significant reduction (35% reduction) in the mitochondrial content but not to the extend we saw at 13 months (WT: 4 ± 0.14 vs. D257A: 2.6 ± 0.06, $p=0.0044$) (Fig 4-10). Combined the above results suggest that mitochondria are probably getting continuously eliminated in skeletal muscle throughout the lifespan of D257A mice.

Skeletal muscle mitochondria from D257A mice produce significantly less ROS

The main tenet of the free radical theory of aging (70) is that aging is due to the progressive accrual of ROS-inflicted damage, including mtDNA mutations, the accumulation of which has been postulated to lead to a "vicious cycle" of further mitochondrial ROS generation and mitochondrial dysfunction (5, 6). To test this hypothesis, we measured H_2O_2 produced by skeletal muscle mitochondria of young and old (3-mo and 11-mo old) WT and D257A mice. H_2O_2 production was measured during state 4 since ROS production is highest when electron flow is low, while during state 3 ROS production is nearly negligible. Levels of H_2O_2 were not

significantly different between genotypes at the 3-mo time point (WT: 0.30 ± 0.05 nmol H_2O_2/ min/mg protein vs. D257A: 0.26 ± 0.06, p=0.6) (Fig A-4). Interestingly, at 11-mo of age, H_2O_2 production was significantly decreased (-36 %) in D257A mice (WT: 0.6 ± 0.07 nmol H_2O_2/ min/mg protein vs. D257A: 0.4 ± 0.05, p=0.01) (Fig 4-11), and coupled to the decreased state-3 respiration (Fig 4-2). The decreased H_2O_2 production by mutant mitochondria also led to the calculation of a significantly lower free radical leak for the D257A mitochondria (WT: 2.6 ± 0.3% vs. D257A: 1.8 ± 0.3%, p=0.04) (Fig 4-11). These observations do not support the "mitochondrial vicious-cycle" hypothesis of aging, but instead suggest that mtDNA mutational load is causal to reduced mitochondrial function, as demonstrated by the marked decrease in oxygen consumption and the significant mitochondrial uncoupling. However, the accumulation of mutations does not induce an increase in mitochondrial ROS production. Similar results regarding mitochondrial ROS production have recently been published using mouse embryonic fibroblasts (MEFs) from D257A mutator mice (79) and this study also questioned the accuracy of the mitochondrial "vicious cycle" theory.

D257A mitochondria produce less ROS in both main ROS generators of the ETC: Complex I and Complex III

When we evaluated site specific ROS generation in 3-mo old mice we found no differences between genotypes in ROS production at either complex I -representing total basal ROS generation (Fig A-4: panels A) (WT: 0.3 ± 0.05 nmol H_2O_2/ min/mg protein vs. D257A: 0.26 ± 0.06, p=0.6) or Complex III (Reverse flux included-WT: 4.6 ± 0.56 vs. D257A: 4.15 ± 0.67, p=0.6) (Reverse flux blocked-WT: 1.13 ± 0.23 vs. D257A: 1.1 ± 0.3, p=0.9) (Fig A-4: panels C, D), or in the maximal capacity of these complexes to generate ROS (Fig A-4: panels B, E) (Maximal complex I production - WT: 1.6 ± 0.19 vs. D257A: 1.75 ± 0.18, p= 0.68) (Maximal complex III production - WT: 8.6± 0.9 vs. D257A: 8.4 ± 0.6, p= 0.84). As expected, the free

radical leak percent (Fig A-4: panel F) was also not different between WT and D257A mice (WT: 2 ± 0.45% vs. D257A: 1.75 ± 0.4%, p=0.7). At 11-mo of age our results were consistent, showing that, D257A mitochondria produce less ROS at complex III, either when reverse electron flux is taken into account (WT: 6.3 ± 0.47 nmol H_2O_2/ min/mg protein vs. D257A: 3.13 ± 0.48, p=0.0002) (Fig 4-12: panel B) or when it's blocked (WT: 1.5 ± 0.14 vs. D257A: 0.9 ± 0.12, p=0.005) (Fig 4-12: panel C), and have reduced maximal capacity to generate ROS at both complex I (WT: 2.9 ± 0.23 vs. D257A: 1.2 ± 0.19, p<0.0001) (Fig 4-12: panel A) and complex III (WT: 11.9 ± 1.2 vs. D257A: 6.75 ± 0.88, p=0.003) (Fig 4-12: panel D) compared to WT. Moreover, the fact that H_2O_2 production is decreased almost fourfold for both WT and D257A mice when the reverse electron flux is blocked (when comparing Y axis values from Fig 4-12, panels B and C) signifies that this reverse flow is a significant source of ROS produced by the ETC. These observations combined provide further support to our previous results regarding total basal ROS production by the mitochondria (see Fig 4-11), as well as, additional evidence against the mitochondrial "vicious cycle" theory.

No difference in antioxidant enzyme mRNA expression between genotypes

We measured mRNA expression of Catalase and the mitochondrial-specific isoform of SOD, MnSOD, in skeletal muscle of 11-mo old WT and D257A mice, via RT-PCR. We found no difference in either Catalase (WT: 1.2 ± 0.08 arbitrary units vs. D257A: 1.1 ± 0.04, p=0.1) (Fig 4-13) or MnSOD (WT: 0.8 ± 0.01 arbitrary units vs. D257A: 0.7 ± 0.07, p=0.3) (Fig 4-13) between genotypes. This provides further support to the notion that mitochondria from D257A mice actually produce less ROS and that the decrease we observed in H_2O_2 production was not due to an adaptive up-regulation of antioxidant defenses in the mutant mice. In fact, in D257A muscle, there was a strong trend toward decrease, especially, in Catalase mRNA expression. The

fact that mutant mice generate less H_2O_2 might explain the no-need for up-regulation of antioxidant defenses compared to WT.

Mitochondrial DNA mutations cause aging phenotypes in the absence of increased oxidative stress

In order to correlate our H_2O_2 results with further oxidative stress, we next examined a marker of ROS-induced oxidative damage to DNA, by assessing the levels of 8-oxo-7,8-dihydro-2'-deoxyguanosine (8-oxodGuo) in skeletal muscle mtDNA of 11-mo old WT and D257A mice, using HPLC with electrochemical detection. We did not find any differences in the levels of mtDNA oxidation between 11-mo old WT and D257A mice (WT: 51.4 ± 6.3 8-oxodGuo/10^6 dGuo vs. D257A: 50.3 ± 7.2, p=0.9) (Fig 4-14). Moreover, in published results, we also showed no significant differences between WT and D257A skeletal muscle in F2-isoprostanes, a marker of lipid peroxidation (13). Thus, an increased load of mtDNA mutations does not appear to be associated with increased levels of oxidative damage to mtDNA (Fig 4-14), or elevated lipid peroxidation in skeletal muscle. A recent publication provided further support to our outcomes showing that protein carbonylation, and thus, oxidative damage to proteins was not significantly different in mtDNA mutator mice compared to WT (79). Hence, despite increased mutational load, mitochondria from D257A mice do not show increased oxidative stress.

Results for Specific Aim 2

D257A mice display significant skeletal muscle loss by 11-mo of age

We obtained data on 3-mo old and 11-mo old WT and D257A mice. At 3-mo-of age there was no significant difference in skeletal muscle weight between WT and D257A mice (WT: 170 ± 6 mg vs. D257A: 150 ± 8, p=0.24) (Fig A-1). However, at 11-mo of age D257A mice exhibited significant skeletal muscle loss in the gastrocnemius (-24 %) (WT: 160 ± 6 mg vs. D257A: 126 ± 5, p=0.0004) (Fig 4-15), and in the quadriceps muscle (-19 %) (WT: 190 ± 6 mg

vs. D257A: 0.156 ± 0.007, p=0.0003) (Fig 4-15) compared to WT, which is indicative of sarcopenia, since normally aged animals (30-mo WT) also showed similar degree of muscle loss compared to young animals (5-mo WT) (WT: 145.7 ± 9.3 mg vs. D257A: 109.9 ± 6.6, p=0.0095) (Fig 4-15).

Apoptosis in D257A skeletal muscle is evident by an increase in cytosolic mono- and oligo-nucleosomes

We quantified apoptotic DNA fragmentation in skeletal muscle of 11-mo old WT and D257A mice by measuring the amount of mono- and oligo-nucleosomes released in the cytosol, using a quantitative "Cell Death" detection ELISA. These, are characteristic fragments of ~180-200 bp or multiples and are specific to apoptosis. We observed a significant release of these fragments into the cytosol in the D257A muscle (WT: 0.11 ± 0.006 OD/mg protein vs. D257A: 0.17 ± 0.03, p=0.035) (Fig 4-16) indicating that apoptosis indeed occurs in these mice and is, at least, partly responsible for the loss of skeletal muscle mass observed in these mice (Fig 4-15, 4-16).

DNA laddering is evident in skeletal muscle of D257A mice

To further demonstrate and corroborate apoptosis in D257A skeletal muscle we performed a standard measure of apoptosis: DNA laddering. This enables the detection and visualization of nucleosomal ladders of ~180-200 bp or multiples, characteristic of apoptosis. Prominent DNA ladders are evident for the D257A mice while ladders are very minimal or non-existent for WT mice (Fig 4-17). This small-scale DNA fragmentation further confirms that apoptosis is an important mechanism of sarcopenia in the mutant mice.

Caspase-3 cleavage and activation is up-regulated in D257A mice and resembles caspse-3 activation during normal aging

We evaluated apoptosis in skeletal muscle by measuring the content of activated (cleaved) caspase-3, by western blotting. Caspase-3 is the final effector caspase for many apoptotic

pathways and its cleavage at the C-terminal side of a specific aspartate residue is considered as one of the hallmarks of apoptosis.

To determine if increased levels of cleaved caspase-3 is a feature of normal aging, we first examined caspase-3 content in tissues of 5 mo-old and 30 mo-old WT mice (Fig 4-18) (13). Cleaved caspase-3 levels significantly increased with normal aging in skeletal muscle of WT mice by ~32% (5-mo old: 43130 ± 4704 arbitrary units vs. 30-mo old: 63620 ± 4510, p=0.0085). We further evaluated caspase-3 levels in skeletal muscle of 3-mo old and 11-mo old D257A and WT mice. Levels of cleaved caspase-3 did not differ between WT and D257A mice at 3-mo of age (WT: 26950 ± 5802 vs. D257A: 21660 ± 3924, p=0.46) (Fig A2), suggesting that the D257A phenotype is age-induced. Similar to normal aging, cleaved caspase-3 levels were also significantly elevated in D257A skeletal muscle by 11 months of age compared to controls (WT: 31580 ± 1408 arbitrary units vs. D257A: 56780 ± 8925, p=0.016) (Fig 4-18) (13), a time point at which mutant animals also displayed significant loss of muscle mass. This suggests that apoptosis, mediated by caspase-3 activation, is probably an important mechanism of skeletal muscle loss in the mutant mice and also during normal aging.

Together, these findings suggest that normal aging, as well as, accelerated aging induced by the accumulation of mtDNA mutations, are associated with the activation of a caspase-3 mediated apoptotic pathway in skeletal muscle. The observation of a similar response between normal and accelerated aging constitutes the D257A an appropriate mouse model to study the possible mechanisms of muscle wasting with age. Moreover, loss of critical, irreplaceable cells through apoptosis may be a central mechanism of skeletal muscle loss associated with the accumulation of mtDNA mutations during the aging process.

Results for Specific Aim 3

Cytochrome c release in the cytosol of D257A and WT skeletal muscle

We measured cytochrome c release in the cytosol by performing a western blot for cytochrome c in the cytosolic fraction isolated from skeletal muscle of 13-mo old WT and D257A mice. We did not detect significant differences between WT and D257A mice in cytosolic cytochrome c content, although we expected that cytochrome c release in the cytosol of D257A skeletal muscle would be significant (WT: 3.6 ± 0.2 arbitrary units vs. 3.56 ± 0.35, p=0.87) (Fig 4-19). It is very possible that our cytosol was contaminated with mitochondrial protein due to the mitochondrial isolation procedure. Basically, during mitochondrial isolation although most of the mitochondria isolated are intact and fully functional, some may get destroyed during homogenization, releasing many of the soluble proteins in the cytosol. Unfortunately, once this occurs, even if we further purify the cytosol nothing changes in the case of cytochrome c because it's a soluble protein.

Caspase-3 and caspase-9 activities are significantly higher in D257A mice: Evidence for induction of the mitochondrial, caspase-dependent pathway of apoptosis

We measured caspase-3 activity in the cytosol of 11-mo old WT and D257A skeletal muscle and found that it is significantly higher in the mutant mice (WT: 43 ± 2.7 RFU/mg protein vs. D257A: 57.7 ± 1.97, p= 0.0003) (Fig 4-20). Similarly, caspase-9 activity showed the same response: significant increase in D257A mice compared to WT (WT: 35.4 ± 2 RFU/mg protein vs. D257A: 45.3 ± 1.7, p= 0.0014) (Fig 4-20). In addition, when we correlated caspase-3 activity with caspase-9 activity we found significant correlations for both WT ($r = 0.97$, $p<0.0001$) and D257A mice ($r = 0.8$, $p=0.0029$) (Fig 4-21). These results provide proof for the induction of the main mitochondrial mediated, caspase-dependent pathway of apoptosis since activation of caspase-9 is evident in the mutant mice, which in turn leads to further cleavage and

activation of the final effector caspase, caspase-3 in this pathway (Fig 4-18, 4-20), which is directly responsible for the downstream events (i.e. cleavage of endo-nucleases and DNA repair enzymes) that lead to apoptosis.

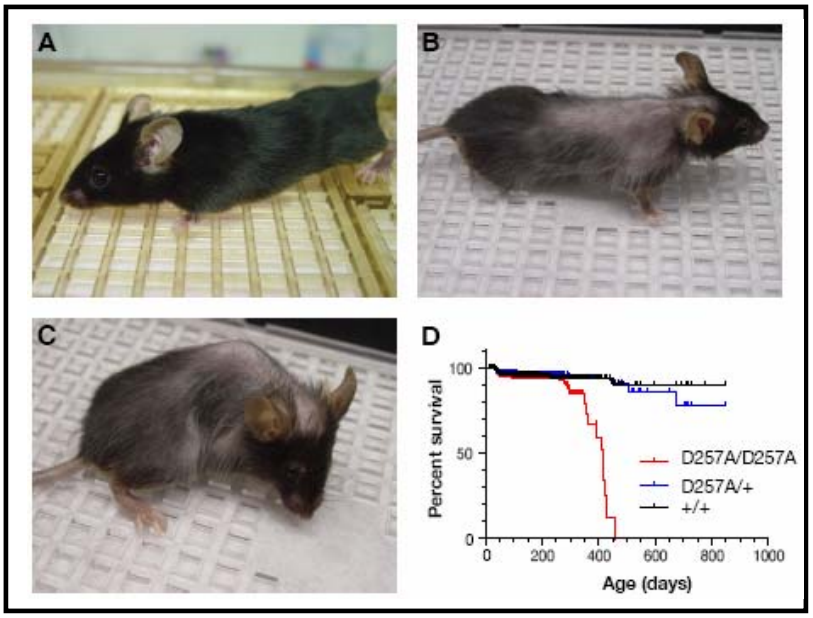

Figure 4 -1. D257A mice display a premature aging phenotype. Shown are (A) WT and (B, C) D257A mice at ~13 months of age. Progeroid features including hair loss, graying and kyphosis become apparent at ~9 months of age. (D) Kaplan-Meier survival analysis of cohorts of WT (+/+), D257A heterozygous mice (D257A/+) and D257A homozygous mice (D257A/D257A). At least 230 mice per genotype are represented in the survival curves.

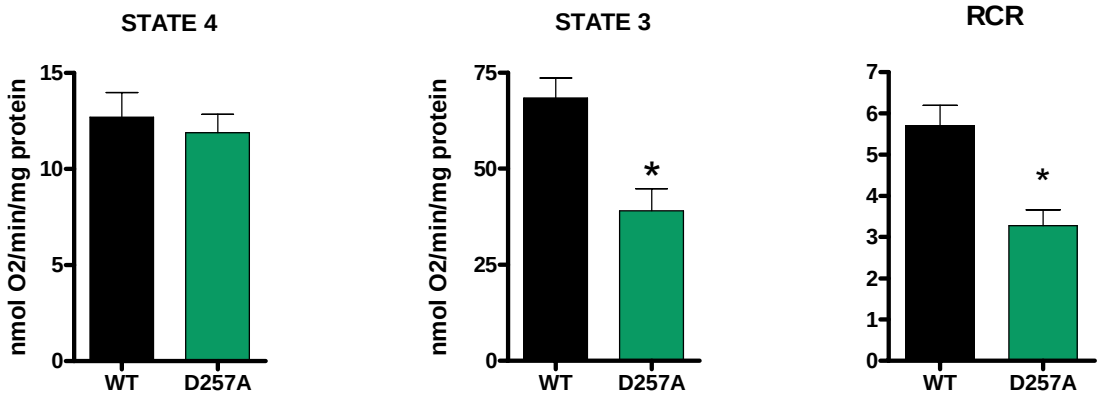

Figure 4- 2. Mitochondrial respiration is compromised in skeletal muscle of D257A mice. We determined the effects of mtDNA mutations on O_2 consumption of skeletal muscle mitochondria obtained from 11-mo old WT and D257A mice. Oxygen consumption was measured during state 4 (non-phosphorylative state and during state 3 (phosphorylative state). The respiratory control ratio (RCR), an index of mitochondrial coupling, was calculated by dividing state 3 to state 4 respiration values. Error bars represent SEM. *P < 0.5.

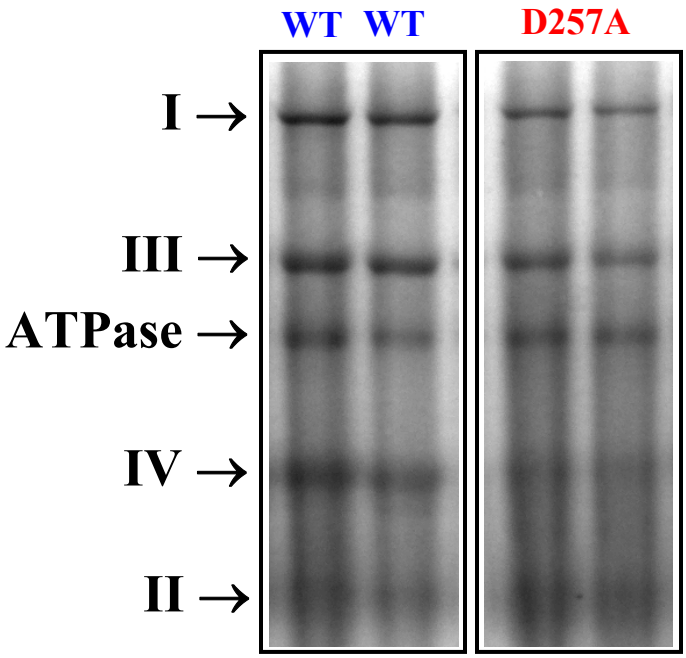

Fig. 4-3. D257A mice display decreased content of ETC Complexes I, III and IV that contain mtDNA-encoded subunits. The total content of ETC complexes I, II, III, IV and the F1 domain of the ATPase from skeletal muscle of 11-mo old WT and D257A mice was determined using Blue Native Page electrophoresis followed by staining with commassie blue stain. Proteins were separated according to molecular weight. Representative blots are depicted above.

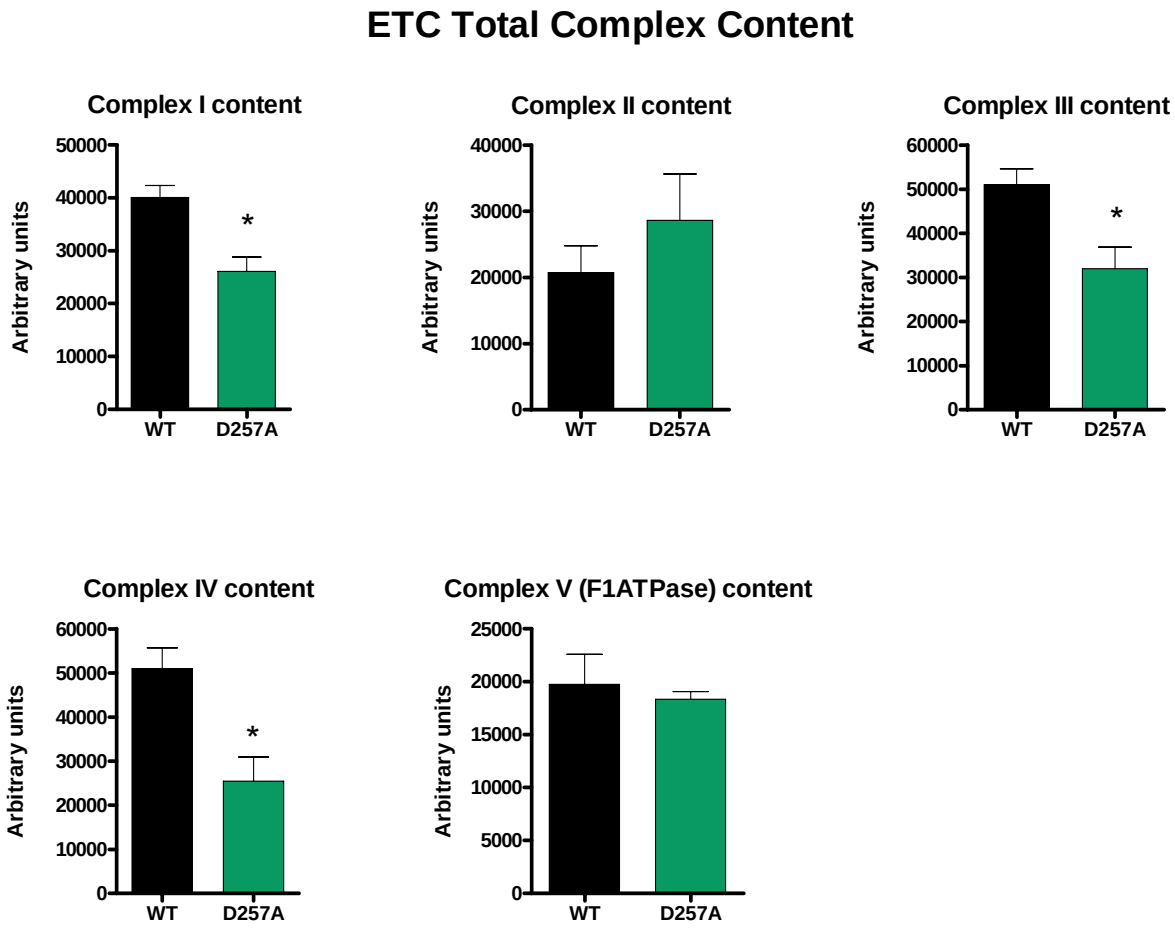

Fig. 4-4. Statistical analysis of ETC complex I, II, III, IV and the F1 domain of the ATPase content measured by Blue Native Page in skeletal muscle of 11-mo old WT and D257A mice. Arbitrary units represent densitometry values normalized to total protein loaded measured by the Bradford assay. Error bars represent SEM. *P < 0.5.

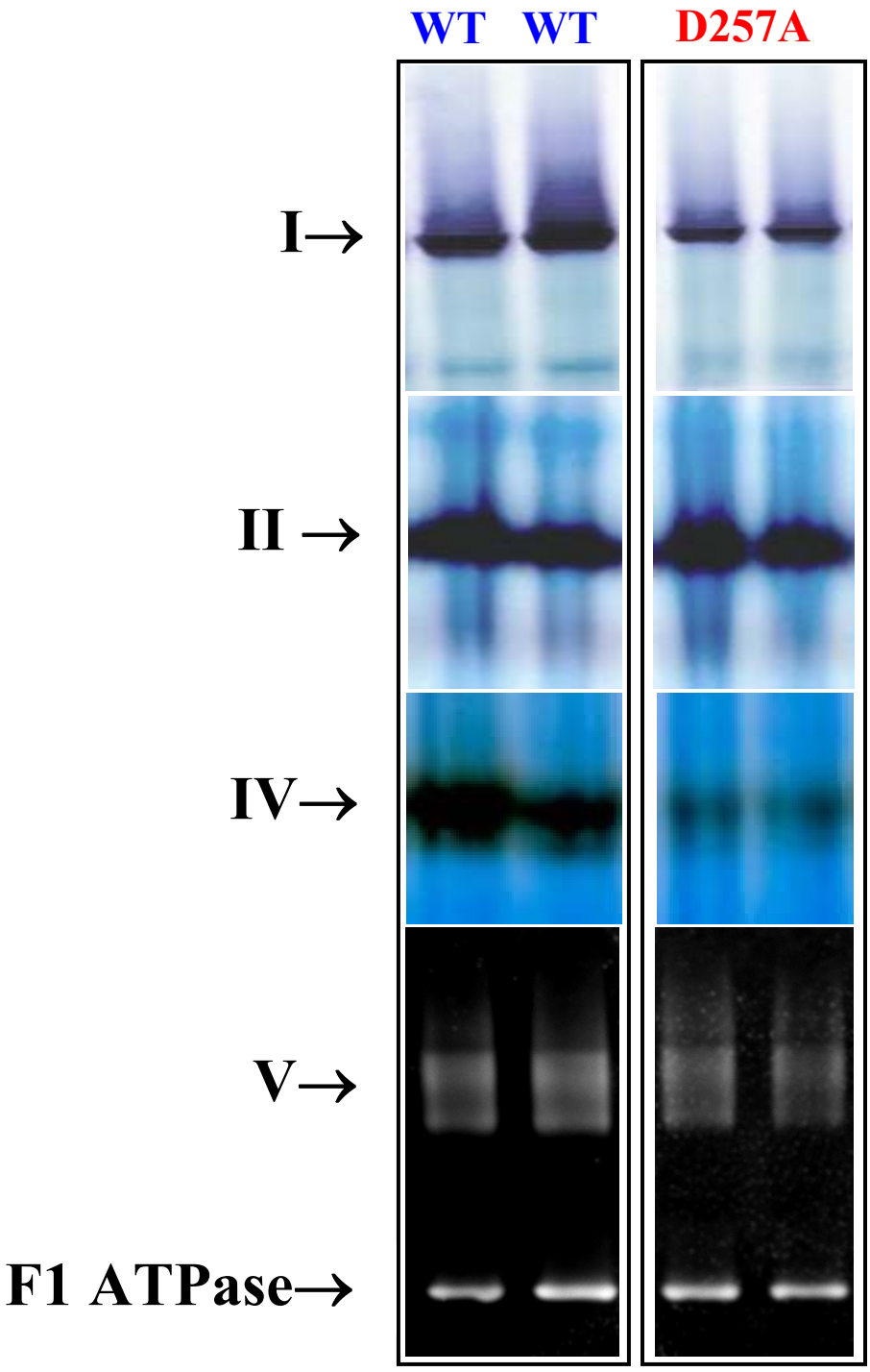

Fig. 4-5. Electron transport chain complex activity in skeletal muscle of 11-mo old WT and D257A mice. The activity of ETC complexes I, II, IV and the F1 domain of the ATPase was determined using Blue Native Page electrophoresis followed by enzymatic colorimetric reactions performed on the gels. Representative blots are depicted above.

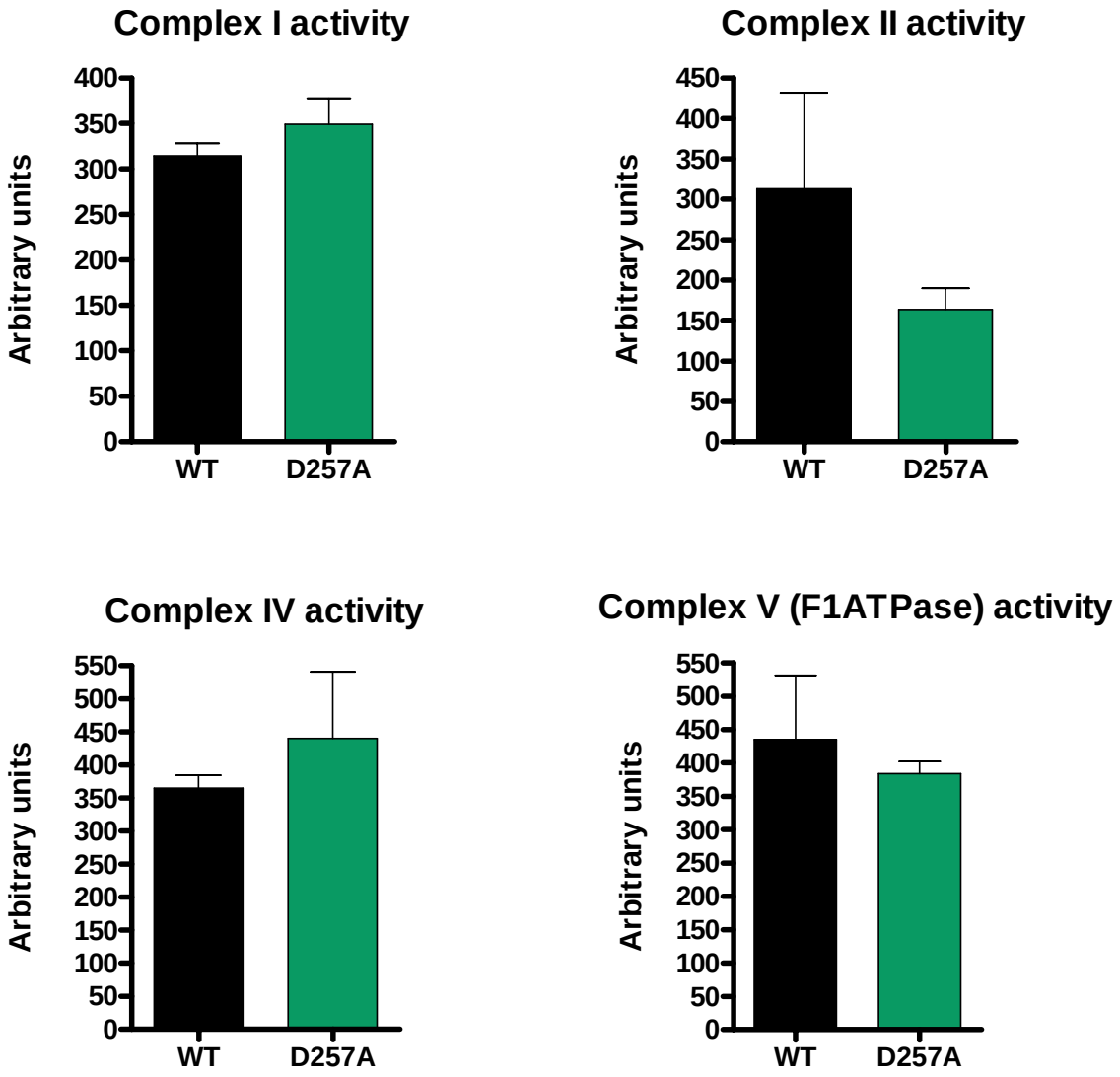

Fig. 4-6. Statistical analysis of ETC complex activity in skeletal muscle of 11-mo old WT and D257A mice. The activity of ETC complexes I, II, IV and the F1 domain of the ATPase was determined using Blue Native Page electrophoresis followed by enzymatic colorimetric reactions performed on the gels. Arbitrary units represent activity densitometry values normalized to respective content densitometry values for each sample. Error bars represent SEM.

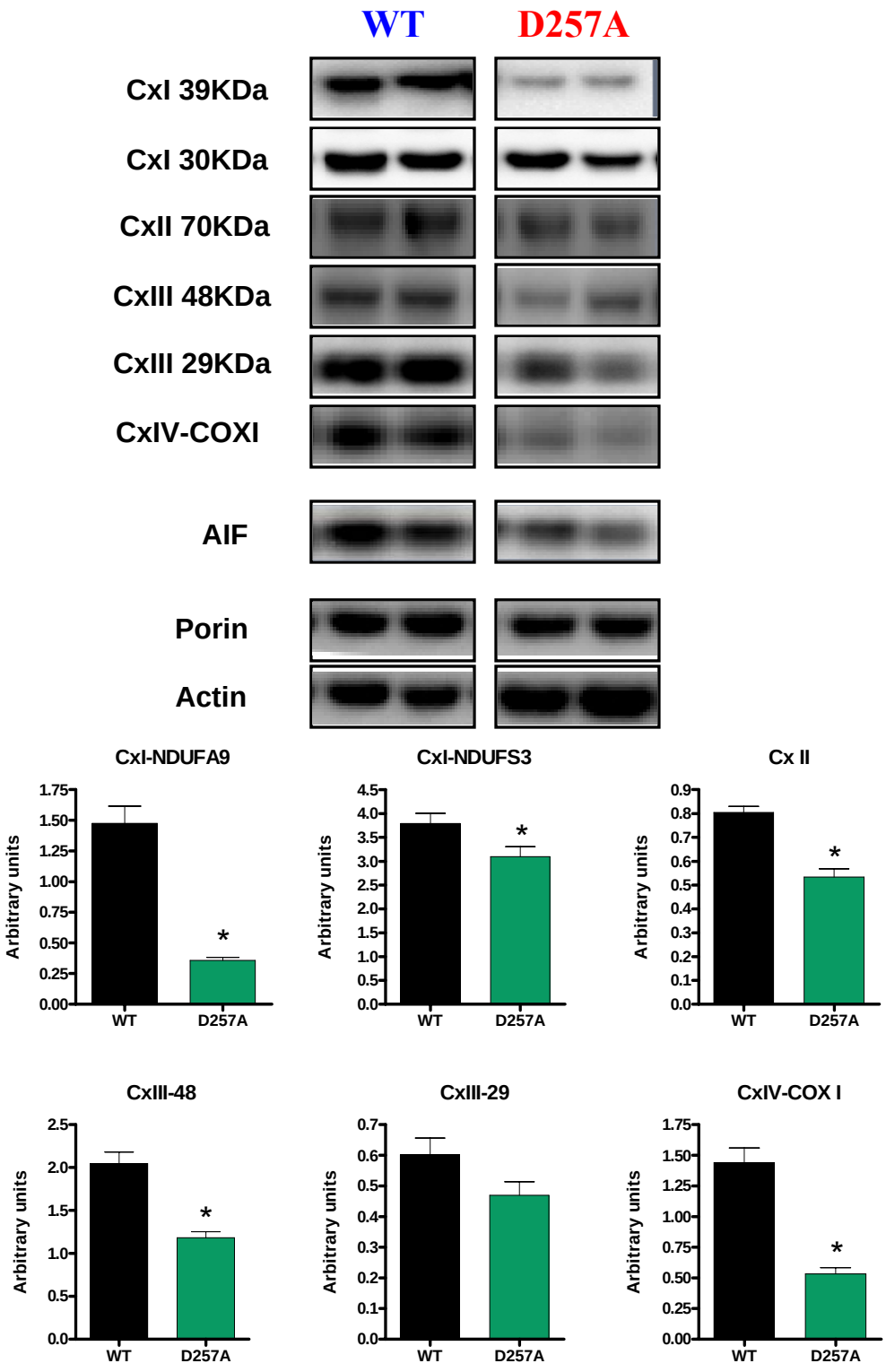

Fig. 4-7. D257A mice show decreased content of both nuclear-encoded and mitochondrial-encoded ETC subunits. The content of selected nuclear- and mitochondrial-encoded subunits from complexes I, II, III and IV, were evaluated by Western Blotting in 11-mo old WT and D257A mice. Representative blots are depicted above. Results shown above were normalized to porin. Error bars represent SEM. *P < 0.5. Cx: complex

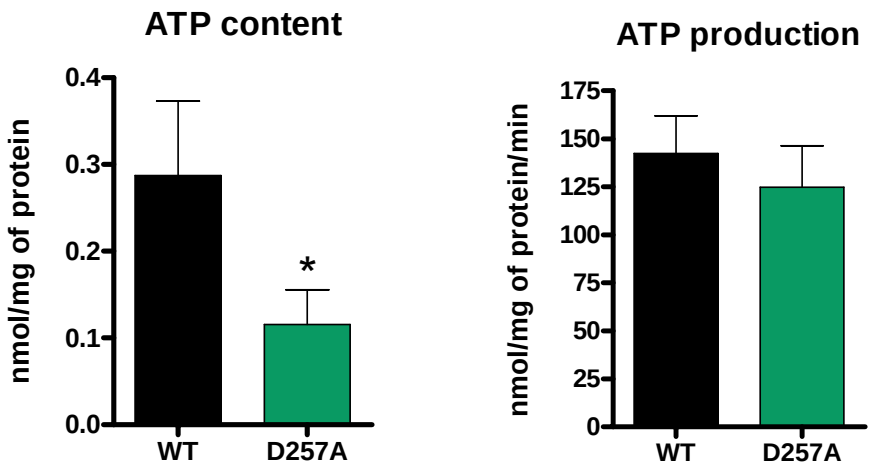

Fig. 4-8. D257A mice display decreased ATP content. We determined the effects of mtDNA mutations on ATP content and production in skeletal muscle mitochondria obtained from 11-mo old WT and D257A mice. Error bars represent SEM. *P < 0.5.

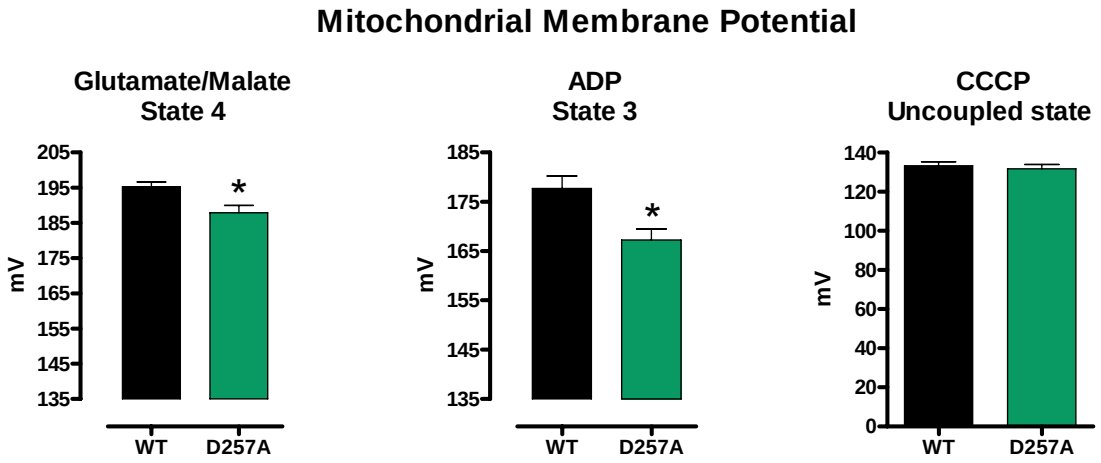

Fig. 4-9. Mitochondrial membrane potential (Δψ) drop in D257A mice. We determined the effects of mtDNA mutations on Δψ in skeletal muscle mitochondria obtained from 13-mo old WT and D257A mice. Changes in Δψ were followed qualitatively by monitoring the fluorescence of TMRM that accumulates in energized mitochondria. Δψ was measured during both state 4 (non-phosphorylative state) and during state 3 (phosphorylative state). Measurement of Δψ after addition of CCCP served as a control for TMRM binding. Error bars represent SEM. *P < 0.5.

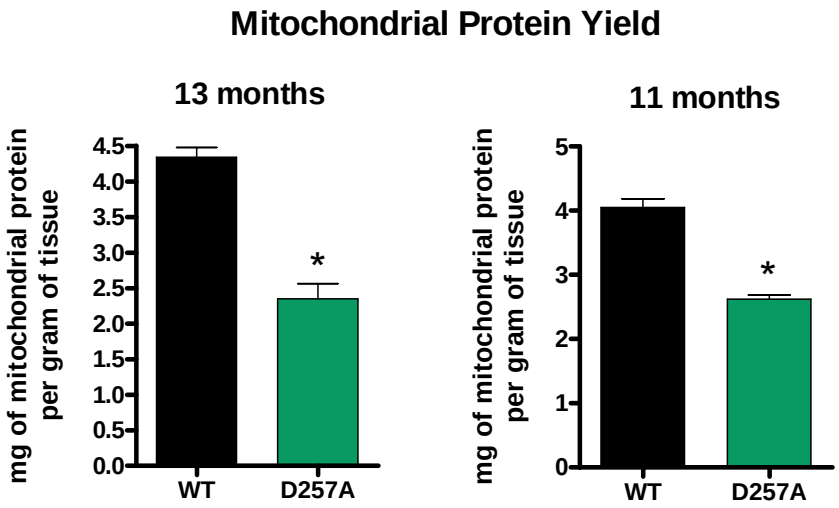

Fig. 4-10. Mitochondrial yield is reduced in D257A skeletal muscle. We determined total mitochondrial yield in 11- and 13-mo old WT and D257A mice by dividing the mitochondrial protein content measured by the Bradford assay by the skeletal muscle weight used each time to obtain the respective mitochondrial fractions. Error bars represent SEM. *P < 0.5.

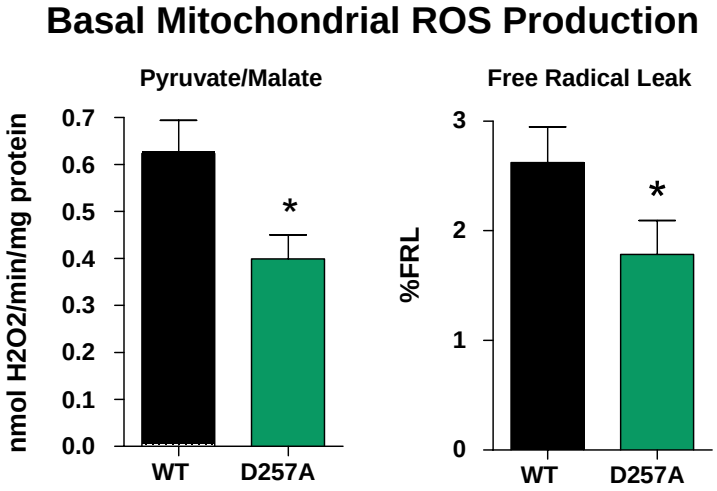

Fig. 4-11. D257A mitochondria produce less reactive oxygen species (ROS) during state 4. We measured H_2O_2 production since it represents total basal mitochondrial ROS generation. Skeletal muscle mitochondria were obtained from 11-mo old, WT and D257A mice and supplemented with pyruvate/malate as substrate for oxidative phosphorylation. Pyruvate/malate was used to study complex I ROS production which also represents total mitochondrial ROS production. Free radical leak percent (FRL%), an index of mitochondrial efficiency, was calculated by dividing the H_2O_2 value by twice the state 4 respiration value and the result was multiplied by 100 to give a % final value. Error bars represent SEM. *P < 0.05.

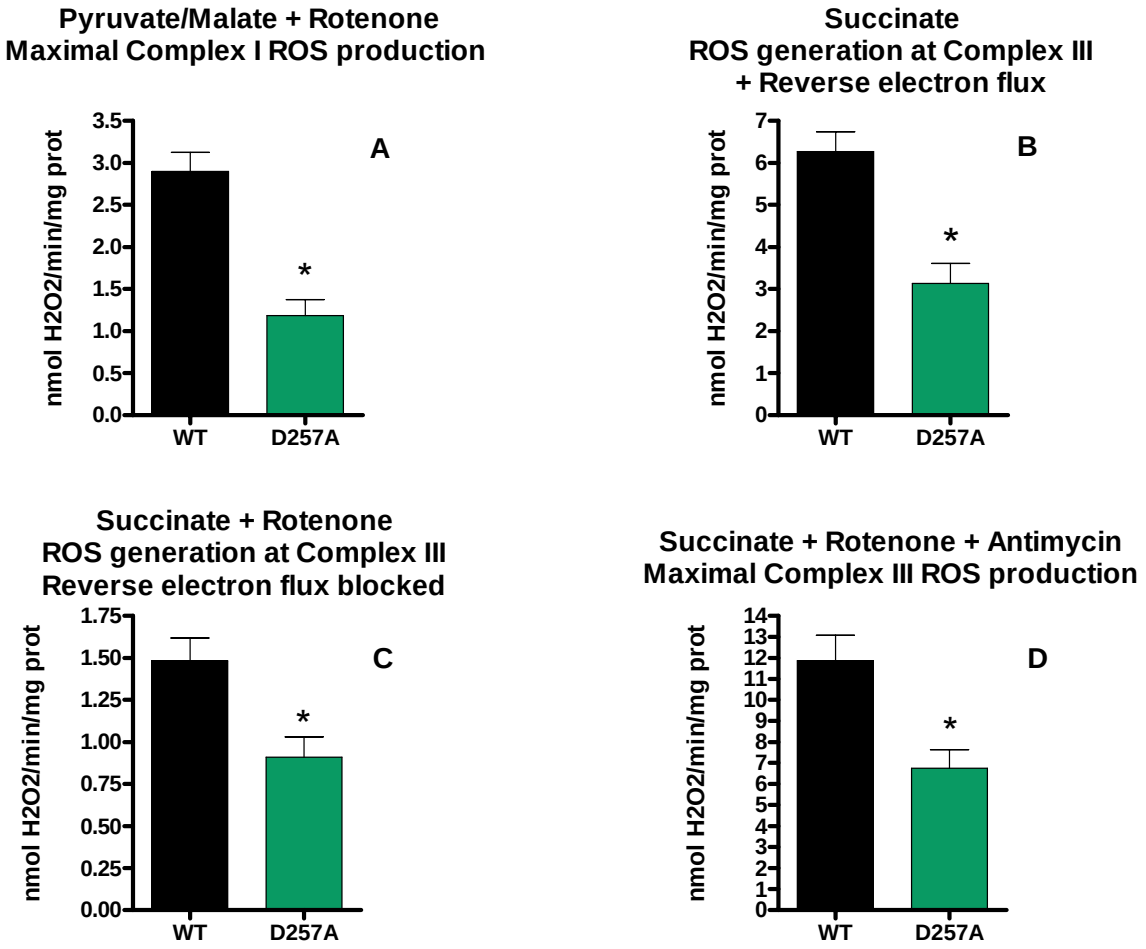

Fig. 4-12. D257A mitochondria produce less ROS in both main ROS generators: Complex I and Complex III. Skeletal muscle mitochondria were obtained from 11-mo old, WT and D257A mice. We used inhibitors of the ETC in order to study maximum rates of H_2O_2 production from complexes I and III, since they represent the main sites of ROS generation within the mitochondria. For complex I maximum rate (panel A) we used rotenone added to pyruvate/malate supplemented mitochondria. For complex III maximum rate (panel D) we used antimycin A plus rotenone, added to succinate supplemented mitochondria. We also used mitochondria supplemented with succinate alone in order to study complex III ROS production under near physiological conditions (panel B). In addition, some of the assays with succinate as substrate were performed in the presence of rotenone (panel C), in order to avoid the backwards flow of electrons to Complex I. Error bars represent SEM. *$P < 0.05$.

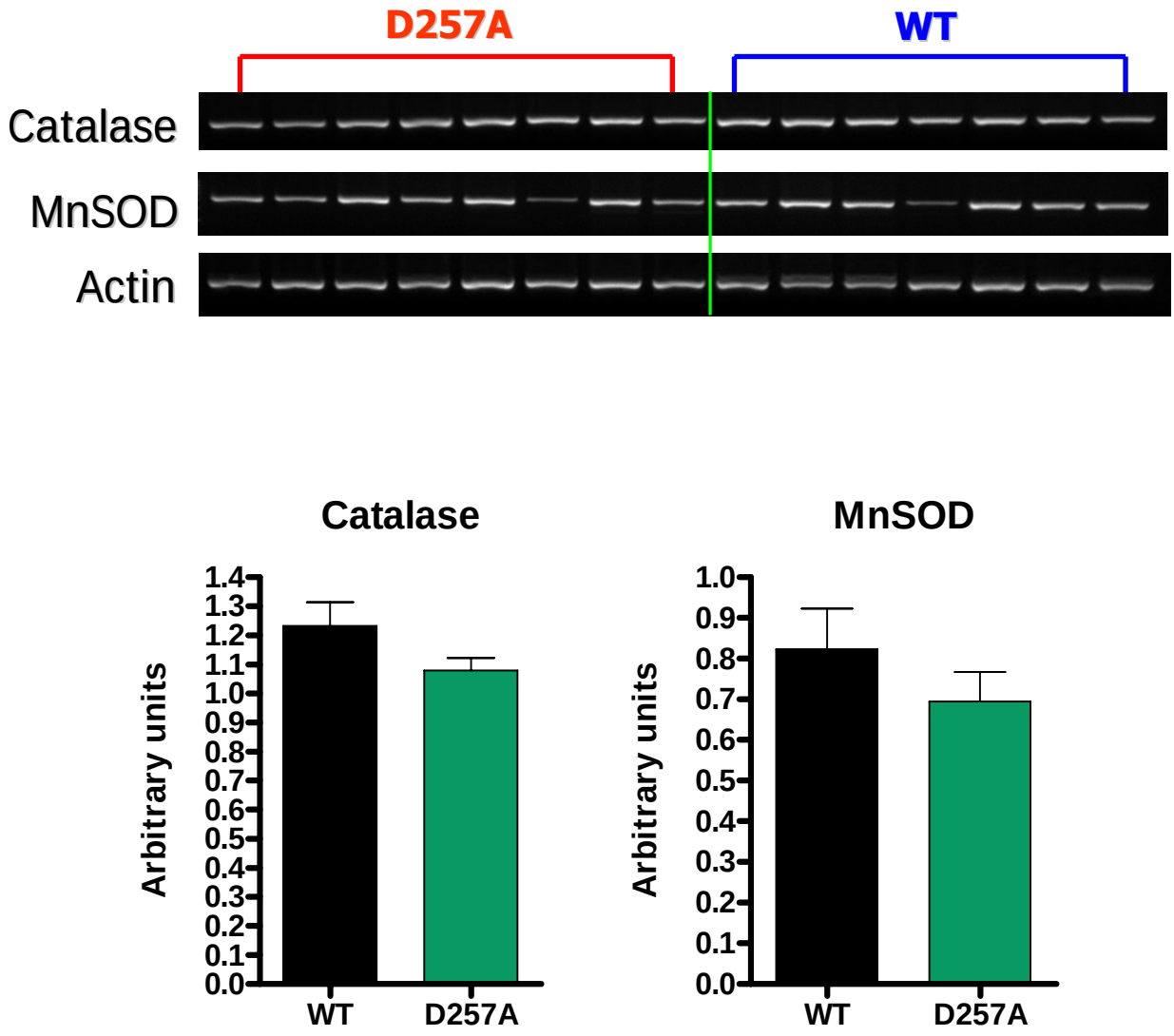

Fig. 4-13. D257A mice show no difference in antioxidant enzyme mRNA expression. We measured Catalase and MnSOD mRNA expression in 11-mo old WT and D257A mice by RT-PCR. Arbitrary units represent specific mRNA densitometry values normalized to actin mRNA densitometry values. Error bars represent SEM.

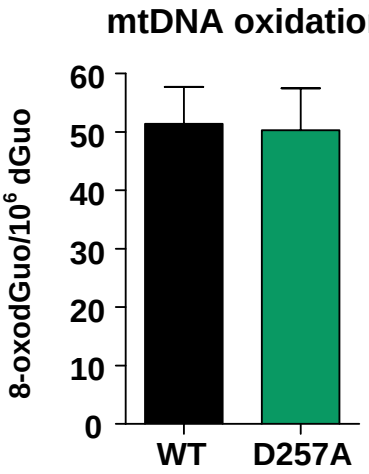

Fig. 4-14. Mitochondrial DNA oxidation in skeletal muscle of WT and D257A mice. We examined a marker of ROS-induced oxidative damage to DNA, by assessing the levels of 8-oxo-7,8-dihydro-2'-deoxyguanosine (8-oxodGuo) in skeletal muscle mtDNA of 11-mo old WT and D257A mice, using HPLC with electrochemical detection. We found no differences between 11-month old WT and D257A mice. Error bars represent SEM.

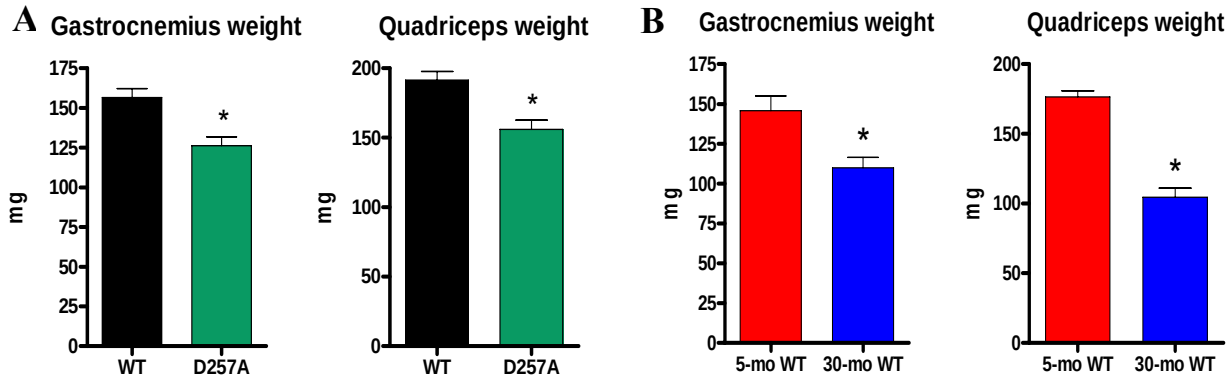

Fig. 4-15. D257A mice display significant skeletal muscle loss by 11-mo of age compared to age-matched WT (panel A) which resembles sarcopenia during normal aging (panel B). Gastrocnemius and quadriceps muscles were extracted immediately following sacrifice, rinsed in saline solution and weighed. Error bars represent SEM. *P < 0.05.

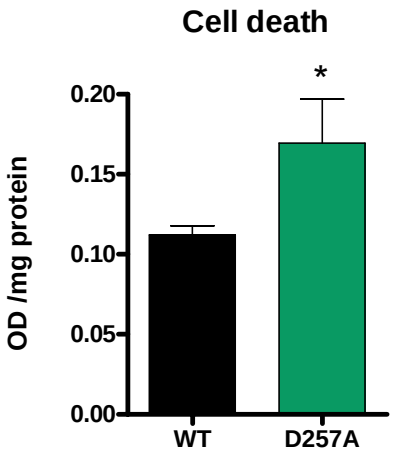

Fig. 4-16. Apoptosis evident in D257A muscle by increase in cytosolic mono- and oligo-nucleosomes. Cytosolic fractions from 11-mo old WT and D257A skeletal muscle were prepared. Apoptosis was quantified as the amount of mono- and oligo-nucleosomes present in the cytosol, using a sandwich ELISA. Error bars represent SEM. *P < 0.05.

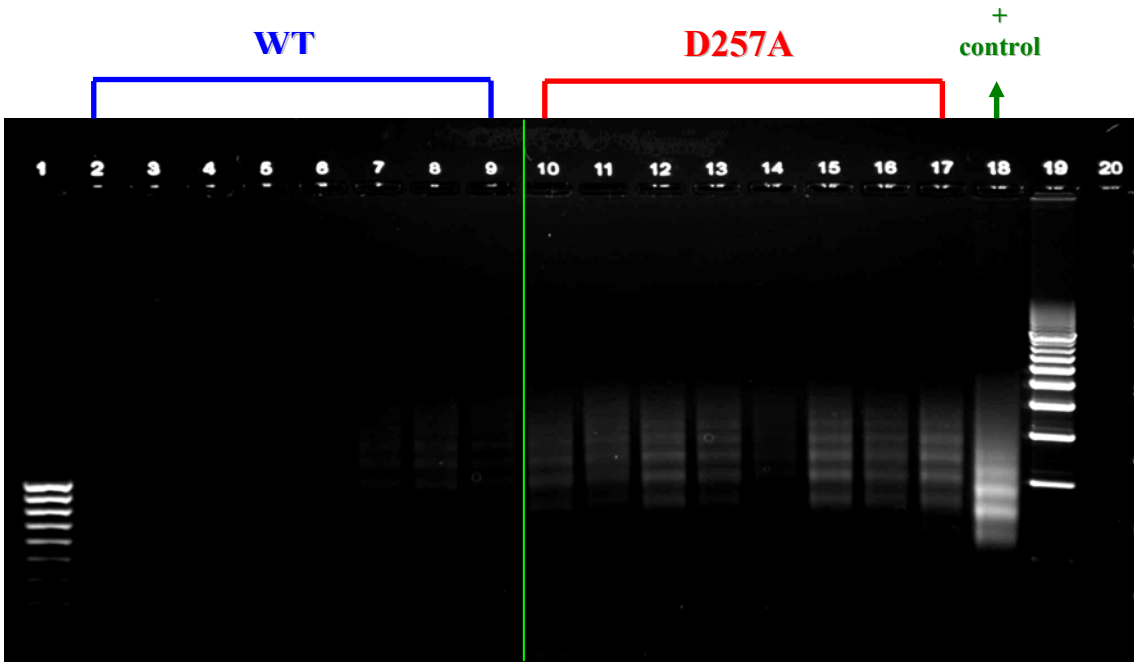

Fig. 4-17. DNA laddering evident in skeletal muscle of D257A mice. DNA from 13-mo old WT and D257A mice was extracted and subjected to a DNA laddering-specific ligation PCR. PCR products were electrophoresed through 1% agarose gels and visualized under UV light for apoptosis-specific DNA ladders of ~180-200bp pr multiples. Lane 1: 100bp molecular marker. Lanes 2-9: WT PCR products. Lanes 10-17: D257A PCR products. Lane 18: Positive control. Lane 19: 500bp molecular marker.

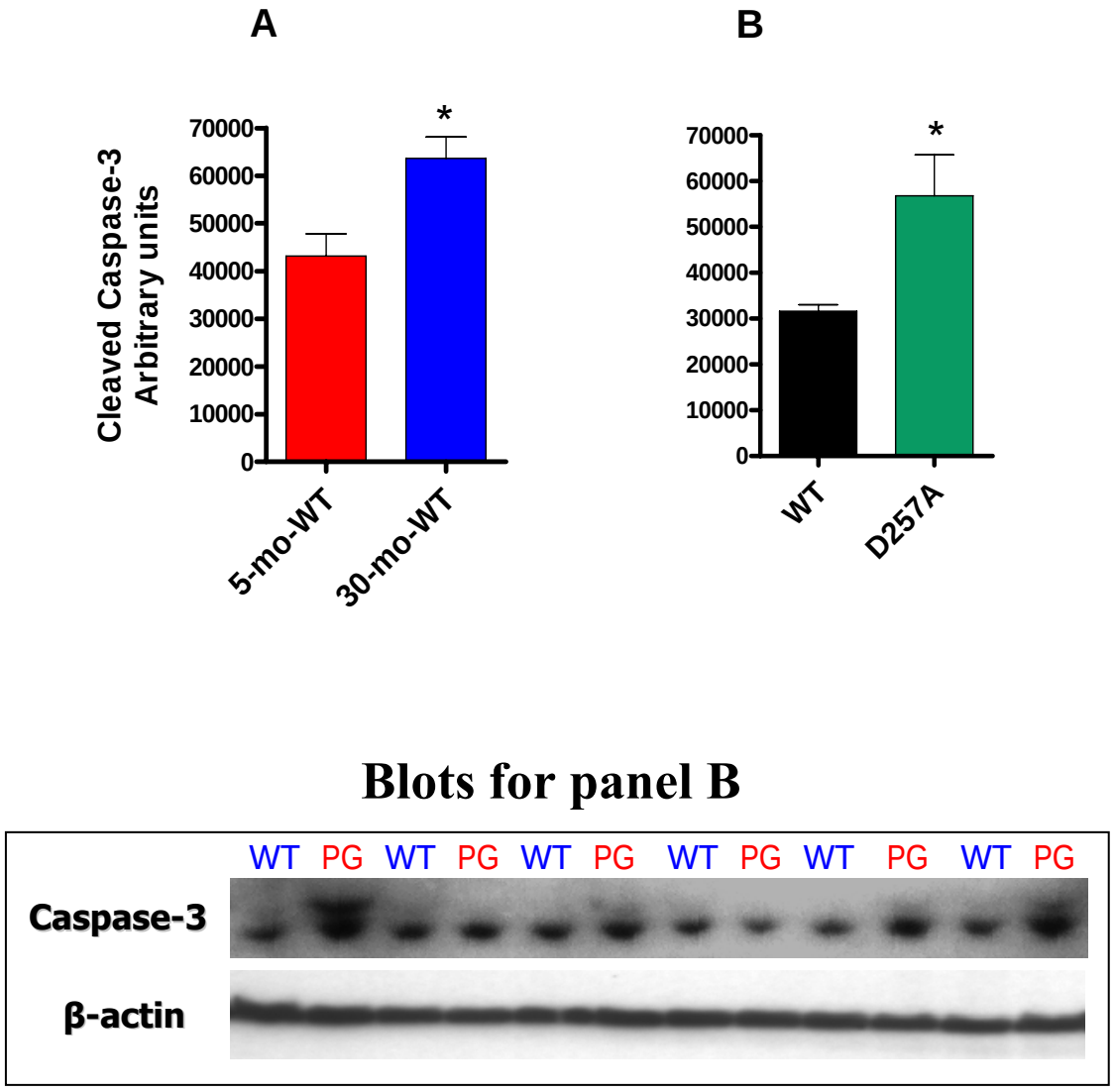

Fig. 4-18. Caspase-3 activation in skeletal muscle of D257A mice resembles caspase-3 activation during normal aging. Panel A: Cleaved (activated) caspase-3 content with normal aging: Comparison of young (5-mo) vs old (30-mo) WT mice. Panel B: Comparison of WT versus D257A cleaved caspase-3 levels at 11-mo of age. Skeletal muscle cytosolic extracts from WT and D257A mice were subjected to SDS-polyacrylamide gel electrophoresis and probed with a rabbit monoclonal antibody against cleaved caspase-3. Representative blots are shown above. Arbitrary units represent caspase-3 densitometry values normalized to β-actin densitometry values. Error bars represent SEM. *P < 0.05.

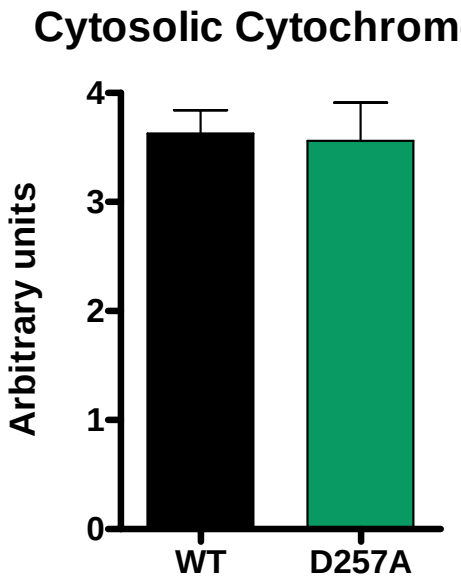

Fig. 4-19. Cytochrome c release in the cytosol of D257A and WT skeletal muscle. Skeletal muscle cytosolic extracts from 13-mo old WT and D257A mice were subjected to SDS-polyacrylamide gel electrophoresis and probed with a mouse monoclonal antibody against cytochrome c. Arbitrary units represent cytochrome c densitometry values normalized to tubulin densitometry values. Error bars represent SEM.

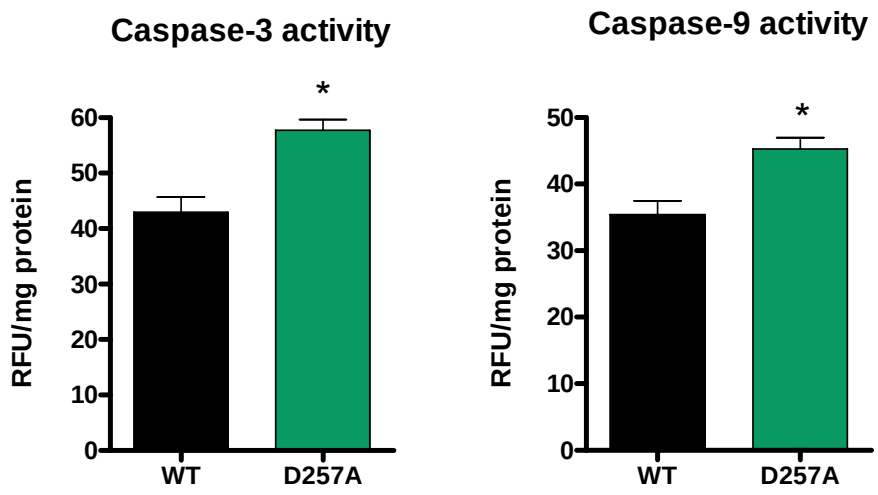

Fig. 4-20. Caspase-3 and -9 activities are elevated in D257A muscle: Proof of activation of the mitochondrial caspase-dependent pathway of apoptosis. Cytosolic fractions from 11-mo old WT and D257A skeletal muscle were prepared. Caspase -3 and -9 activities were measured using a fluorometric protease assay kit which is based on detection of cleavage of the substrate DEVD-AFC or LEHD-AFC by caspase-3 and -9 respectively. Error bars represent SEM. *P < 0.05.

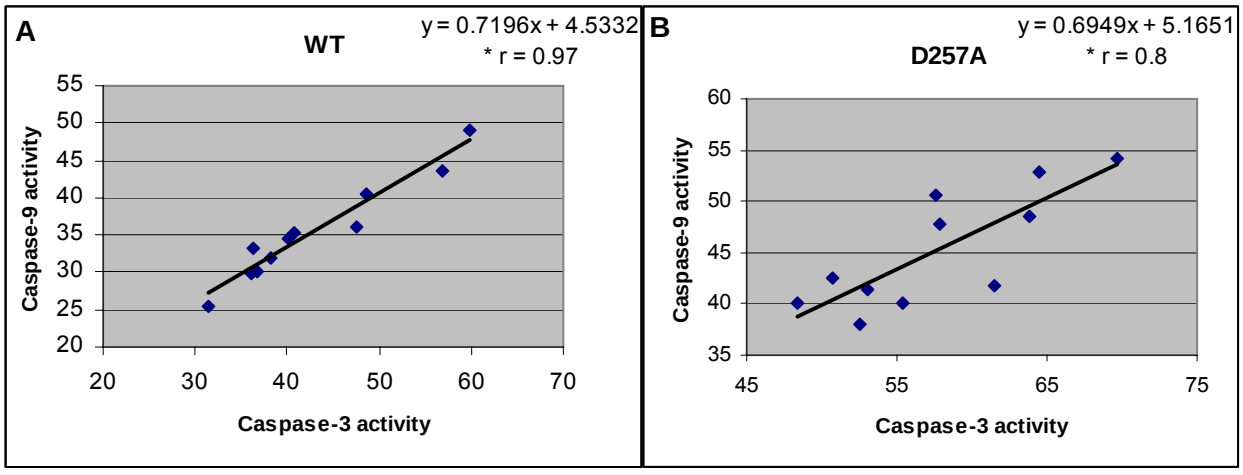

Fig. 4-21. Caspase-3 and caspase-9 activity Pearson correlations in WT and D257A mice: Caspase-3 activity was correlated with caspase-9 activity in WT (panel A) and D257A (panel B) mice. Pearson r values are shown on top right corner. Correlations were significant for both genotypes. *P < 0.05.

CHAPTER 5
DISCUSSION

Overview of Principal Findings

The overall goal of this project was to determine "*in vivo*" whether mtDNA mutations, known to accumulate with aging in skeletal muscle fibers, are causal to the demise of skeletal muscle with age, the condition commonly termed sarcopenia. For this purpose mice having a progeroid syndrome, due to a mutation in the exonuclease domain of POLγ that led to an increase in spontaneous mutation rates in mtDNA, were utilized. The experiments conducted examined the impact of increased mtDNA mutational load on both mitochondrial function and mitochondrial-induced apoptosis in skeletal muscle via three separate groups of experiments.

Specific aim 1 tested the following questions: (a) Do mtDNA mutations lead to mitochondrial dysfunction? (b) If mitochondrial dysfunction is evident is it associated with an increase in mitochondrial ROS production? (c) If mitochondrial ROS generation is elevated does it lead to further oxidative damage in mtDNA? (d) What is the primary mechanism by which mtDNA mutations induce mitochondrial dysfunction? Our results reveal that mtDNA mutations induce mitochondrial dysfunction, apparent by compromised mitochondrial respiration during state 3, decreased ATP content, and a significant drop in membrane potential during both state 3 and state 4. Importantly, this compromised mitochondrial function is not accompanied by elevations in ROS production or further oxidative damage to mtDNA, which is in contrast to the main premise of the "Vicious Cycle" theory of aging. In fact, it appears that in skeletal muscle, the accumulation of mtDNA mutations is associated with a significant decrease in mitochondrial ROS production which was coupled to the decrease in state 3 respiration. Moreover, the primary cause of the mitochondrial dysfunction appears to be the abrogation of ETC complexes I, III and IV, all of which contain mtDNA-encoded subunits. In addition, energy deficits due to the latter

are likely responsible for the drop in $\Delta\psi$ we observed which in turn is likely responsible for the induction of apoptosis intrinsic to the mitochondria.

Specific aim 2 tested the following questions: (a) Is apoptosis the mechanism responsible for skeletal muscle loss in D257A mice? (b) If apoptosis is evident, is it caspase-dependent? Our data indeed confirms that apoptosis is induced in skeletal muscle of D257A mice. Apoptosis was evident by DNA laddering and increased release of mono-and oligo-nucleosomes in the cytosol. Furthermore, apoptosis was caspase-dependent since significant increases in both the content and activity of the final effector caspase, caspase-3, were observed.

Specific aim 3 tested the question: Is apoptosis mitochondrial-mediated? Although we were not able to show differences in cytochrome c release in the cytosol between genotypes, we detected a significant up-regulation of caspase-9 activity with further downstream activation of caspase-3 (as the caspase-3-,caspase-9 correlations suggest on Fig 4-21), in D257A skeletal muscle. This proves that the main, caspase-dependent mitochondrial pathway is activated in D257A mice and is at least, partly responsible for the sarcopenia observed in these mice.

Hypothesis One: The Effect of mtDNA Mutations in Skeletal Muscle Mitochondrial Function

The goal of this aim was to determine that mtDNA mutations are directly responsible for a measurable deficiency in cellular oxidative phosphorylation activity and if this was proven to be true, to identify the series of events that lead to mitochondrial dysfunction. Therefore, an important aspect of this aim was to test the mitochondrial "Vicious Cycle" theory of aging, or in other words to examine whether mtDNA mutations indeed lead to an enhanced ROS production, which in turn gives rise to the rate of mtDNA damage and mutagenesis, thus causing a 'Vicious Cycle' of exponentially increasing oxidative damage and dysfunction, which ultimately culminates in death.

Mitochondrial DNA Mutations Cause Profound Deficiencies in Mitochondrial Function

Information on the specific contribution of mtDNA instability to human aging phenotypes can be inferred through the analysis of disorders associated with increased mtDNA mutation or deletion frequency. For example, in mitochondrial diseases, it is well demonstrated that mtDNA deletions, when present at concentrations of 30% and greater in muscle tissue, can cause three disorders, Kearns-Sayre syndrome (KSS), chronic progressive external opthalmoplegia (CPEO), and Pearson's syndrome (PS) (20, 151, 152). The affected tissues show impaired electron transport activity, ATP production, and mitochondrial protein synthesis and decreased mitochondrial membrane potential (153-156). Furthermore, muscle biopsies from patients with KSS or CPEO show ragged red fibers and cytochrome oxidase (COX) -negative fibers (157, 158). Tissues most affected by disorders associated with inherited mtDNA mutations are the same tissues markedly affected by normal aging; these include the brain, heart, skeletal muscle, kidney and the endocrine system (159). Because the most obvious consequence of mtDNA mutations is an impairment of energy metabolism, most studies addressing aging effects have focused on tissues that are post mitotic and display high energetic demands, such as the heart, skeletal muscle, and the brain. Indeed, several studies have unambiguously demonstrated that mtDNA base substitution mutations accumulate as a result of aging in a variety of tissues and species, including rodents, rhesus monkeys, and humans.

An ongoing debate in the field relates to the issue of causality: are mtDNA mutations merely markers of biological age, or do they lead to a decline in physiological function that contributes to the aging process? Studies on sarcopenia in rodents and human samples have helped to address this issue. Studies using laser capture microdissection to study the role of mtDNA deletion mutations in single skeletal muscle fibers from sarcopenic rats have shown that mtDNA deletions colocalize with electron transport chain dysfunction and fiber atrophy (7).

Interestingly, the mutations are largely clonal and absent from phenotypically normal regions within individual muscle fibers (43). In a similar study of aged (69–82 years old) human muscle biopsies, an association between a deficiency in the mitochondrially encoded cytochrome c oxidase (COX) and clonally expanded base-substitution mutations and deletions in mtDNA was shown (49).

Perhaps the strongest evidence that clonally expanded mtDNA mutations can be causal in both age-related dysfunction and disease comes from recent studies of neurons present in the substantia nigra region of the human brain. These dopamine-rich, pigmented neurons contain very high levels of mtDNA deletions. Deleted mtDNA molecules are clonal in each neuron, can accumulate, reaching up to 60% of the total mtDNA and are associated with oxidative phosphorylation defects (160). Cytochrome c oxidase–deficient cells have also been shown to increase with age in both hippocampal pyramidal neurons and choroid plexus epithelial cells (161). Although these studies do not prove causality, they provide strong evidence in support of the hypothesis that mtDNA deletions play a contributing role in age-related mitochondrial dysfunction leading to aging phenotypes in post-mitotic tissues of mammals.

In order to test the in vivo effects of increased somatic mtDNA mutation accumulation, Larsson's group was the first to report results on the D257A knock-in mice (the same mice used in this project) showing that mtDNA mutations and deletions are responsible for a progressive decline in respiratory function of mitochondrially encoded complexes, that was evident as early as 12 weeks, resulting in decreased oxygen consumption and ATP production (14, 79). In accordance with the aforementioned studies in this section, we also found profound decreases in mitochondrial O_2 consumption during state 3, the active state of the mitochondria when ATP is

produced (Fig 4-2). Moreover, ATP content was significantly lower in D257A mice, compared to WT (Fig 4-8).

These findings clearly indicate that oxidative phosphorylation is compromised in skeletal muscle of mutant mice and provide a causal role of mtDNA mutations specifically in skeletal muscle mitochondrial dysfunction. In addition, since mitochondrial ETC enzyme activity declines, decreases in ATP synthesis and state 3 respiration, and energy depletion are all well documented in normal aging in various species and tissues, including human skeletal muscle (39, 40, 162-165) (see also more extensive background info on mitochondrial function with aging in chapter 2), it can be deduced that mtDNA mutations may contribute to the sarcopenic phenotype not only in D257A mice but also during normal aging.

Furthermore, D257A skeletal muscle mitochondria were uncoupled since respiratory control ratios (state 3/state 4 O_2 consumption) in our experiments were less than 3.5 (Fig 4-2). These defects in oxidative phosphorylation we have observed are likely the cause for the disruption of mitochondrial membrane potential we have also detected in mitochondria from mutant mice (Fig 4-9). In support of the latter, it has been shown that in mitochondrial diseases, the accumulation of mtDNA deletions causes deficits in basic bioenergetic parameters including mitochondrial membrane potential (156, 166, 167). For example, in Leber's hereditary optic neuropathy (LHON), a late onset neurological disorder associated with specific mtDNA point mutations, Battisti et al., showed that lymphocytes from patients with LHON treated with the oxidizing agent dRib had significant depolarization of the mitochondrial membrane potential compared to control cells and an increase in the percentage of apoptotic cells with respect to controls (166). The authors concluded that their results confirmed the notion of a direct link between complex I (commonly altered in patients with LHON) and changes in mitochondrial

membrane permeability. Furthermore, in cybrid cells incorporating two pathogenic mitochondrial DNA point mutations, 3243A > G and 3302A > G in tRNALeu(UUR), it was shown that the lowered mitochondrial membrane potentials exhibited by the cells led to a disturbed intramitochondrial calcium homeostasis, which was postulated to be a major pathomechanism in mitochondrial diseases, according to the authors (167). Lower mitochondrial $\Delta\psi$s have also been observed in normally aged mitochondria of rodents and in skin fibroblasts from elderly human subjects (34, 168-171), and low $\Delta\psi$s were found to correlate with reduced ATP synthesis. As the levels of mtDNA mutations have also been shown to increase with age in both humans and rodents (as has been extensively discussed in chapter 2), these observations provide further support to the notion that mtDNA mutations are important culprits for tissue dysfunction with age.

Mitochondrial DNA Mutations Cause Mitochondrial Dysfunction in the Absence of Increased ROS Production or Oxidative Damage to mtDNA: Implications for the Mitochondrial "Vicious Cycle" Theory of Aging

It has been thought that loss of mitochondrial function and increased mitochondrial ROS production are important causal factors in aging. Every human cell contains hundreds of mitochondria, and each mitochondrion has multiple copies of mitochondrial DNA (mtDNA). Because the mitochondrial genome codes for 13 polypeptides constituting the respiratory enzyme complexes required for normal functioning of the oxidative phosphorylation system, somatic mutations in mtDNA may be directly involved in the mechanism by which ROS initiate a vicious cycle and cause aging. The previously mentioned vicious cycle theory of oxidative damage to mtDNA (172) holds that oxidative damage, or resultant mutation, of the mtDNA causes the assembly of a defective respiratory chain, which in turn causes the production of more

ROS, and the cycle repeats, with ever increasing dysfunctions of the respiratory chain. Eventually the cell dies (172).

Studies from aging humans and animals have shown good correlations between aging and increased mitochondrial production of ROS and between mitochondrial function decline and accumulation of mtDNA mutations (173). Certainly, oxidative stress could be playing a role in the generation of mtDNA mutations in wild-type animals. The rate of mitochondrial ROS production, extent of mtDNA (but not nuclear DNA), oxidative damage, and degree of membrane fatty acid unsaturation (a determinant of vulnerability to lipid peroxidation) are all inversely correlated with longevity across species (174-177). Mice expressing mitochondrion-targeted catalase show reduced total DNA oxidative damage in skeletal muscle, fewer mtDNA deletions, and extended mean and maximal lifespan (178), suggesting that mitochondrial accumulation of oxidative damage can limit rodent lifespan.

The increased production of ROS as a consequence of a mtDNA mutation has been demonstrated in some occasions, as discussed below. The presence of a specific mutation in ATPase 6, a subunit of the F0 portion of the ATP synthase, caused massive apoptosis in cultured fibroblasts when glucose in the culture medium was replaced with galactose (179). Because both the mitochondrial and cytosolic SOD activities were shown to be elevated, it was inferred that superoxide production was increased, and it was proposed that it was the superoxide, rather than the defect in oxidative phosphorylation, that directly caused the apoptosis. This hypothesis was supported from an experiment in which a spin trap molecule, added to the medium, was able to prevent apoptosis. The explanation for why this particular point mutation in mtDNA would cause superoxide production is rather straightforward. The specific mutation inhibits the activity of the ATP synthase (180), and, in coupled mitochondria, this inhibition would arrest respiration,

putting the mitochondria in ‘‘state 4.’’ In this state, the electron carriers of the respiratory chain are fully reduced, and superoxide production is maximal compared to almost negligible superoxide formation in actively respiring (state 3) mitochondria (181, 182). Moreover, cells in culture that have defects in complex I (the respiratory NADH dehydrogenase) produce higher amounts of superoxide (183).

It should be noted that measurements of the level of one particular ROS may not provide the complete picture of the relevant changes in the cell. For example, the amount of superoxide at a given time is the net result of a balance between its formation and its degradation by superoxide dismutase. In the study mentioned above (183) the more serious diseases resulting from complex I deficiency were found to be associated with normal levels of superoxide and greatly increased SOD activities, suggesting that the greater the superoxide production, the greater the SOD activity. The data of Geromel et al. (179), mentioned previously, is also consistent with the idea that SOD increases to compensate for increased superoxide production. In our study, we measured the amount of H_2O_2 released by intact mitochondria in a surrounding medium during state 4, as an index of total basal mitochondrial ROS production. By the addition of SOD in the medium, we ensured that any superoxide remaining would be converted to H_2O_2. Furthermore, H_2O_2 production in intact mitochondria is thought to be closer to a more physiologic situation, while superoxide production is usually assayed in sub-mitochondrial particles, since its half life is very short and it readily gets dismutated to H_2O_2 by SOD before it exits the mitochondria (141). In contrast to the above studies, we and others have clearly demonstrated that mitochondrial mutator mice do not have increased levels of oxidative stress (13, 79, 80).

In this study we provide further support against the vicious cycle theory, showing that specifically in skeletal muscle, mitochondrial ROS production is not only unchanged (as we showed in the past for other tissues) but significantly decreased in mutant mice compared to WT (Fig 4-11). These results suggest that ROS production is regulated in a tissue specific way and does not necessarily play a role in the increased sensitivity to apoptosis. More importantly, since we also found no up-regulation in either MnSOD or Catalase mRNA levels (Fig 4-13), we can conclude that in contrast to previous studies mentioned above (179, 183), ROS levels are decreased in mutant mice due to a lower ROS production and not due to a reactive up-regulation in antioxidant defenses.

Respiratory enzyme complex I and the protonmotive Q cycle operating in complex III are the major sites that generate ROS within the ETC (184). In order to evaluate whether D257A mice produce different amounts of ROS compared to WT at these main generators, we used specific complex inhibitors: rotenone in pyruvate/malate supplemented mitochondria, and rotenone plus antimycin in succinate supplemented mitochondria, in order to assess maximal ROS formation at complex I (Fig 4-12, panel A) and complex III (Fig 4-12, panel D) respectively. Besides basal and maximal ROS production we also assessed the production from complex III under normal conditions using succinate-supplemented mitochondria (Fig 4-12, panels B and C). In every instance, we detected a decrease in the amount of ROS produced by mutant mitochondria at complex I or complex III under physiological conditions, or when ETC inhibitors were used for maximal ROS production at either complex. This reinforces the hypothesis that mtDNA mutations are likely to induce mitochondrial dysfunction leading to apoptosis in the absence of increased ROS, and that oxidative stress is not an obligate mediator of aging phenotypes provoked by mitochondrial DNA mutations.

Furthermore, the ROS data fit very well with the lowered mitochondrial Δψ data in D257A mice, since increased ROS generation has been reported to occur at high mitochondrial Δψs while the opposite is also true (181, 185). For example, in 1973 Boveris and Chance have shown that the protonophorous uncoupler of oxidative phosphorylation (CCCP) or ADP+Pi inhibit H_2O_2 formation by mitochondria (185). Moreover, Skulachev and colleagues have shown that the inhibition of H_2O_2 formation by the uncoupler malonate and ADP+Pi was proportional to the Δψ decrease by these compounds (181), and proposed that that a high proton motive force in state 4 is potentially dangerous for the cell due to an increase in the probability of superoxide formation (186). This is likely because at high Δψs electron flow is not efficient and the chance that electrons flow out of sequence - thus leaking to form superoxide instead of reducing O_2 to H_2O at the terminal cytochrome oxidase (complex IV) - increases. Another hypothesis is that activation of ROS production in state 4, when protonic potential is high and respiration rate is limited by lack of ADP, is due to the fact that some transients of the respiratory chain electron transport, capable of reducing O_2 to superoxide, such as $CoQH^{\bullet}$, become long-lived (181).

In agreement with the ROS data, we also found that mtDNA oxidative damage, measured by 8-oxodG was not different between genotypes. This is the second time our group shows no differences in oxidative damage in D257A mice. In 2005, we demonstrated that the amount of 8-oxodG lesions in total liver DNA was not different compared to WT and 8-oxoG was actually lower in liver RNA of mutant mice (13). In addition, mitochondrial protein carbonyl levels and F2-isoprostanes were also unchanged compared to WT (13). The oxidative stress findings in mitochondrial mutator mice were also confirmed by Larsson's group that showed no differences in protein oxidation and no up-regulation of antioxidant enzymes in the heart and liver (79). Furthermore, Zassenhaus and colleagues using mice with a heart-specific POLG mutation have

demonstrated no elevations in protein carbonyls, no differences in mtDNA 8-oxodG levels, no up-regulation of antioxidant defense systems, normal ubiquitination levels and intact (not oxidatively damaged) iron-sulfur centers in aconitase enzyme (80). The fact that we did not detect an actual decrease in mtDNA 8-oxodG levels, like we did in H_2O_2 production in the present study, may indicate that it is not only the ROS produced by the mitochondria that damage mtDNA.

Taken all together, we do not postulate that chronic accumulation of ROS production and oxidative stress are not important factors contributing to mtDNA damage and mutagenesis, leading to aging and age-related phenotypes, such as sarcopenia. However, using the D257A model, we do support the idea that, the mutagenesis partly due to chronic ROS insults to mtDNA, does not lead to further increases in ROS production and oxidative stress and may not be an important mediator of apoptosis. Hence, based on our results, we contradict and question an important part of the mitochondrial vicious cycle theory (Fig 2-2) and we propose instead that respiratory chain dysfunction *per se* is the primary inducer of the sarcopenic phenotype in mtDNA mutator mice.

Studies on different transgenic mice further support the idea that increased mitochondrial oxidative damage is not sufficient for accelerated aging. Mice with reduced levels of the mitochondrial MnSOD enzyme ($Sod2^{+/-}$) do not appear to age any faster than their wild-type counterparts, despite harboring increased levels of oxidative damage to both nuclear and mtDNA (187). Similarly, mice deficient for 8-oxoguanine DNA glycosylase (that repairs the vast majority of 8-oxoguanine lesions) or 8-oxoGTPase (that prevents oxidized dGTP from being incorporated into DNA) do not exhibit accelerated aging features (188-190). On the other hand, mouse models such as the $Ant1^{-/-}$ mice exhibit elevated levels of ROS production (191) and

mitochondria treated with specific chemical electron transport chain (ETC) inhibitors can indeed produce increased ROS levels (192). However, it should be noted that, inhibition of ETC function in Ant1$^{-/-}$ mice or by chemical inhibitors may generate ROS because all mitochondria show the same defect (e.g., lack of available ADP or blockage of electron flow at a specific point in the ETC) (193). Upstream complexes can still function, resulting in electron stalling and transfer to O_2 to generate superoxide. By contrast, in the D257A mice, a variety of mutations is present and multiple upstream complexes could be nonfunctional or be lacking subunits if mitochondrial rRNA or tRNA mutations are numerous. Thus, electron flow through all the complexes (except nucleus encoded complex II) may be impaired and reduced intermediates may not be accumulating. In the case where mtDNA mutation levels are much lower, the presence of many wild-type copies of mtDNA will mask the effects of specific respiratory mutations (193).

It is also important not to forget the observations of Bandy and Davison, the first investigators to put forward a mechanistic elaboration of what later became known as the mitochondrial 'vicious cycle' theory: while they showed that some mtDNA mutations may have the same effect on the respiratory chain as small-molecule inhibitors of respiration, that is, to stimulate ROS production, they also carefully noted that not all mutations stimulate superoxide production (72). Specifically, they pointed out that mutations preventing the synthesis of cytochrome b would actually abolish any superoxide production at complex III that normal mitochondria might exhibit, because without cytochrome b in place, complex III cannot be assembled (72). Later studies also reported that cells possessing large deletions, which eliminated the genes for at least a couple of respiratory chain subunits, but also removed at least one tRNA gene, would indisputably preclude assembly of both the enzyme complexes known to be responsible for mitochondrial ROS production, complexes I and III (73-76).

Mitochondrial DNA Mutations Lead to Mitochondrial Dysfunction, Via Alterations of ETC Complex Composition

One of the main goals of this specific aim was to characterize the D257A mice in terms of skeletal muscle mitochondrial function and ROS production, and if dysfunction was evident to try to identify how this dysfunction is induced. Since the mtDNA encodes a total of 13 polypeptides all-subunits of the complexes of the ETC, our hypothesis was that accumulation of mutations will have a direct impact on transcription and translation of these genes leading to miscoded, truncated and dysfunctional proteins, which in turn could preclude assembly of functional complexes within the inner mitochondrial membrane. We therefore, went on to assess the content and activity of the five ETC protein complexes. In order to determine whether complete complex content corresponds with protein expression levels of individual subunits, we further analyzed selected mitochondrial- or nuclear-encoded subunits from each complex.

Certainly, one can argue that mitochondrial dysfunction observed during normal aging is not only due to mutations in mitochondrial genes leading to ETC complex misassembly. For example, in WT old mice a compromised state 3 respiration, such as the one we observed in D257A mice, could be due to several different factors. To name a few: (a) decrease in the content and/or activity of respiratory complexes (due to the disruption in subunits encoded by mitochondrial DNA) leading to impaired electron flux, (b) disruption of ADP phosphorylation due to the decline in the activity of ATP Synthase (194), (c) impairment in the transport of ADP in the mitochondria due to alterations in Adenine Nucleotide Translocase (ANT) due to carbonylation or nitration (195), or (d) alterations in enzymes involved in TCA cycle or fatty acid oxidation. In our mtDNA mutator mice a suboptimal concentration and/or activity of respiratory complexes may be the primary cause of the observed mitochondrial dysfunction, and (b), (c), (d) could be consequences of (a) rather than the cause.

Of course in D257A mitochondria it is almost certain that from the ~1,500 nuclear-encoded proteins that exist in the mitochondria at any given time, translation, interaction and/or activity of many of these proteins are likely to be impacted by the high load of mtDNA mutations. In this project we only focused on proteins that comprise the five ETC complexes since we believe ETC complex dysfunction is directly and primarily affected by the high load of mtDNA mutations. Furthermore, we are aware that aging and sarcopenia are complex processes, that likely result from deregulation and interaction of multiple pathways. However, here, we only tested one of these hypotheses, the role of mtNA mutations in sarcopenia which also appears to be very relevant, specifically for skeletal muscle, since multiple papers show strong correlations between the rate of somatic mtDNA mutations and skeletal muscle dysfunction.

Decreases in the content and/or activity of ETC complexes with age, and as a result of accumulated mtDNA mutations, especially in skeletal muscle are well-documented in the literature. Aiken's group has repeatedly demonstrated loss of COX (complex VI) staining combined with hyperactive SDH staining in aged rat skeletal muscle cross-sections (also known as ragged red fibers) (7, 87, 102, 196). Interestingly, these abnormalities co-localized with clonal intracellular expansions of unique somatically derived mtDNA deletion mutations. In the areas of the fiber where the mutation abundance surpassed 90% of the total mitochondrial genomes, the fibers lost COX activity and displayed abnormal morphology such as fiber splitting and breakage, while normal areas of the same fiber contained only wild type mitochondrial genomes and did not exhibit de-regulation of ETC complex activities (7, 196). Decreased activities of complex I, III and IV with age were also reported in gastrocnemius muscle of mice, while the nuclear-encoded complex II did not show significant changes with age (28). In the same study the authors conducted a kinetic analysis for complex III and IV and indicated that V_{max} for both

complexes decreased with age, which suggested a decrease in the total enzyme content (28). Similarly, muscle biopsies from aged humans revealed that randomly deleted mtDNA appeared mainly in the oldest subjects (beyond 80 years old), affecting up to 70% of mtDNA molecules with the activities of partly mitochondrial-encoded complexes III and IV being lower in the aged subjects (48) (see also chapter 2 for more extensive review on mtDNA mutations and ETC abnormalities with age).

Our findings are in agreement with some of the findings mentioned above. We detected a significant decrease in the content of complex I, III and IV, all of which contain subunits encoded by mtDNA while the content of all nuclear-encoded complexes II and F1 domain of ATPase showed no difference between genotypes (Figs 4-3, 4-4). This confirms our hypothesis that indeed accumulation of mtDNA mutations directly impacts the assembly of ETC complexes that are comprised of mtDNA encoded subunits and suggests that complex formation in D257A mice is abolished. Interestingly, we did not detect significant differences between genotypes in any of the complex activities (Fig 4-6), when each complex activity was normalized to the respective complex content assessed by BN-page. Since per amount of mitochondrial protein loaded on the BN-page we detected a lower ETC content in D257A mice but no differences in activity, this suggests that although a significant amount of ETC complexes is lost the activity of the remaining complexes in D257A muscle is for the most part normal. Based on these results, it is reasonable to propose that per single D257A mitochondrion the amount to electron transport chains assembled is probably significantly lower compared to a WT mitochondrion. Thus, even if the activity of the remaining ETCs in mutant mitochondria are normal, the lower amount of complexes still creates energy deficits in the mitochondria, leading to an overall decrease in ETC activity in mitochondria and thus, in mutant skeletal muscle cells. It is also important to note that

even if maximum activity of isolated complexes is normal that does not exclude the possibility that some of these complexes do not assemble into fully functional electrons transport chains, especially in the case of mutant mitochondria.

Furthermore, a point that requires special attention regarding measurements of ETC complex enzymatic activities is how the complex activities are expressed. In most cases complex enzymatic activities are normalized just to total protein content used (usually expressed as nmol/min/mg of protein) (162), or expressed as a ratio to nuclear-encoded citrate synthase activity (48). In our case, we normalized the activity densitometry values to the respective content densitometry values (content value was first normalized to total protein content loaded per well). In this way we evaluated complex activity per unit of ETC complex content which gives a more precise picture of what may be occurring. In most other cases the overall activity per amount of mitochondrial protein is evaluated which may not always reflect decreases in the actual activity of the individual complexes, but in many cases, decreases in the complex content. In line with our assumptions, very recently Dubessay et al, reported significant decreases in the activities of complex I, III and IV with age, expressed in nmol/min/mg, in *drosophila melanogaster* (162). However, the authors clearly stated that these activity decreases may have various causes, such as reduced concentrations of respiratory complexes in the inner mitochondrial membrane or partial inactivation of the biological functions of the constituent subunits of these complexes (162).

Moreover, we observed a significant down-regulation of protein expression in the D257A muscle, for almost all of the ETC protein subunits evaluated either nuclear- or mitochondrial-encoded (Fig 4-7). The reduced expression of mitochondrial-encoded subunits fits well with our total complex content data: if expression of mtDNA-encoded subunits is abolished due to the

accumulation of mtDNA mutations that may impact their transcription or translation, it would be expected that assembly of whole functional complexes may also be abolished, as we have observed (see Figs 4-3, 4-4).

The reduction in the expression of nuclear-encoded subunits may be explained by the fact that a reactive adaptation of the nucleus is occurring: if less ETC complexes are assembled due to the miscoding of mtDNA-encoded subunits, expression of nuclear-encoded subunits would also have to be reduced since there would be no need for the expression of extra subunits if more fully functional electron transport chains are not created. However, the fact that, there is no down-regulation in the content of all-nuclear encoded ETC complex II and F1 in mutant mice (see Figs 4-3, 4-4), cannot be fully explained by these results and needs to be further substantiated. It is possible that although there is a down-regulation of nuclear-encoded subunits still these subunits more often combine to assemble functional complexes since it is less likely that nuclear-encoded subunits would be truncated or have altered active sites, leading to loss of activity and misassembly of a complex, etc., as it would be the case for mtDNA-encoded subunits. However, this does not mean that functional nuclear-encoded complexes are necessarily inserted in the inner membrane to assemble functional ETCs. In agreement with our hypothesis of a reactive adaptation of the nucleus to the defects induced by mtDNA mutations, Alemi et al. recently demonstrated that pathogenic mtDNA deletions in cells derived from KSS and CPEO patients had a strong negative effect on nuclear-encoded mitochondrially targeted genes (156). This was especially evident on Complex I transcripts, but also on Complex II and Complex IV assembly genes, on Complex V, on several TCA cycle genes, and on components of the mitochondrial ribosome (156). Based on their results, these authors also suggested that the nucleus senses the irreversible depletion of mtDNA-encoded mitochondrial subunits and tRNAs,

and responds by down-regulating the interacting subunits that would normally form a functional complex (156). They proposed that, the down-regulation of nuclear-encoded mitochondrial ribosomal subunits, oxidative phosphorylation, and TCA cycle transcripts, possibly reinforces the mitochondrial defect initiated by the deletions, and adds to the mitochondrial metabolic defect in these patients (156).

Total Skeletal Muscle Mitochondrial Protein Yield Continuously Decreases as Time Progresses in Mutant Mice

Several studies in the past, performed in skeletal muscle of rodents have reported decreases in mitochondrial protein yield with aging (197, 198). To evaluate the overall oxidative capacity of skeletal muscle of adult (6-mo) and elderly (24-mo) Fischer 344 rats, Hoppel and colleagues determined the mitochondrial content. They measured the activity of two exclusively mitochondrial enzymes, citrate synthase (CS) and succinate dehydrogenase (SDH), and they used these data to calculate the mitochondrial content (198). They found that the activity of both mitochondrial marker enzymes was significantly lower in skeletal muscle homogenates of 24-mo-old compared with 6-mo-old adult animals (198). The average decrease for both CS and SDH activities was 31%. In contrast to CS and SDH, no age-associated decrease was found in lactate dehydrogenase activity, a cytosolic marker enzyme. The calculated mitochondrial content was significantly lower in skeletal muscle of elderly rats with both mitochondrial marker enzymes (25 and 20% based on CS and SDH, respectively). They concluded that aged skeletal muscle has a significantly lower content of mitochondria in Fischer 344 rats. Moreover, the yield of mitochondrial protein per gram wet weight of skeletal muscle was also less in elderly compared with the adult animals, consistent with the lower mitochondrial content. Lower skeletal muscle mitochondrial yield from elderly rats also has been reported by Beyer et al.

These authors reported a 35% decrease in mitochondrial protein yield from quadriceps femoris of elderly Sprague-Dawley rats (197).

Consistent with the above findings we also found that in our accelerated-aging mice the total mitochondrial protein yield, expressed as mg of mitochondrial protein per gram wet weight of skeletal muscle, was significantly decreased compared to WT animals (Fig 4-10). By 11-mo of age we detected a 35% reduction (Fig 4-10) which agrees with previous data in normally aged skeletal muscle (197). Interestingly, at ~13 months we saw a drastic, 46% reduction in the protein yield (Fig 4-10) suggesting that mitochondrial content is continuously reduced in these animals as they are approaching their mean lifespan which is ~14 months. Although our data in this area is limited to the only measurement of mitochondrial protein yield, it is tempting to suggest that mitochondria in D257A mice are probably getting continuously eliminated. This would make sense especially in the case where the accumulation of mtDNA mutations reach a reported critical threshold (42, 51, 193, 196) before significant tissue dysfunction is observed. And in the case of the post-mitotic skeletal muscle this threshold appears to be much later in the D257A animal's lifespan compared to that of other tissues. For example, at 3-mo of age, the aging phenotype for skeletal muscle is not evident in D257A mice, while in the case of rapidly dividing cells in duodenum, thymus, and testes, we detected significant tissue dysfunction at the same time point (13). Once the critical threshold of mtDNA mutations is reached, mitochondrial dysfunction may ensue possibly leading to mitochondrial-mediated apoptosis and the elimination of dysfunctional mitochondria. As the accumulation of mtDNA mutations was shown to be exponential over time in several post mitotic tissues, with the most well-documented being skeletal muscle (51, 73, 193, 199, 200), we also see that the mitochondrial protein yield in D257A skeletal muscle further decreases over time.

In line with the above, our BN-page results, showing that mitochondrial complex content is decreased and suggesting that less ETC complexes may exist per mutant mitochondrion, also point to the direction that indeed elimination of these mitochondria is a very likely hypothesis, since these mitochondria would not be able to keep up with the energy demands of the cell. Mitochondrial elimination in skeletal muscle would lead to compromised oxidative capacity and tissue dysfunction. On the other hand, one can argue that accumulation of dysfunctional mitochondria and inhibition of mitochondrial autophagy may be the cause for tissue dysfunction. However, based on the fact that mitochondrial protein yield is profoundly decreased in the D257A mice we don not believe this is the case. Nevertheless, our hypothesis remains to be further explored and confirmed.

If indeed mitochondria from D257A muscle are eliminated this creates an important question as to the mechanism responsible for their elimination (Fig 5-1). Would dysfunctional mitochondria in D257A muscle trigger an autophagic response? How is mitochondrial biogenesis impacted by the accumulation of dysfunctional mitochondria? Very recently Cortopassi's group showed that specific cell types with pathogenic mtDNA deletions derived from KSS and CPEO patients had a significant induction of the ATG12 transcript (156). The ATG12 transcript encodes the first and most important product in the mammalian autophagy cascade (201, 202) and was induced in the microarray data from fibroblasts, lymphoblasts, and myoblasts from KSS patients, and in NT2 neural cells bearing deletions. To determine whether the induction of ATG12 was a specific consequence of mtDNA deletions, they quantified ATG12 transcript levels in 143B osteosarcoma cybrid fusion controls (i.e., cell lines that had gone through the process of cybridization but with normal mtDNA), in osteosarcoma cybrids harboring deletions, and in osteosarcoma cell lines lacking the mitochondrial genome. The

ATG12 transcript levels were highly correlated with the presence of deletions, were significantly higher in cells bearing deletions, and highest in cells lacking mtDNA (156). Consistent with the hypothesis of an induction of autophagy in mutant cells, they also observed the induction of several SNARE/vesicular transcripts, proteins that are also essential for the process of autophagy (203, 204). The authors concluded that the induction of autophagic transcripts is a specific consequence of mtDNA deletions (156). Based on the above findings, activation of autophagy could also be a plausible mechanism mediating mitochondrial removal in D257A mice.

Regarding mitochondrial biogenesis, it has been shown that the expression of nuclear genes encoding the transcription factors TFAM, TFB1, TFB2 and DmTTF, which are essential for the maintenance and expression of mtDNA, are decreased in old and dysfunctional mitochondria (162). It is possible that attenuation in mitochondrial biogenesis in conjunction with an up-regulation of autophagy may be occurring in skeletal muscle of mutant mice, and are responsible for the robust declines in mitochondrial yield. Although the mitochondrial protein yield responses in normal aging and accelerated aging in D257A mice appear to be similar, the respective mechanisms responsible for the decreases in mitochondrial protein yields remain to be determined.

Hypothesis Two: the Effect of mtDNA Mutations on Skeletal Muscle Apoptosis

The goal of this aim was to demonstrate that mitochondrial dysfunction - observed in aim # 1 – ultimately culminates in apoptosis, and to prove that the sarcopenia observed in D257A mice was due to apoptosis. In this way we could show a direct causal relationship between the accumulation of mtDNA mutations and skeletal muscle loss through apoptosis and since the D257A model is an aging model we could extrapolate our results to normal aging and deduce that: a) Accumulation of mtDNA mutations with age is an important culprit for tissue

dysfunction, in this case, skeletal muscle loss and b) Apoptosis is a central mechanism responsible for the age-induced sarcopenia.

Apoptosis is a programmed process of cell death that has a tightly regulated initiation and execution. In Greek, apoptosis means "dropping off" of petals or leaves from plants or trees. The phrase had a medical meaning to the Greeks over two thousand years ago. Hippocrates (460-370 BC) used the term to describe "the falling off of the bones" and Galen extended its meaning to "the dropping of the scabs". A re-introduction of the term for medical use occurred in 1972 when Kerr, Wyllie, and Currie deduced that there was a specific controlled mechanism of cell death distinct from uncontrolled necrotic death (205). They noticed a characteristic, identical sequence of events in many different types of cells and published their observations in a seminal 1972 paper that coined the phrase "apoptosis" and was largely ignored for fifteen years (205)! The concept that death is essential for life according to Wyllie went "against twentieth century philosophy".

Apoptosis with Aging

To date, evidence has been accumulating to suggest that de-regulation of apoptosis may contribute to age-associated changes such as progressive decline of physiologic function and significant increases in the incidence of cancer and degenerative diseases (206). Progressive cell loss mediated by apoptosis is linked to many age-related disorders. Moreover, many studies have demonstrated that apoptosis is up-regulated during aging in various post-mitotic cells such as those of the central nervous system, cardiomyocytes, and skeletal muscle fibers (206-210). For example, the loss of neurons through apoptosis is closely associated with functional impairments such as dementia and motor neuron disability in neurodegenerative diseases such as Alzheimer disease, amyotrophic lateral sclerosis, and Parkinson disease (211). The aging process that occurs in the heart is characterized in animals and humans by a loss of cardiomyocytes and

reactive hypertrophy of the remaining cells, which ultimately results in impairment of cardiac function in advanced age (206). In skeletal muscle, there is increasing evidence indicating that deregulation of apoptosis plays a key role in the pathophysiology of skeletal muscle cell loss. Indeed, accelerated skeletal muscle apoptosis has been well documented to occur with aging (105, 207).

In accordance with the above published reports we found a significant skeletal muscle loss in WT aging mice compared to young WT counterparts (Fig 4-15). Sarcopenia in normally aged mice was also associated with up-regulation in cleaved caspase-3 content (Fig 4-18), suggesting that the apoptotic program is activated in skeletal muscle of old animals. Cell loss in these tissues can cause functional deterioration, thereby leading to aging. These observations suggest that aging enhances apoptosis under physiologic conditions and increases the susceptibility to apoptosis triggered by challenges.

Mitochondrial DNA Mutations and Apoptosis

Aging-associated accumulation of oxidative damage to macromolecules in mitochondria results in mitochondrial dysfunction. Oxidative damage to mtDNA induced by ROS is probably a major source of mitochondrial genomic instability since much of this damage can be mutagenic (212). Indeed, MtDNA mutations are gradually accumulated and the activity/efficiency of energy metabolism declines in aging tissue cells that often exhibit a higher susceptibility to apoptosis (213, 214). This instability of mtDNA, leading to respiratory dysfunction and apoptosis, is thought to be one of the most important factors in aging (212). Pathogenic A3243G and A8344G mutations as well as the 4977-bp deletion in mtDNA render human cells more susceptible to apoptosis stimuli such as UV irradiation (215, 216). In addition, studies on mice with a knockout of the mitochondrial transcription factor showed that defects in the respiratory chain are associated with massive apoptosis of affected cells (217). It is conceivable that impairment of

mitochondrial ATP production and the resulting energy depletion can lead to apoptosis (212). Therefore, aging-induced inadequate supply of energy from mitochondria may contribute to an increased susceptibility of aging human and animal cells to apoptosis.

Several laboratories have addressed the question of whether apoptosis is a part of the pathogenic mechanisms associated with mtDNA deletions and point mutations. In support of this hypothesis, human cells bearing mutations causing Leber's hereditary optic neuropathy, an inherited mtDNA disease, are sensitized to Fas-induced apoptosis (218). Furthermore, TUNEL positive staining was observed in up to 75% or more of the muscle fibers in patients with mitochondrial encephalomyopathy, carrying a high percentage (>40%) of a mtDNA deletion (219). In patients carrying high proportions (>70%) of the A32443G MELAS mutation in the mitochondrial tRNALeu (UUR) gene, or the A8344G MERRF mutation in the mitochondrial tRNALys gene, 25–75% of the muscle fibers exhibited TUNEL-positive nuclei. It appears that the apoptotic program is initiated in muscle fibers of patients carrying high proportions of mutations affecting mitochondrial tRNAs. Recently, Zassenhaus and colleagues proposed an intriguing mechanism whereby mtDNA mutations would generate a pool of misfolded mitochondrial proteins, some small proportion of which might have the conformation necessary to bind to Bax or Bak and thereby activate apoptosis or perhaps bind to cyclophilin D and inhibit its chaperone function (220). This hypothesis could explain how heteroplasmic mtDNA mutations could elicit a cell-death response in the presence of many wild-type copies of mtDNA.

Very recently, Aiken and colleagues demonstrated that aged rat muscle fibers possessed segmental, clonal intracellular expansions of unique somatically derived mtDNA deletion mutations (196). In the areas where less than wild type genomes were detected the fibers displayed ETC abnormalities and abnormal morphology such as fiber splitting, atrophy, and

breakage (196). Deletion mutation accumulation was linked to these aberrant morphologies with more severe cellular pathologies resulting from higher deletion mutation abundance. In addition, in fiber regions distant from the ETC abnormalities with normal morphology, only wild type genomes were detected, and mtDNA deletion mutations were undetectable (196).

In summary, these measurements corroborate previous studies of the same group (7, 43, 87), and indicate that age-induced mtDNA deletion mutations expand within individual muscle fibers, eliciting fiber dysfunction and atrophy. Our study is in agreement with those findings showing that mtDNA mutations lead to ETC abnormalities and skeletal muscle atrophy, and extends the conclusions by showing that the skeletal muscle atrophy observed in the D257A mice is actually due to apoptosis (Figs 4-16, 4-17, 4-18, 4-20). Therefore, the mitochondrial mutator mice suggest that activation of apoptosis is important for the induction of the aging phenotype in skeletal muscle. While previous studies demonstrated an increased susceptibility of cells with pathogenic mtDNA mutations to apoptotic stimuli, or showed a correlative relationship between mtDNA mutations and apoptosis in mitochondrial diseases, we are showing a direct causal relationship between the accumulation of somatic mtDNA mutations *in vivo* and apoptosis in skeletal muscle. Hence, loss of myonuclear domain through apoptosis, possibly leading to the loss of irreplaceable skeletal muscle fibers, appears to be a central mechanism of sarcopenia associated with the accumulation of mtDNA mutations.

Disruption of Mitochondrial Membrane Potential and Role for Apoptosis

During mitochondrial-mediated apoptosis, the release of cytochrome c from the mitochondrial intermembrane space induces the assembly of the apoptosome that is required for activating downstream caspases. However, the actual mechanism of its release is still debatable. In particular, the relation between mitochondrial physiology and the release of cytochrome c and other apoptogenic factors from mitochondria is not clear (221). It is conceivable that the ETC

abnormalities we have detected in the D257A model, leading to energy depletion is likely the cause for the drop in membrane potential we observed in D257A mice (Fig 4-9). Previous studies have described the relationship between mitochondrial membrane potential and apoptosis showing that a reduction in $\Delta\psi$ leads to matrix condensation and exposure of cytochrome c to the intermembrane space, facilitating cytochrome c release and cell death following an apoptotic insult (221).

Changes in the $\Delta\psi$ have been originally postulated to be early, obligate events in the apoptotic signaling pathway (222, 223). Multiple lines of research demonstrate that the nuclear features of apoptosis are preceded by changes in mitochondrial structure and $\Delta\psi$ in some regimes of induction of apoptosis. Rat embryo cells induced to undergo apoptosis by the SV40 large T antigen, show a lowered $\Delta\psi$ and a decrease in mitochondrial respiration and translation, which is detectable early in the apoptotic process (224). Human peripheral blood mononuclear cells treated with dexamethasone show a reduced uptake of the mitochondrial $\Delta\psi$ determining fluorochrome, 3,3'dihexyloxacarbocyanine iodide before the appearance of any morphological signs of apoptosis (223). The separation of these cells prior to dexamethasone treatment into populations with high $\Delta\psi$ and low $\Delta\psi$ revealed that cells with a lowered $\Delta\psi$ undergo spontaneous apoptosis after a short term in culture at 37◦C (223). Also, dexamethasone induces early mitochondrial effects in thymocytes undergoing apoptosis, which show both an early decrease in $\Delta\psi$ as determined by another $\Delta\psi$ fluorochrome, 5,5,6,6-tetrachloro-1,1',3,3'-tetraethyl benzimidazolylcarbocyanine iodide (JC-1), and altered mitochondrial structure as demonstrated by electron microscopy (225). Furthermore, cell death in the Dictyostelium discoideum, a single-celled slime mold involves early disruption of $\Delta\psi$ that precedes

phosphatidylserine exposure, nuclear shrinkage, DNA fragmentation and the release of AIF (226), suggesting the evolutionary conservation between unicellular and multicellular organisms.

In contrast to the above results, ρ^0 cells, (devoid of mitochondrial DNA) which typically have only 40–60% of the $\Delta\psi$ of their parental cell line, can also undergo apoptosis in response to range of agents with similar kinetics as the parental cells. These include Ca^{2+} and atractyloside (227), staurosporine (228), anti-Fas antibodies (229), TNFα plus cycloheximide (227), or didemnin B (230). As there seems to be no acceleration in the apoptotic process, even though the $\Delta\psi$ in these ρ^0 cells is already significantly decreased compared to their parental cell line(230), the notion that lowering $\Delta\psi$ will predispose cells for apoptosis cannot be generalized (223).

Based on our outcomes, we suggest that it is the drop in $\Delta\psi$ observed in skeletal muscle mitochondria from mutant mice that leads to the leakage of pro-apoptotic proteins into the cytosol and triggers apoptosis, although other mechanisms not investigated in the present project (e.g. Bax-Bak pores in the mitochondrial outer membrane) could also be additionally responsible for this induction, and thus, cannot be excluded.

Apoptosis is Evident in Skeletal Muscle of D257A Mice

Apoptosis in our model was evident by an increased release of mono- and oligo-nuclesomal fragments into the cytosol (Fig 4-16). Cells undergoing apoptosis can release mono- or oligo-nucleosomes comprising DNA fragments and histones from their nuclei into the cytoplasm or even into the extracellular compartment and this process is very characteristic to apoptosis (231, 232).

Moreover, degradation of chromosomal DNA is one of the biochemical hallmarks of apoptosis: Late in the apoptotic process, caspase-activated endogenous endonucleases cleave chromosomal DNA between the nucleosomes, generating a series of DNA fragments with

multiples of 180 to 220 bases (233-235) that form a ladder when the extracted DNA is separated by gel electrophoresis and stained by ethidium bromide. We have detected prominent DNA ladders in D257A mice while DNA ladders were almost not detectable in WT mice (Fig 4-17), which further confirms that apoptosis is the mechanism responsible for the sarcopenia observed in D257A mice.

In addition, protein cleavage by caspases, the central executioners of the apoptotic pathway, accounts for the distinctive cytoplasmic and structural changes seen in apoptotic cells. Cleavage and activation of the effector caspase-3 during apoptosis has been very well documented in the scientific literature (119, 236-239). Here, we also show that the DNA fragmentation we detected in D257A muscle is caspase-3-mediated since we demonstrated up-regulation in both the content and the activity of caspase-3 (Figs 4-18, 4-20). As mentioned previously, caspase-3 is activated by proteolytic cleavage at the C-terminal side of a specific aspartate residue. In figure 4-18 we show the content of the large (17/19 kDa) activated fragment of caspase-3 resulting from cleavage adjacent to Asp175. Furthermore, disruption of mitochondrial membrane potential leading to activation of caspase-3 and subsequent apoptosis, has been well documented (240-242), and this is also in agreement with our findings showing a drop in $\Delta\psi$, caspase-3 activation and subsequent apoptotic DNA fragmentation. More importantly, we showed that apoptosis through caspase-3 activation is also an important mechanism for skeletal muscle loss during normal aging (Fig 4-18), providing further support to the usefulness of our model to study mechanisms of sarcopenia in aging skeletal muscle.

Hypothesis Three: Identify the Specific Apoptotic Signaling Pathway Responsible for Sarcopenia in D257A Mice

The goal of this aim was to demonstrate that the apoptosis observed in mutator mice is intrinsic to the mitochondria. In this way, we intended to show that the mitochondrial-mediated

pathway is the pathway responsible for the apoptosis induced by increased mtDNA mutational load, and make the inference that mitochondrial-mediated apoptosis is an important mechanism for the age-associated skeletal muscle loss.

Studies have suggested that age-related apoptosis and/or necrosis in response to energy depletion may occur through activation of the mitochondria-mediated signaling pathway (41, 212, 213, 221). Izyumov et al. has shown that in HeLa cells, complete inhibition of oxidative phosphorylation by oligomycin, myxothiazol or FCCP (trifluoromethoxycarbonylcyanide Phenylhydrazone) combined with partial inhibition of glycolysis by 2-deoxyglucose resulted in a steady threefold decrease in the intracellular ATP level (41). In 48 h after a transient (3 h) [ATP] lowering followed by recovery of the ATP level, the majority of the cells had committed suicide by means of mitochondrial-mediated apoptosis. Apoptosis was accompanied by Bax translocation to mitochondria, cytochrome c release into cytosol, caspase activation, and reorganization and decomposition of chromatin (41). Similarly, it has been shown that, in mitochondria isolated from healthy cells, matrix condensation can be induced by either depletion of oxidizable substrates or by protonophores that dissipate the membrane potential (221). Matrix remodeling to the condensed state results in cristae unfolding and exposes cytochrome c to the intermembrane space facilitating its release from the mitochondria and the induction of apoptosis (221).

In accordance with the above studies, we showed that disruption of oxidative phosphorylation and a drop in the ATP content in the D257A skeletal muscle (Figs 4-2, 4-8) indeed leads to mitochondrial-mediated apoptosis evident by up-regulation in the activity of the initiator caspase-9 which mediated the downstream cleavage and activation of caspase-3 (Figs 4-18, 4-20, 4-21). The significant positive correlation between caspase-3 and caspase-9 (Fig 4-21) adds

further support to the notion that the up-regulation of caspase-9, and thus the activation of the caspase-dependent mitochondrial pathway, is indeed responsible for the activation of caspase-3. In addition, disruption of mitochondrial membrane potential followed by caspase-9 activation and downstream caspase-3 activation has also been previously demonstrated (240). Although we were unable to show differences in cytochrome c release into the cytosol - most probably due to contamination of our cytosolic fraction with ruptured mitochondria which can occur during the mitochondrial isolation procedure - we would expect that cytochrome c release is indeed the case in D257A animals, since activation of caspase-9 can only occur after formation of the apoptosome, which requires cytochrome c release in the cytosol.

Furthermore, studies exist to support a critical role of mtDNA mutations in apoptosis intrinsic to the mitochondria (82, 243). Zassenhaus's group studied mice that express a proofreading-deficient POLγ specifically in the heart, and develop cardiac mtDNA mutations, in order to determine whether low frequency mitochondrial mtDNA mutations are pathogenic. They found that sporadic myocytic death occurred in all regions of the heart, due to apoptosis as assessed by histological analysis and TUNEL staining (82). While in their model they showed that mitochondrial respiratory function, ultrastructure, and number remained normal, they also pointed out that cytochrome c was released from mitochondria and concluded that mtDNA mutations are pathogenic, and seem to trigger apoptosis through the mitochondrial pathway (82).

In another study and in order to confirm whether apoptotic processes are truly related to muscle fiber degeneration in mitochondrial encephalomyopathies, Ikezoe et al. evaluated apoptosis in muscle fibers from patients with chronic progressive external ophthalmoplegia (CPEO; associated with a mtDNA deletion), MELAS, or MERRF (243). The criterion for selecting the patients for this study was that ≥5% of the muscle fibers were ‘‘ragged red fibers,’’

(RRFs) i.e., fibers with the characteristic subsarcolemmal accumulation of mitochondria found in mitochondrial diseases with deficient mitochondrial protein synthesis (usually RRFs show loss of COX activity with concomitant hyperactivation of SDH activity). The proportion of mtDNA carrying the relevant mutation was unknown. However, markers of mitochondrial-mediated apoptosis appeared to be upregulated in RRFs: Bax and Apaf-1 expression and cytochrome c release from mitochondria were seen in RRFs (243). Caspase-3 activation was also confirmed in RRFs of MELAS, CPEO and MERRF, but not in control muscles (243).

It is therefore evident from the current literature that a rise in mtDNA mutations can lead to apoptosis mediated by the mitochondria. The present dissertation study confirms results from previous studies and ties these studies together showing that an induced *in vivo* rise in somatic mtDNA mutations results in ETC abnormalities, such as profound decreases in complex I and COX content, and compromised oxidative phosphorylation, which in turn lead to energy depletion, loss of mitochondrial membrane potential and induction of apoptosis mediated by the mitochondria.

Proposed Mechanism for the Skeletal Muscle Loss Induced by High Load of Somatic mtDNA Mutations

Based on our outcomes, we describe below a hypothetical mechanism of how somatic mtDNA mutations can lead to apoptosis, responsible for the sarcopenia observed in D257A skeletal muscle (Figure 5-1).

From the blue native page results we observed that the content of mitochondrial ETC complexes I, III and IV is significantly lower in D257A mice (Figs 4-3, 4-4) while their activities remain unaffected (Figs 4-5, 4-6). We have also determined that total mitochondrial content per gram of skeletal muscle tissue in D257A mice is ~35% lower by 11 months, and almost half (~46% lower) compared to that of WT by 13-mo of age (Fig 4-13), which suggests that

mitochondria in D257A mice are getting continuously eliminated. The decreased ETC complex content per total protein loaded may suggests that assembly of ETC complexes, specifically those containing mtDNA-encoded subunits, is abolished. We can still detect normal levels of all-nuclear-encoded complexes, such as, complex II. However, if formation of partly mitochondrial-encoded complexes is abrogated that means that possibly fewer fully functional electron transport chains exist per skeletal muscle mitochondrion in D257A mice. Thus, even if levels of all-nuclear encoded complexes are not different compared to WT it is most possible that they may just accumulate in mitochondria without being inserted in the mitochondrial inner membrane to form fully functional ETCs. If fewer ETCs exists per mitochondrion this would still leave the mitochondrion at energy deficit even though the activity of the remaining ETCs is normal. Our results fit very well this hypothesis since we indeed show impairment of mitochondrial oxygen consumption at state 3 (Fig 4-2), as well as, decreased ATP content (Fig 4-8) in mitochondria isolated from D257A mice. We believe that these energy deficits due to the assembly of fewer ETCs in mutant mitochondria lead to the disturbance in the mitochondrial membrane potential we have observed (Fig 4-9). A decrease in membrane potential in turn, may be directly responsible for the rupture of the mitochondrial outer membrane and the release of cytochrome *c* and other pro-apoptotic proteins from the inter-membrane space into the cytosol, which triggers apoptosis. Release of cytochrome c will lead to the formation of the apoptosome causing activation of caspase-9 and downstream activation of the final effector caspase, caspase-3, which will be responsible for carrying out the proteolytic events that lead to DNA fragmentation. In accordance with the above we demonstrated increased skeletal muscle apoptosis in D257A mice (Figs 4-16, 4-17, 4-18, 4-20) which was indeed intrinsic to the mitochondria, since activation of caspase-9 and caspase-3 was observed (Figs 4-18, 4-20). We

believe that the main, mitochondrial caspase-dependent pathway is a central pathway responsible for sarcopenia associated with the accumulation of somatic mtDNA mutations and, it may be also as critical for the skeletal muscle loss associated with normal aging. A mechanistic series of events is depicted in Figure 5-1. Last, and as previously mentioned, based on our total mitochondrial protein yield findings, it appears that mitochondria in skeletal muscle fibers are getting eliminated. Although this provides support to our hypotheses, since we would expect that mutant mitochondria with energy deficits and disrupted membrane potentials would eventually get destroyed, it also poses the important question as to how their distraction is mediated. What is the mechanism of their elimination? These are important questions that await answers.

Synopsis

This project utilized the D257A knock in mouse, as an "*in vivo*" model of increased spontaneous mutation rates in mtDNA in order to elucidate the role of mtDNA mutations in sarcopenia. This mouse contained a mutation that resulted in the functional disruption of the exonuclease domain of mouse mitochondrial DNA polymerase γ, leading to the abolishment of its proofreading function without significantly affecting the polymerase activity (13, 14, 148).

Three separate but interrelated hypotheses were tested. Major findings include the following: (a) mtDNA mutations in skeletal muscle lead to compromised mitochondrial bioenergetics, evident by profound decreases in mitochondrial O_2 consumption, ATP content, and a significant drop in $\Delta\psi$. (b) The accumulation of mtDNA mutations in skeletal muscle of D257A mice leads to a significant decrease in the content of ETC complexes I, III, and IV, all of which contain mtDNA-encoded subunits. This finding represents the primary mechanism responsible for the impaired mitochondrial bioenergetics observed and the disturbance in the $\Delta\psi$, since elimination of ETC complexes from the inner mitochondrial membrane are likely to leave

mitochondria and cells in energy deficits. (c) Importantly, our observations, thus far, do not support the idea that mtDNA mutations contribute to increased mitochondrial ROS production and further oxidative damage to mtDNA, in contrast to the main tenet of the free radical theory of aging (4-6, 19, 71). Instead, it is evident that mtDNA mutations can induce mitochondrial dysfunction in the absence of increased ROS production, and this finding has been also demonstrated by other groups (79). (d) Up-regulation of apoptosis in D257A mice is evident by DNA laddering, increased release of mono- and oligo-nucleosomes in the cytosol, and increases in cleaved cas-3 content and activity. The apoptosis data when combined with the significant loss of muscle mass in 11-mo-old D257A mice suggest that loss of irreplaceable, post-mitotic cells through apoptosis may be a central mechanism of sarcopenia induced by the accumulation of mtDNA mutations. (e) Involvement of the main mitochondrial caspase-dependent pathway is apparent by the up-regulation of caspase-9 activity resulting in downstream activation of the final effector caspase-3 in D257A mice. The drop in mitochondrial membrane potential is likely the trigger for mitochondrial-mediated apoptosis in the D257A mice. A mechanistic series of events is depicted in Figure 5-1.

The results of these experiments provide a unique contribution to the existing research, utilizing the first *"in vivo"* mammalian system to examine the role of mtDNA mutations in skeletal muscle aging. In contrast to previous correlative studies, these new outcomes establish a direct link between the accumulation of mtDNA mutations and sarcopenia. Importantly, this work is also the first to demonstrate that, specifically in skeletal muscle, mtDNA mutations do not lead to increases in mitochondrial ROS production, introducing a break in the mitochondrial "Vicious Cycle" theory.

Conclusions

Concurrent with the age-dependent loss of muscle fibers, multiple mtDNA mutations accumulate over time in many tissues and species (11, 73, 200, 244, 245). MtDNA mutations and deletions were initially considered to be at low abundance (<0.1%) when calculated against the total mitochondria pool in tissue homogenates (246, 247). When, however, discrete numbers of muscle fibers were analyzed, the abundance of mtDNA mutations was found to be inversely proportional to the number of cells analyzed (248). In situ hybridization studies demonstrated that mtDNA deletion mutations were not distributed homogeneously throughout a tissue, but amplified focally within a subset of individual cells, appearing as a segmental pattern along the length of muscle fibers and as a mosaic distribution between cells (75, 158, 249-253). This provides a mechanism for significant tissue dysfunction induced by mtDNA mutations, the focal accumulation of which may cause significant impairment of mitochondrial function in individual cells in spite of low overall levels of mitochondrial DNA mutations in muscle (49).

The hypothesis that aging is due in part to mtDNA damage and associated mutations (5, 6) was based on the observations that mtDNA is located in the organelle that generates most cellular ROS, that mtDNA is relatively unprotected from ROS damage due to a lack of histones, and also that mtDNA repair may be limited. It is important to note that aging and aging – associated phenotypes, such as sarcopenia, are complex processes that are likely to have multifactorial causes. Mitochondrial DNA mutations can arise directly from errors during DNA replication (193). Oxidative stress may also generate mtDNA mutations as well as damaged proteins that might be able to directly signal apoptosis through a misfolded protein response (193, 220). Respiratory deficiency could contribute to apoptotic signaling or be directly responsible for some aspects of tissue dysfunction (193) . The limited and sometimes contradictory evidence available concerning the capacity of pathogenic mtDNA mutations to

start and support the development of the apoptotic process and the role of the production of ROS in this phenomenon makes it difficult to reach general conclusions.

The still limited understanding of the pathogenic mechanisms of many of the disease-causing mutations and of all the factors capable of promoting and controlling the various apoptotic pathways adds greatly to the complexity of the problem. Last, because cells may have hundreds of mitochondria, and each carries multiple copies of mtDNA, the contribution of mtDNA mutations and deletions to normal aging and aging phenotypes, remains a controversial issue. It is clear, however, that progress in these areas will lead to a better understanding of the resources available to the cell for compensating and possibly reversing the process leading to cell death, with potential implications for the therapy of sarcopenia, as well as degenerative diseases associated with mtDNA mutations.

Future Directions

Since the D257A mouse model represents a relatively new model to study aging, there is a lot of work left to be done.

A significant finding of this study was that the total mitochondrial protein content per gram of skeletal muscle tissue is getting continually decreased in D257A mice, being half that in WT by 13-mo of age. This, points out to the fact that mitochondria are probably getting continuously eliminated in these mice which very nicely agrees with the fact that current examined mitochondria exhibit loss of ETC complexes and disruptions in membrane potential. However, it also poses a question as to the mechanism responsible for the elimination of mitochondria. Is it autophagy that is responsible for the decrease in mitochondrial content or maybe a decrease in mitochondrial biogenesis, or maybe a combination of both?

In this project we evaluated what would be directly impacted by the increased mtDNA mutational load, assessing mostly proteins of the ETC, however, future research is needed to

determine the adaptive responses of nuclear genes to the changes in mitochondrial-encoded genes or in other words, how mtDNA mutations affect nuclear-encoded genes in the mitochondria, especially the ones involved in the Krebs cycle, ATP production, as well as, genes involved in the regulation of the permeability transition pore opening.

Moreover, more work is required to clarify the role of Bcl-2 family proteins such as Bax, Bad, Bak, and Bcl-2 in apoptosis induced in the D257A model and the formation of pores in the outer membrane that also lead to mitochondrial-mediated apoptosis.

Importantly, future work should also focus on answering the very interesting question of why skeletal muscle mitochondria with accumulated mtDNA mutations produce significantly less ROS, which is in contrast to the mitochondrial "Vicious Cycle" theory. We provided the first indications /observations to that, suggesting that, it is the abrogation of ETC complexes I and III, the main generators of ROS within the ETC, that lead to a decrease in ROS production in the mutant mice. The drop in mitochondrial $\Delta\psi$ can also be a potential mechanism explaining the decrease in ROS production but this may also be linked back to the energy deficits due to the decrease in the content of ETC complexes, specifically those containing mtDNA-encoded subunits. The exact mechanism for this significant decline in ROS generation is far from being completely understood and warrants additional research.

Ultimately, testing the effect of reduced mtDNA mutation accumulation on lifespan and aging phenotypes, including sarcopenia, will provide the strongest support of a causal relationship between mtDNA mutations and aging.

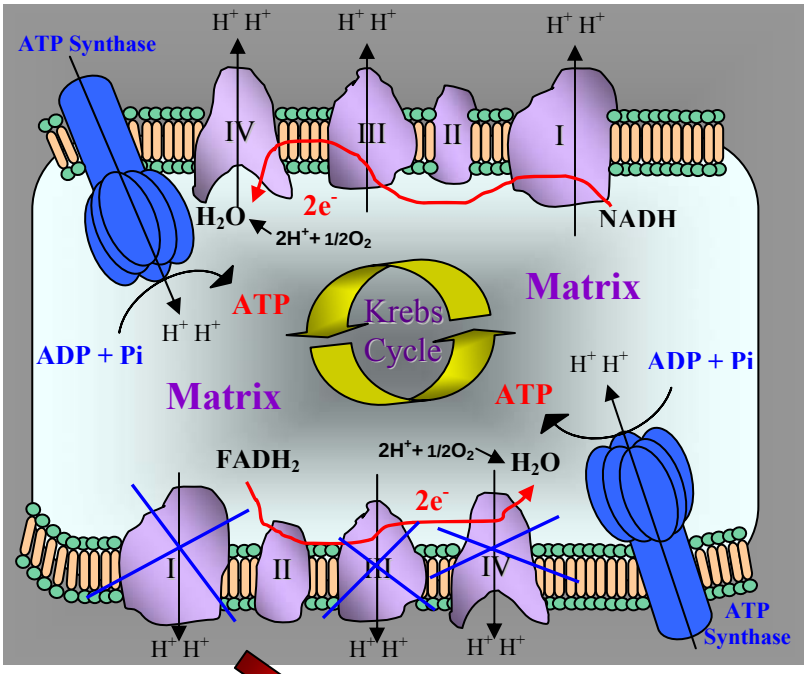

D257A Mitochondrion

Energy deficits in mitochondria → **↓ O2 Consumption**
↓ ATP Content

Muscle Fiber

↓Δψ

Cyt c

ATP **Apaf-1** **Cas-9**

Cas-3

Apoptosis

??? Mechanism

↑ Mitochondrial Autophagy?? **(+)** **↓ Mitochondrial Biogenesis??**

Fig 5-1. Proposed mechanism for the skeletal muscle loss induced by high load of somatic mtDNA mutations. Abolishment of ETC complexes in D257A mice leads to assembly of less functional electron transport chains per mutant mitochondrion. This can create energy deficits leading to mitochondrial dysfunction, evident by severely compromised mitochondrial respiration and reduced ATP content in D257A muscle. Ultimately, this dysfunction results in significant drop in mitochondrial membrane potential and release of cytochrome c from the intermembrane space into the cytosol. Cytochrome c in the cytosol results in apoptosome formation, activation of caspase-9 and downstream activation of caspase-3 which ultimately results in apoptotic DNA fragmentation. Apoptosis appears to be a central mechanism of skeletal muscle loss in D257A mice. Moreover, the observation of reduced mitochondrial yield in D257A skeletal muscle suggests that mitochondria are eliminated. The mechanism for their elimination still remains to be determined although up-regulation of autophagy, down-regulation of mitochondrial biogenesis or both are likely mechanisms.

APPENDIX: ADDITIONAL FIGURES

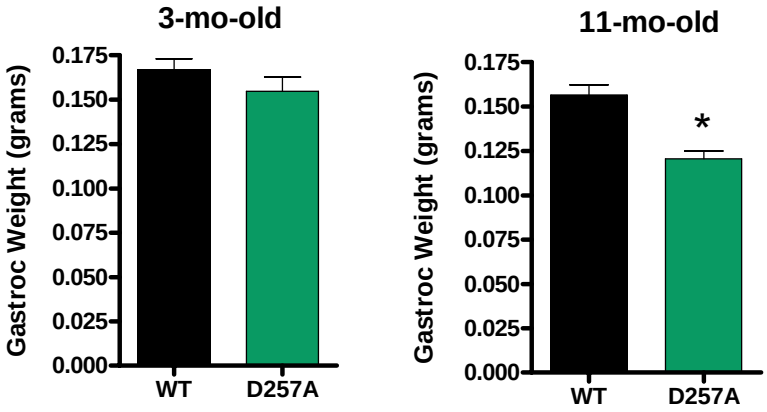

Fig A-1. Skeletal muscle mass (gastrocnemius) in 3-mo old (N=8 per group), and 11-mo old (N=11 per group), WT and D257A mice. Error bars represent SEM. *P < 0.05.

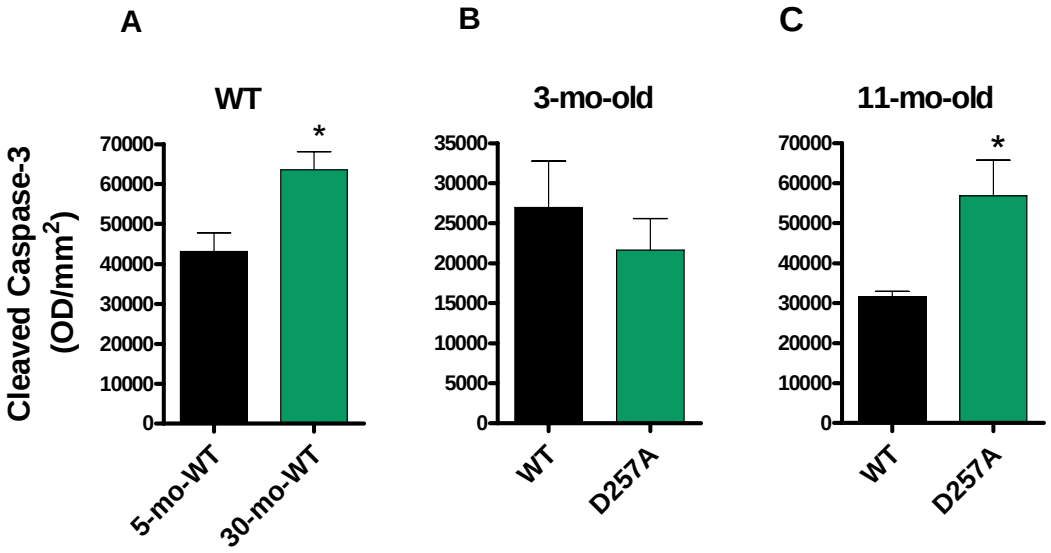

Fig A-2. Caspase-3 activation in gastrocnemius muscle. (A): Caspase-3 content with normal aging: Comparison of young (5-mo) versus old (30-mo) WT mice. (B): Comparison of WT versus D257A caspase-3 levels at 3 months of age. (C): Comparison of WT versus D257A caspase-3 levels at 11 months of age. Cytosolic extracts from WT and D257A mice of the indicated ages were subjected to SDS-polyacrylamide gel electrophoresis and probed with a rabbit monoclonal antibody against cleaved caspase-3. Error bars represent SEM. N=7 per group. *P < 0.05.

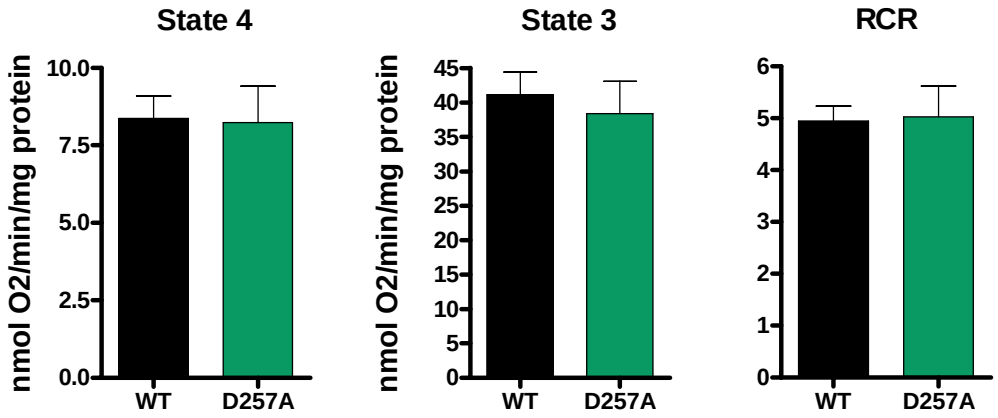

Fig A-3. Mitochondrial respiration in skeletal muscle of 3-mo old mice. We determined the effects of mtDNA mutations on O_2 consumption of skeletal muscle mitochondria obtained from 3-mo old (N=8 per group) WT and D257A mice. The respiratory control ratio (RCR), an index of mitochondrial coupling, was calculated by dividing state 3 to state 4 respiration values. Error bars represent SEM.

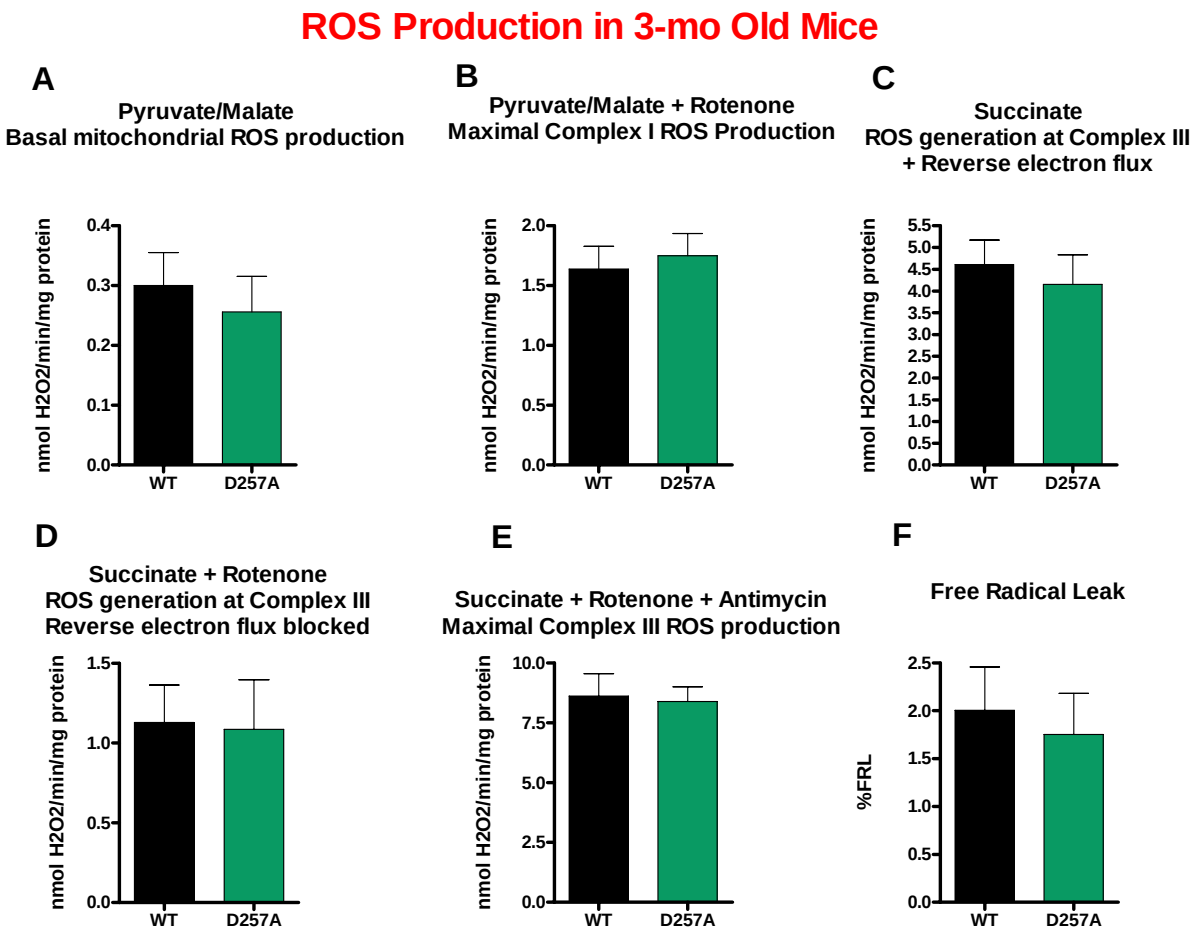

Fig A-4. Reactive oxygen species production during state 4 in isolated mitochondria from 3-mo old mice. Skeletal muscle mitochondria were obtained from 3-mo old (N=8 per group) WT and D257A mice. We measured H_2O_2 production in mitochondria supplemented with pyruvate/malate (panel A) since it represents total basal mitochondrial ROS generation. We also used inhibitors of the ETC in order to study maximum rates of H_2O_2 production from complexes I and III, since they represent the main sites of ROS generation within the mitochondria. For complex I maximum rate (panel B) we used rotenone added to pyruvate/malate supplemented mitochondria. For complex III maximum rate (panel E) we used antimycin A plus rotenone, added to succinate supplemented mitochondria. We also used mitochondria supplemented with succinate alone in order to study complex III ROS production under near physiological conditions (panel C). In addition, some of the assays with succinate as substrate were performed in the presence of rotenone (panel D), in order to avoid the backwards flow of electrons to Complex I. Free radical leak percent (FRL%), an index of mitochondrial efficiency (panel F), was calculated by dividing the H_2O_2 value by twice the state 4 respiration value and the result was multiplied by 100 to give a % final value. Error bars represent SEM.

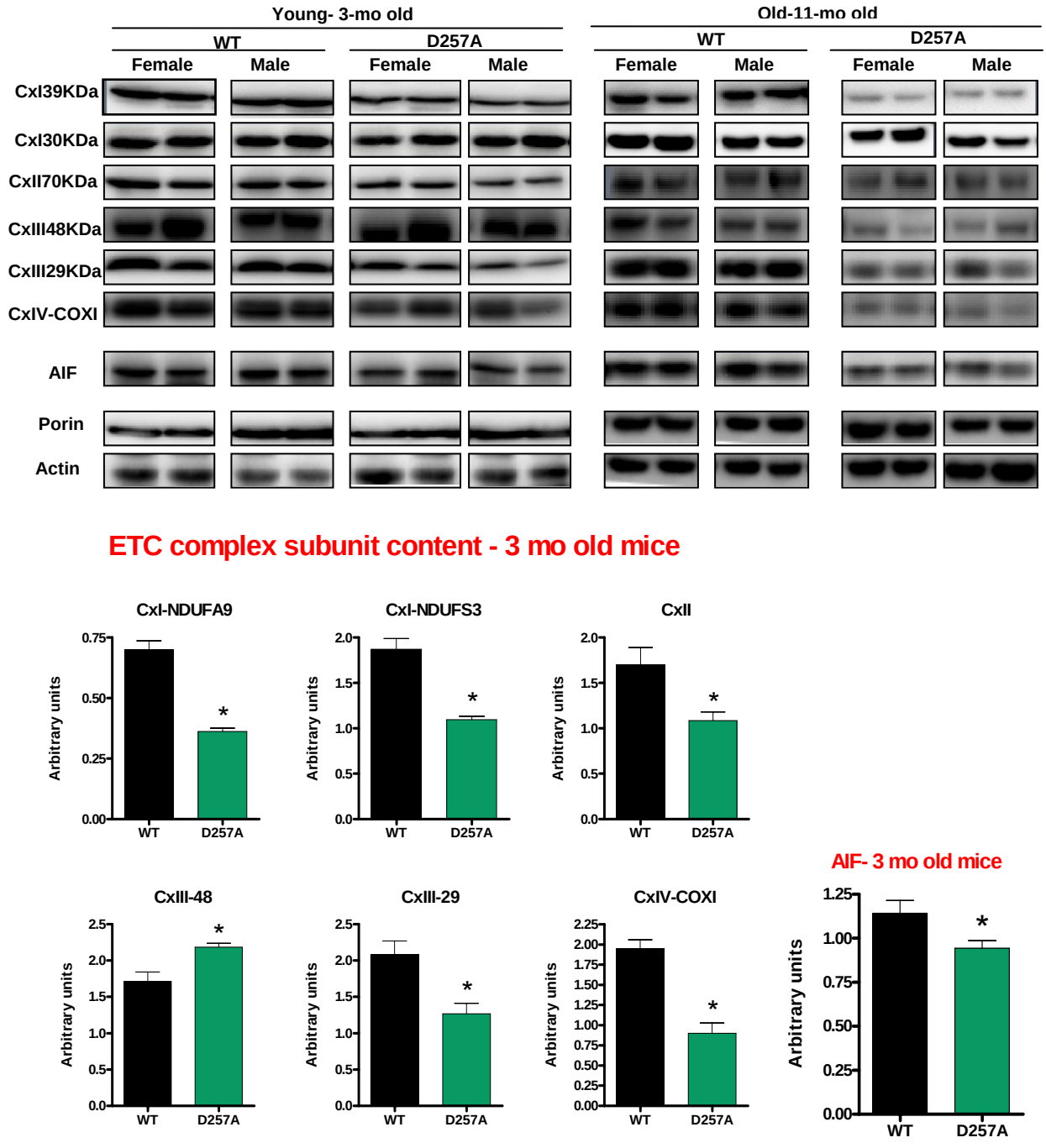

Fig. A-5. Protein expression of nuclear-encoded and mitochondrial-encoded ETC subunits in skeletal muscle of 3-mo old and 11-mo old WT and D257A mice. The content of selected nuclear- and mitochondrial-encoded subunits from complexes I, II, III and IV, as well as, AIF were evaluated by Western Blotting. Representative blots are depicted above. Results shown above were normalized to porin. Error bars represent SEM. *P < 0.5.

LIST OF REFERENCES

1. Marcell, T. J. (2003) Sarcopenia: causes, consequences, and preventions. *J Gerontol A Biol Sci Med Sci* **58**, M911-916

2. Roubenoff, R. (2000) Sarcopenia and its implications for the elderly. *Eur J Clin Nutr* **54 Suppl 3**, S40-47

3. Janssen, I., Baumgartner, R. N., Ross, R., Rosenberg, I. H., and Roubenoff, R. (2004) Skeletal muscle cutpoints associated with elevated physical disability risk in older men and women. *Am J Epidemiol* **159**, 413-421

4. Harman, D. (1972) Free radical theory of aging: dietary implications. *Am J Clin Nutr* **25**, 839-843

5. Harman, D. (1972) The biologic clock: the mitochondria? *J Am Geriatr Soc* **20**, 145-147

6. Fleming, J. E., Miquel, J., Cottrell, S. F., Yengoyan, L. S., and Economos, A. C. (1982) Is cell aging caused by respiration-dependent injury to the mitochondrial genome? *Gerontology* **28**, 44-53

7. Wanagat, J., Cao, Z., Pathare, P., and Aiken, J. M. (2001) Mitochondrial DNA deletion mutations colocalize with segmental electron transport system abnormalities, muscle fiber atrophy, fiber splitting, and oxidative damage in sarcopenia. *Faseb J* **15**, 322-332

8. Khaidakov, M., Heflich, R. H., Manjanatha, M. G., Myers, M. B., and Aidoo, A. (2003) Accumulation of point mutations in mitochondrial DNA of aging mice. *Mutat Res* **526**, 1-7

9. Corral-Debrinski, M., Shoffner, J. M., Lott, M. T., and Wallace, D. C. (1992) Association of mitochondrial DNA damage with aging and coronary atherosclerotic heart disease. *Mutat Res* **275**, 169-180

10. Corral-Debrinski, M., Horton, T., Lott, M. T., Shoffner, J. M., Beal, M. F., and Wallace, D. C. (1992) Mitochondrial DNA deletions in human brain: regional variability and increase with advanced age. *Nat Genet* **2**, 324-329

11. Lee, C. M., Chung, S. S., Kaczkowski, J. M., Weindruch, R., and Aiken, J. M. (1993) Multiple mitochondrial DNA deletions associated with age in skeletal muscle of rhesus monkeys. *J Gerontol* **48**, B201-205

12. Wang, Y., Michikawa, Y., Mallidis, C., Bai, Y., Woodhouse, L., Yarasheski, K. E., Miller, C. A., Askanas, V., Engel, W. K., Bhasin, S., and Attardi, G. (2001) Muscle-specific mutations accumulate with aging in critical human mtDNA control sites for replication. *Proc Natl Acad Sci U S A* **98**, 4022-4027

13. Kujoth, G. C., Hiona, A., Pugh, T. D., Someya, S., Panzer, K., Wohlgemuth, S. E., Hofer, T., Seo, A. Y., Sullivan, R., Jobling, W. A., Morrow, J. D., Van Remmen, H., Sedivy, J. M., Yamasoba, T., Tanokura, M., Weindruch, R., Leeuwenburgh, C., and Prolla, T. A. (2005) Mitochondrial DNA mutations, oxidative stress, and apoptosis in mammalian aging. *Science* **309**, 481-484

14. Trifunovic, A., Wredenberg, A., Falkenberg, M., Spelbrink, J. N., Rovio, A. T., Bruder, C. E., Bohlooly, Y. M., Gidlof, S., Oldfors, A., Wibom, R., Tornell, J., Jacobs, H. T., and Larsson, N. G. (2004) Premature ageing in mice expressing defective mitochondrial DNA polymerase. *Nature* **429**, 417-423

15. Ojaimi, J., Masters, C. L., Opeskin, K., McKelvie, P., and Byrne, E. (1999) Mitochondrial respiratory chain activity in the human brain as a function of age. *Mech Ageing Dev* **111**, 39-47

16. Trounce, I., Byrne, E., and Marzuki, S. (1989) Decline in skeletal muscle mitochondrial respiratory chain function: possible factor in ageing. *Lancet* **1**, 637-639

17. Cooper, J. M., Mann, V. M., and Schapira, A. H. (1992) Analyses of mitochondrial respiratory chain function and mitochondrial DNA deletion in human skeletal muscle: effect of ageing. *J Neurol Sci* **113**, 91-98

18. Yen, T. C., Chen, Y. S., King, K. L., Yeh, S. H., and Wei, Y. H. (1989) Liver mitochondrial respiratory functions decline with age. *Biochem Biophys Res Commun* **165**, 944-1003

19. Harman, D. (1981) The aging process. *Proc Natl Acad Sci U S A* **78**, 7124-7128

20. Holt, I. J., Harding, A. E., and Morgan-Hughes, J. A. (1988) Deletions of muscle mitochondrial DNA in patients with mitochondrial myopathies. *Nature* **331**, 717-719

21. Wallace, D. C., Singh, G., Lott, M. T., Hodge, J. A., Schurr, T. G., Lezza, A. M., Elsas, L. J., 2nd, and Nikoskelainen, E. K. (1988) Mitochondrial DNA mutation associated with Leber's hereditary optic neuropathy. *Science* **242**, 1427-1430

22. Clayton, D. A. (1982) Replication of animal mitochondrial DNA. *Cell* **28**, 693-705

23. Robin, E. D., and Wong, R. (1988) Mitochondrial DNA molecules and virtual number of mitochondria per cell in mammalian cells. *J Cell Physiol* **136**, 507-513

24. Abu-Erreish, G. M., and Sanadi, D. R. (1978) Age-related changes in cytochrome concentration of myocardial mitochondria. *Mech Ageing Dev* **7**, 425-432

25. Boffoli, D., Scacco, S. C., Vergari, R., Solarino, G., Santacroce, G., and Papa, S. (1994) Decline with age of the respiratory chain activity in human skeletal muscle. *Biochim Biophys Acta* **1226**, 73-82

26. Bowling, A. C., Mutisya, E. M., Walker, L. C., Price, D. L., Cork, L. C., and Beal, M. F. (1993) Age-dependent impairment of mitochondrial function in primate brain. *J Neurochem* **60**, 1964-1967

27. Hansford, R. G., and Castro, F. (1982) Age-linked changes in the activity of enzymes of the tricarboxylate cycle and lipid oxidation, and of carnitine content, in muscles of the rat. *Mech Ageing Dev* **19**, 191-200

28. Desai, V. G., Weindruch, R., Hart, R. W., and Feuers, R. J. (1996) Influences of age and dietary restriction on gastrocnemius electron transport system activities in mice. *Arch Biochem Biophys* **333**, 145-151

29. Hudson, E. K., Tsuchiya, N., and Hansford, R. G. (1998) Age-associated changes in mitochondrial mRNA expression and translation in the Wistar rat heart. *Mech Ageing Dev* **103**, 179-193

30. Sugiyama, S., Takasawa, M., Hayakawa, M., and Ozawa, T. (1993) Changes in skeletal muscle, heart and liver mitochondrial electron transport activities in rats and dogs of various ages. *Biochem Mol Biol Int* **30**, 937-944

31. Takasawa, M., Hayakawa, M., Sugiyama, S., Hattori, K., Ito, T., and Ozawa, T. (1993) Age-associated damage in mitochondrial function in rat hearts. *Exp Gerontol* **28**, 269-280

32. Muller-Hocker, J. (1989) Cytochrome-c-oxidase deficient cardiomyocytes in the human heart--an age-related phenomenon. A histochemical ultracytochemical study. *Am J Pathol* **134**, 1167-1173

33. Muller-Hocker, J., Schafer, S., Link, T. A., Possekel, S., and Hammer, C. (1996) Defects of the respiratory chain in various tissues of old monkeys: a cytochemical-immunocytochemical study. *Mech Ageing Dev* **86**, 197-213

34. Hagen, T. M., Liu, J., Lykkesfeldt, J., Wehr, C. M., Ingersoll, R. T., Vinarsky, V., Bartholomew, J. C., and Ames, B. N. (2002) Feeding acetyl-L-carnitine and lipoic acid to old rats significantly improves metabolic function while decreasing oxidative stress. *Proc Natl Acad Sci U S A* **99**, 1870-1875

35. Hagen, T. M., Ingersoll, R. T., Wehr, C. M., Lykkesfeldt, J., Vinarsky, V., Bartholomew, J. C., Song, M. H., and Ames, B. N. (1998) Acetyl-L-carnitine fed to old rats partially restores mitochondrial function and ambulatory activity. *Proc Natl Acad Sci U S A* **95**, 9562-9566

36. Paradies, G., and Ruggiero, F. M. (1990) Age-related changes in the activity of the pyruvate carrier and in the lipid composition in rat-heart mitochondria. *Biochim Biophys Acta* **1016**, 207-212

37. Paradies, G., Ruggiero, F. M., Gadaleta, M. N., and Quagliariello, E. (1992) The effect of aging and acetyl-L-carnitine on the activity of the phosphate carrier and on the phospholipid composition in rat heart mitochondria. *Biochim Biophys Acta* **1103**, 324-326

38. Liu, J., Killilea, D. W., and Ames, B. N. (2002) Age-associated mitochondrial oxidative decay: improvement of carnitine acetyltransferase substrate-binding affinity and activity in brain by feeding old rats acetyl-L- carnitine and/or R-alpha -lipoic acid. *Proc Natl Acad Sci U S A* **99**, 1876-1881

39. Drew, B., Phaneuf, S., Dirks, A., Selman, C., Gredilla, R., Lezza, A., Barja, G., and Leeuwenburgh, C. (2003) Effects of aging and caloric restriction on mitochondrial energy production in gastrocnemius muscle and heart. *Am J Physiol Regul Integr Comp Physiol* **284**, R474-480

40. Short, K. R., Bigelow, M. L., Kahl, J., Singh, R., Coenen-Schimke, J., Raghavakaimal, S., and Nair, K. S. (2005) Decline in skeletal muscle mitochondrial function with aging in humans. *Proc Natl Acad Sci U S A* **102**, 5618-5623

41. Izyumov, D. S., Avetisyan, A. V., Pletjushkina, O. Y., Sakharov, D. V., Wirtz, K. W., Chernyak, B. V., and Skulachev, V. P. (2004) "Wages of fear": transient threefold decrease in intracellular ATP level imposes apoptosis. *Biochim Biophys Acta* **1658**, 141-147

42. Nagley, P., Zhang, C., Lim, M. L., Merhi, M., Needham, B. E., and Khalil, Z. (2001) Mitochondrial DNA deletions parallel age-linked decline in rat sensory nerve function. *Neurobiol Aging* **22**, 635-643

43. Cao, Z., Wanagat, J., McKiernan, S. H., and Aiken, J. M. (2001) Mitochondrial DNA deletion mutations are concomitant with ragged red regions of individual, aged muscle fibers: analysis by laser-capture microdissection. *Nucleic Acids Res* **29**, 4502-4508

44. Lezza, A. M., Pesce, V., Cormio, A., Fracasso, F., Vecchiet, J., Felzani, G., Cantatore, P., and Gadaleta, M. N. (2001) Increased expression of mitochondrial transcription factor A and nuclear respiratory factor-1 in skeletal muscle from aged human subjects. *FEBS Lett* **501**, 74-78

45. Pesce, V., Cormio, A., Fracasso, F., Vecchiet, J., Felzani, G., Lezza, A. M., Cantatore, P., and Gadaleta, M. N. (2001) Age-related mitochondrial genotypic and phenotypic alterations in human skeletal muscle. *Free Radic Biol Med* **30**, 1223-1233

46. Cormio, A., Milella, F., Vecchiet, J., Felzani, G., Gadaleta, M. N., and Cantatore, P. (2005) Mitochondrial DNA mutations in RRF of healthy subjects of different age. *Neurobiol Aging* **26**, 655-664

47. Michikawa, Y., Mazzucchelli, F., Bresolin, N., Scarlato, G., and Attardi, G. (1999) Aging-dependent large accumulation of point mutations in the human mtDNA control region for replication. *Science* **286**, 774-779

48. Chabi, B., de Camaret, B. M., Chevrollier, A., Boisgard, S., and Stepien, G. (2005) Random mtDNA deletions and functional consequence in aged human skeletal muscle. *Biochem Biophys Res Commun* **332**, 542-549

49. Fayet, G., Jansson, M., Sternberg, D., Moslemi, A. R., Blondy, P., Lombes, A., Fardeau, M., and Oldfors, A. (2002) Ageing muscle: clonal expansions of mitochondrial DNA point mutations and deletions cause focal impairment of mitochondrial function. *Neuromuscul Disord* **12**, 484-493

50. Chinnery, P. F., Samuels, D. C., Elson, J., and Turnbull, D. M. (2002) Accumulation of mitochondrial DNA mutations in ageing, cancer, and mitochondrial disease: is there a common mechanism? *Lancet* **360**, 1323-1325

51. Wang, E., Wong, A., and Cortopassi, G. (1997) The rate of mitochondrial mutagenesis is faster in mice than humans. *Mutat Res* **377**, 157-166

52. Wallace, D. C. (1999) Mitochondrial diseases in man and mouse. *Science* **283**, 1482-1488

53. DiMauro, S., and Moraes, C. T. (1993) Mitochondrial encephalomyopathies. *Arch Neurol* **50**, 1197-1208

54. Kobayashi, Y., Momoi, M. Y., Tominaga, K., Momoi, T., Nihei, K., Yanagisawa, M., Kagawa, Y., and Ohta, S. (1990) A point mutation in the mitochondrial tRNA(Leu)(UUR) gene in MELAS (mitochondrial myopathy, encephalopathy, lactic acidosis and stroke-like episodes). *Biochem Biophys Res Commun* **173**, 816-822

55. Wallace, D. C. (1992) Diseases of the mitochondrial DNA. *Annu Rev Biochem* **61**, 1175-1212

56. de Grey, A. D. (1997) A proposed refinement of the mitochondrial free radical theory of aging. *Bioessays* **19**, 161-166

57. Yoneda, M., Chomyn, A., Martinuzzi, A., Hurko, O., and Attardi, G. (1992) Marked replicative advantage of human mtDNA carrying a point mutation that causes the MELAS encephalomyopathy. *Proc Natl Acad Sci U S A* **89**, 11164-11168

58. Bohr, V. A., and Dianov, G. L. (1999) Oxidative DNA damage processing in nuclear and mitochondrial DNA. *Biochimie* **81**, 155-160

59. Larsen, N. B., Rasmussen, M., and Rasmussen, L. J. (2005) Nuclear and mitochondrial DNA repair: similar pathways? *Mitochondrion* **5**, 89-108

60. Dirks, A. J., Hofer, T., Marzetti, E., Pahor, M., and Leeuwenburgh, C. (2006) Mitochondrial DNA mutations, energy metabolism and apoptosis in aging muscle. *Ageing Res Rev*

61. Lewis, L. K., and Resnick, M. A. (2000) Tying up loose ends: nonhomologous end-joining in Saccharomyces cerevisiae. *Mutat Res* **451**, 71-89

62. Michel, B., Ehrlich, S. D., and Uzest, M. (1997) DNA double-strand breaks caused by replication arrest. *Embo J* **16**, 430-438

63. Alexeyev, M. F., Ledoux, S. P., and Wilson, G. L. (2004) Mitochondrial DNA and aging. *Clin Sci (Lond)* **107**, 355-364

64. Wunderlich, V., Schutt, M., Bottger, M., and Graffi, A. (1970) Preferential alkylation of mitochondrial deoxyribonucleic acid by N-methyl-N-nitrosourea. *Biochem J* **118**, 99-109

65. Allen, J. A., and Coombs, M. M. (1980) Covalent binding of polycyclic aromatic compounds to mitochondrial and nuclear DNA. *Nature* **287**, 244-245

66. Backer, J. M., and Weinstein, I. B. (1980) Mitochondrial DNA is a major cellular target for a dihydrodiol-epoxide derivative of benzo[a]pyrene. *Science* **209**, 297-299

67. Niranjan, B. G., Bhat, N. K., and Avadhani, N. G. (1982) Preferential attack of mitochondrial DNA by aflatoxin B1 during hepatocarcinogenesis. *Science* **215**, 73-75

68. Neubert, D., Hopfenmuller, W., and Fuchs, G. (1981) Manifestation of carcinogenesis as a stochastic process on the basis of an altered mitochondrial genome. *Arch Toxicol* **48**, 89-125

69. Miyaki, M., Yatagai, K., and Ono, T. (1977) Strand breaks of mammalian mitochondrial DNA induced by carcinogens. *Chem Biol Interact* **17**, 321-329

70. Harman, D. (1956) Aging: a theory based on free radical and radiation chemistry. *J Gerontol* **11**, 298-300

71. Harman, D. (1973) Free radical theory of aging. *Triangle* **12**, 153-158

72. Bandy, B., and Davison, A. J. (1990) Mitochondrial mutations may increase oxidative stress: implications for carcinogenesis and aging? *Free Radic Biol Med* **8**, 523-539

73. Cortopassi, G. A., and Arnheim, N. (1990) Detection of a specific mitochondrial DNA deletion in tissues of older humans. *Nucleic Acids Res* **18**, 6927-6933

74. Katayama, M., Tanaka, M., Yamamoto, H., Ohbayashi, T., Nimura, Y., and Ozawa, T. (1991) Deleted mitochondrial DNA in the skeletal muscle of aged individuals. *Biochem Int* **25**, 47-56

75. Muller-Hocker, J., Seibel, P., Schneiderbanger, K., and Kadenbach, B. (1993) Different in situ hybridization patterns of mitochondrial DNA in cytochrome c oxidase-deficient extraocular muscle fibres in the elderly. *Virchows Arch A Pathol Anat Histopathol* **422**, 7-15

76. Brierley, E. J., Johnson, M. A., Lightowlers, R. N., James, O. F., and Turnbull, D. M. (1998) Role of mitochondrial DNA mutations in human aging: implications for the central nervous system and muscle. *Ann Neurol* **43**, 217-223

77. Anderson, S., Bankier, A. T., Barrell, B. G., de Bruijn, M. H., Coulson, A. R., Drouin, J., Eperon, I. C., Nierlich, D. P., Roe, B. A., Sanger, F., Schreier, P. H., Smith, A. J., Staden, R., and Young, I. G. (1981) Sequence and organization of the human mitochondrial genome. *Nature* **290**, 457-465

78. de Grey, A. D. (2005) Reactive oxygen species production in the mitochondrial matrix: implications for the mechanism of mitochondrial mutation accumulation. *Rejuvenation Res* **8**, 13-17

79. Trifunovic, A., Hansson, A., Wredenberg, A., Rovio, A. T., Dufour, E., Khvorostov, I., Spelbrink, J. N., Wibom, R., Jacobs, H. T., and Larsson, N. G. (2005) Somatic mtDNA mutations cause aging phenotypes without affecting reactive oxygen species production. *Proc Natl Acad Sci U S A* **102**, 17993-17998

80. Mott, J. L., Zhang, D., Stevens, M., Chang, S., Denniger, G., and Zassenhaus, H. P. (2001) Oxidative stress is not an obligate mediator of disease provoked by mitochondrial DNA mutations. *Mutat Res* **474**, 35-45

81. Wallace, D. C. (2000) Mitochondrial defects in cardiomyopathy and neuromuscular disease. *Am Heart J* **139**, S70-85

82. Zhang, D., Mott, J. L., Farrar, P., Ryerse, J. S., Chang, S. W., Stevens, M., Denniger, G., and Zassenhaus, H. P. (2003) Mitochondrial DNA mutations activate the mitochondrial apoptotic pathway and cause dilated cardiomyopathy. *Cardiovasc Res* **57**, 147-157

83. Lexell, J. (1995) Human aging, muscle mass, and fiber type composition. *J Gerontol A Biol Sci Med Sci* **50 Spec No**, 11-16

84. Lexell, J., Taylor, C. C., and Sjostrom, M. (1988) What is the cause of the ageing atrophy? Total number, size and proportion of different fiber types studied in whole vastus lateralis muscle from 15- to 83-year-old men. *J Neurol Sci* **84**, 275-294

85. Young, A., Stokes, M., and Crowe, M. (1985) The size and strength of the quadriceps muscles of old and young men. *Clin Physiol* **5**, 145-154

86. Overend, T. J., Cunningham, D. A., Paterson, D. H., and Lefcoe, M. S. (1992) Thigh composition in young and elderly men determined by computed tomography. *Clin Physiol* **12**, 629-640

87. McKenzie, D., Bua, E., McKiernan, S., Cao, Z., and Aiken, J. M. (2002) Mitochondrial DNA deletion mutations: a causal role in sarcopenia. *Eur J Biochem* **269**, 2010-2015

88. Cartee, G. D., Bohn, E. E., Gibson, B. T., and Farrar, R. P. (1996) Growth hormone supplementation increases skeletal muscle mass of old male Fischer 344/brown Norway rats. *J Gerontol A Biol Sci Med Sci* **51**, B214-219

89. Barton-Davis, E. R., Shoturma, D. I., Musaro, A., Rosenthal, N., and Sweeney, H. L. (1998) Viral mediated expression of insulin-like growth factor I blocks the aging-related loss of skeletal muscle function. *Proc Natl Acad Sci U S A* **95**, 15603-15607

90. Cartee, G. D. (1995) What insights into age-related changes in skeletal muscle are provided by animal models? *J Gerontol A Biol Sci Med Sci* **50 Spec No**, 137-141

91. Sato, T., Akatsuka, H., Kito, K., Tokoro, Y., Tauchi, H., and Kato, K. (1984) Age changes in size and number of muscle fibers in human minor pectoral muscle. *Mech Ageing Dev* **28**, 99-109

92. Brown, M., Ross, T. P., and Holloszy, J. O. (1992) Effects of ageing and exercise on soleus and extensor digitorum longus muscles of female rats. *Mech Ageing Dev* **63**, 69-77

93. Larsson, L., and Edstrom, L. (1986) Effects of age on enzyme-histochemical fibre spectra and contractile properties of fast- and slow-twitch skeletal muscles in the rat. *J Neurol Sci* **76**, 69-89

94. Ishihara, A., Naitoh, H., and Katsuta, S. (1987) Effects of ageing on the total number of muscle fibers and motoneurons of the tibialis anterior and soleus muscles in the rat. *Brain Res* **435**, 355-358

95. Carlson, B. M. (1995) Factors influencing the repair and adaptation of muscles in aged individuals: satellite cells and innervation. *J Gerontol A Biol Sci Med Sci* **50 Spec No**, 96-100

96. Wallace, D. C., Shoffner, J. M., Trounce, I., Brown, M. D., Ballinger, S. W., Corral-Debrinski, M., Horton, T., Jun, A. S., and Lott, M. T. (1995) Mitochondrial DNA mutations in human degenerative diseases and aging. *Biochim Biophys Acta* **1271**, 141-151

97. Manfredi, G., Vu, T., Bonilla, E., Schon, E. A., DiMauro, S., Arnaudo, E., Zhang, L., Rowland, L. P., and Hirano, M. (1997) Association of myopathy with large-scale mitochondrial DNA duplications and deletions: which is pathogenic? *Ann Neurol* **42**, 180-188

98. Ferri, K. F., and Kroemer, G. (2001) Organelle-specific initiation of cell death pathways. *Nat Cell Biol* **3**, E255-263

99. Wong, A., Yang, J., Cavadini, P., Gellera, C., Lonnerdal, B., Taroni, F., and Cortopassi, G. (1999) The Friedreich's ataxia mutation confers cellular sensitivity to oxidant stress which is rescued by chelators of iron and calcium and inhibitors of apoptosis. *Hum Mol Genet* **8**, 425-430

100. Cortopassi, G. A., and Wong, A. (1999) Mitochondria in organismal aging and degeneration. *Biochim Biophys Acta* **1410**, 183-193

101. Carrozzo, R., Rizza, T., Stringaro, A., Pierini, R., Mormone, E., Santorelli, F. M., Malorni, W., and Matarrese, P. (2004) Maternally-inherited Leigh syndrome-related mutations bolster mitochondrial-mediated apoptosis. *J Neurochem* **90**, 490-501

102. Bua, E. A., McKiernan, S. H., Wanagat, J., McKenzie, D., and Aiken, J. M. (2002) Mitochondrial abnormalities are more frequent in muscles undergoing sarcopenia. *J Appl Physiol* **92**, 2617-2624

103. Lee, C. K., Klopp, R. G., Weindruch, R., and Prolla, T. A. (1999) Gene expression profile of aging and its retardation by caloric restriction. *Science* **285**, 1390-1393.

104. Dirks, A., and Leeuwenburgh, C. (2002) Apoptosis in skeletal muscle with aging. *Am J Physiol Regul Integr Comp Physiol* **282**, R519-527.

105. Dirks, A. J., and Leeuwenburgh, C. (2004) Aging and lifelong calorie restriction result in adaptations of skeletal muscle apoptosis repressor, apoptosis-inducing factor, X-linked inhibitor of apoptosis, caspase-3, and caspase-12. *Free Radic Biol Med* **36**, 27-39

106. Strasser, H., Tiefenthaler, M., Steinlechner, M., Eder, I., Bartsch, G., and Konwalinka, G. (2000) Age dependent apoptosis and loss of rhabdosphincter cells [In Process Citation]. *J Urol* **164**, 1781-1785

107. Whitman, S. A., Wacker, M. J., Richmond, S. R., and Godard, M. P. (2005) Contributions of the ubiquitin-proteasome pathway and apoptosis to human skeletal muscle wasting with age. *Pflugers Arch* **450**, 437-446

108. Cortopassi, G. A., Shibata, D., Soong, N. W., and Arnheim, N. (1992) A pattern of accumulation of a somatic deletion of mitochondrial DNA in aging human tissues. *Proc Natl Acad Sci U S A* **89**, 7370-7374

109. Pollack, M., and Leeuwenburgh, C. (2001) Apoptosis and aging: role of the mitochondria. *J Gerontol A Biol Sci Med Sci* **56**, B475-482

110. Fitts, R. H., Troup, J. P., Witzmann, F. A., and Holloszy, J. O. (1984) The effect of ageing and exercise on skeletal muscle function. *Mech Ageing Dev* **27**, 161-172

111. Song, W., Kwak, H. B., and Lawler, J. M. (2006) Exercise training attenuates age-induced changes in apoptotic signaling in rat skeletal muscle. *Antioxid Redox Signal* **8**, 517-528

112. Leeuwenburgh, C., Gurley, C. M., Strotman, B. A., and Dupont-Versteegden, E. E. (2005) Age-related differences in apoptosis with disuse atrophy in soleus muscle. *Am J Physiol Regul Integr Comp Physiol* **288**, R1288-1296

113. Alison, M. R., and Sarraf, C. E. (1992) Apoptosis: a gene-directed programme of cell death. *J R Coll Physicians Lond* **26**, 25-35

114. Green, D. R., and Reed, J. C. (1998) Mitochondria and apoptosis. *Science* **281**, 1309-1312.

115. Green, D., and Kroemer, G. (1998) The central executioners of apoptosis: caspases or mitochondria? *Trends Cell Biol* **8**, 267-271.

116. Cai, J., Yang, J., and Jones, D. P. (1998) Mitochondrial control of apoptosis: the role of cytochrome c. *Biochim Biophys Acta* **1366**, 139-149.

117. Susin, S. A., Zamzami, N., and Kroemer, G. (1998) Mitochondria as regulators of apoptosis: doubt no more. *Biochim Biophys Acta* **1366**, 151-165

118. Lemasters, J. J., Nieminen, A. L., Qian, T., Trost, L. C., and Herman, B. (1997) The mitochondrial permeability transition in toxic, hypoxic and reperfusion injury. *Mol Cell Biochem* **174**, 159-165

119. van Loo, G., Saelens, X., van Gurp, M., MacFarlane, M., Martin, S. J., and Vandenabeele, P. (2002) The role of mitochondrial factors in apoptosis: a Russian roulette with more than one bullet. *Cell Death Differ* **9**, 1031-1042

120. Li, P., Nijhawan, D., Budihardjo, I., Srinivasula, S. M., Ahmad, M., Alnemri, E. S., and Wang, X. (1997) Cytochrome c and dATP-dependent formation of Apaf-1/caspase-9 complex initiates an apoptotic protease cascade. *Cell* **91**, 479-489

121. Joza, N., Susin, S. A., Daugas, E., Stanford, W. L., Cho, S. K., Li, C. Y., Sasaki, T., Elia, A. J., Cheng, H. Y., Ravagnan, L., Ferri, K. F., Zamzami, N., Wakeham, A., Hakem, R., Yoshida, H., Kong, Y. Y., Mak, T. W., Zuniga-Pflucker, J. C., Kroemer, G., and Penninger, J. M. (2001) Essential role of the mitochondrial apoptosis-inducing factor in programmed cell death. *Nature* **410**, 549-554.

122. Daugas, E., Susin, S. A., Zamzami, N., Ferri, K. F., Irinopoulou, T., Larochette, N., Prevost, M. C., Leber, B., Andrews, D., Penninger, J., and Kroemer, G. (2000) Mitochondrio-nuclear translocation of AIF in apoptosis and necrosis. *Faseb J* **14**, 729-739.

123. Loeffler, M., Daugas, E., Susin, S. A., Zamzami, N., Metivier, D., Nieminen, A. L., Brothers, G., Penninger, J. M., and Kroemer, G. (2001) Dominant cell death induction by extramitochondrially targeted apoptosis-inducing factor. *Faseb J* **15**, 758-767.

124. Mignotte, B., and Vayssiere, J. L. (1998) Mitochondria and apoptosis. *Eur J Biochem* **252**, 1-15.

125. Cande, C., Cecconi, F., Dessen, P., and Kroemer, G. (2002) Apoptosis-inducing factor (AIF): key to the conserved caspase-independent pathways of cell death? *J Cell Sci* **115**, 4727-4734

126. Susin, S. A., Lorenzo, H. K., Zamzami, N., Marzo, I., Snow, B. E., Brothers, G. M., Mangion, J., Jacotot, E., Costantini, P., Loeffler, M., Larochette, N., Goodlett, D. R., Aebersold, R., Siderovski, D. P., Penninger, J. M., and Kroemer, G. (1999) Molecular characterization of mitochondrial apoptosis-inducing factor. *Nature* **397**, 441-446

127. Irvine, R. A., Adachi, N., Shibata, D. K., Cassell, G. D., Yu, K., Karanjawala, Z. E., Hsieh, C. L., and Lieber, M. R. (2005) Generation and characterization of endonuclease G null mice. *Mol Cell Biol* **25**, 294-302

128. Wang, X., Yang, C., Chai, J., Shi, Y., and Xue, D. (2002) Mechanisms of AIF-mediated apoptotic DNA degradation in Caenorhabditis elegans. *Science* **298**, 1587-1592

129. Arnoult, D., Parone, P., Martinou, J. C., Antonsson, B., Estaquier, J., and Ameisen, J. C. (2002) Mitochondrial release of apoptosis-inducing factor occurs downstream of cytochrome c release in response to several proapoptotic stimuli. *J Cell Biol* **159**, 923-929

130. Weil, M., Jacobson, M. D., Coles, H. S., Davies, T. J., Gardner, R. L., Raff, K. D., and Raff, M. C. (1996) Constitutive expression of the machinery for programmed cell death. *J Cell Biol* **133**, 1053-1059

131. Haunstetter, A., and Izumo, S. (1998) Apoptosis: basic mechanisms and implications for cardiovascular disease. *Circ Res* **82**, 1111-1129.

132. Reed, J. C., Jurgensmeier, J. M., and Matsuyama, S. (1998) Bcl-2 family proteins and mitochondria. *Biochim Biophys Acta* **1366**, 127-137. bin/cas/tree/store/bbabio/cas_sub/browse/browse.cgi?year=1998&volume=1136 1996&issue=1991-1992&aid=44652

133. Pollack, M., Phaneuf, S., Dirks, A., and Leeuwenburgh, C. (2002) The role of apoptosis in the normal aging brain, skeletal muscle, and heart. *Ann N Y Acad Sci* **959**, 93-107

134. Deveraux, Q. L., Takahashi, R., Salvesen, G. S., and Reed, J. C. (1997) X-linked IAP is a direct inhibitor of cell-death proteases. *Nature* **388**, 300-304

135. Deveraux, Q. L., Roy, N., Stennicke, H. R., Van Arsdale, T., Zhou, Q., Srinivasula, S. M., Alnemri, E. S., Salvesen, G. S., and Reed, J. C. (1998) IAPs block apoptotic events induced by caspase-8 and cytochrome c by direct inhibition of distinct caspases. *Embo J* **17**, 2215-2223

136. Salvesen, G. S., and Duckett, C. S. (2002) IAP proteins: blocking the road to death's door. *Nat Rev Mol Cell Biol* **3**, 401-410

137. Wu, T. Y., Wagner, K. W., Bursulaya, B., Schultz, P. G., and Deveraux, Q. L. (2003) Development and characterization of nonpeptidic small molecule inhibitors of the XIAP/caspase-3 interaction. *Chem Biol* **10**, 759-767

138. Ludwig, L. M., Tanaka, K., Eells, J. T., Weihrauch, D., Pagel, P. S., Kersten, J. R., and Warltier, D. C. (2004) Preconditioning by isoflurane is mediated by reactive oxygen species generated from mitochondrial electron transport chain complex III. *Anesth Analg* **99**, 1308-1315; table of contents

139. Stowe, D. F., and Kevin, L. G. (2004) Cardiac preconditioning by volatile anesthetic agents: a defining role for altered mitochondrial bioenergetics. *Antioxid Redox Signal* **6**, 439-448

140. Bradford, M. M. (1976) A rapid and sensitive method for the quantitation of microgram quantities of protein utilizing the principle of protein-dye binding. *Anal Biochem* **72**, 248-254

141. Barja, G. (2002) The quantitative measurement of H2O2 generation in isolated mitochondria. *J Bioenerg Biomembr* **34**, 227-233

142. Barja, G. (1999) Mitochondrial oxygen radical generation and leak: sites of production in states 4 and 3, organ specificity, and relation to aging and longevity. *J Bioenerg Biomembr* **31**, 347-366

143. Drew, B., and Leeuwenburgh, C. (2003) Method for measuring ATP production in isolated mitochondria: ATP production in brain and liver mitochondria of Fischer-344 rats with age and caloric restriction. *Am J Physiol Regul Integr Comp Physiol* **285**, R1259-1267

144. Scaduto, R. C., Jr., and Grotyohann, L. W. (1999) Measurement of mitochondrial membrane potential using fluorescent rhodamine derivatives. *Biophys J* **76**, 469-477

145. Schagger, H., and von Jagow, G. (1991) Blue native electrophoresis for isolation of membrane protein complexes in enzymatically active form. *Anal Biochem* **199**, 223-231

146. Sanz, A., Gredilla, R., Pamplona, R., Portero-Otin, M., Vara, E., Tresguerres, J. A., and Barja, G. (2005) Effect of insulin and growth hormone on rat heart and liver oxidative stress in control and caloric restricted animals. *Biogerontology* **6**, 15-26

147. Aure, K., Fayet, G., Leroy, J. P., Lacene, E., Romero, N. B., and Lombes, A. (2006) Apoptosis in mitochondrial myopathies is linked to mitochondrial proliferation. *Brain* **129**, 1249-1259

148. Foury, F., and Vanderstraeten, S. (1992) Yeast mitochondrial DNA mutators with deficient proofreading exonucleolytic activity. *Embo J* **11**, 2717-2726

149. Derbyshire, V., Freemont, P. S., Sanderson, M. R., Beese, L., Friedman, J. M., Joyce, C. M., and Steitz, T. A. (1988) Genetic and crystallographic studies of the 3',5'-exonucleolytic site of DNA polymerase I. *Science* **240**, 199-201

150. Ollis, D. L., Brick, P., Hamlin, R., Xuong, N. G., and Steitz, T. A. (1985) Structure of large fragment of Escherichia coli DNA polymerase I complexed with dTMP. *Nature* **313**, 762-766

151. Rotig, A., Cormier, V., Blanche, S., Bonnefont, J. P., Ledeist, F., Romero, N., Schmitz, J., Rustin, P., Fischer, A., Saudubray, J. M., and et al. (1990) Pearson's marrow-pancreas syndrome. A multisystem mitochondrial disorder in infancy. *J Clin Invest* **86**, 1601-1608

152. Moraes, C. T., DiMauro, S., Zeviani, M., Lombes, A., Shanske, S., Miranda, A. F., Nakase, H., Bonilla, E., Werneck, L. C., Servidei, S., and et al. (1989) Mitochondrial DNA deletions in progressive external ophthalmoplegia and Kearns-Sayre syndrome. *N Engl J Med* **320**, 1293-1299

153. Jacobs, H. T. (2003) Disorders of mitochondrial protein synthesis. *Hum Mol Genet* **12 Spec No 2**, R293-301

154. Gellerich, F. N., Deschauer, M., Chen, Y., Muller, T., Neudecker, S., and Zierz, S. (2002) Mitochondrial respiratory rates and activities of respiratory chain complexes correlate linearly with heteroplasmy of deleted mtDNA without threshold and independently of deletion size. *Biochim Biophys Acta* **1556**, 41-52

155. Porteous, W. K., James, A. M., Sheard, P. W., Porteous, C. M., Packer, M. A., Hyslop, S. J., Melton, J. V., Pang, C. Y., Wei, Y. H., and Murphy, M. P. (1998) Bioenergetic consequences of accumulating the common 4977-bp mitochondrial DNA deletion. *Eur J Biochem* **257**, 192-201

156. Alemi, M., Prigione, A., Wong, A., Schoenfeld, R., DiMauro, S., Hirano, M., Taroni, F., and Cortopassi, G. (2007) Mitochondrial DNA deletions inhibit proteasomal activity and stimulate an autophagic transcript. *Free Radic Biol Med* **42**, 32-43

157. Rollins, S., Prayson, R. A., McMahon, J. T., and Cohen, B. H. (2001) Diagnostic yield muscle biopsy in patients with clinical evidence of mitochondrial cytopathy. *Am J Clin Pathol* **116**, 326-330

158. Mita, S., Schmidt, B., Schon, E. A., DiMauro, S., and Bonilla, E. (1989) Detection of "deleted" mitochondrial genomes in cytochrome-c oxidase-deficient muscle fibers of a patient with Kearns-Sayre syndrome. *Proc Natl Acad Sci U S A* **86**, 9509-9513

159. Wallace, D. C. (2005) A mitochondrial paradigm of metabolic and degenerative diseases, aging, and cancer: a dawn for evolutionary medicine. *Annu Rev Genet* **39**, 359-407

160. Kraytsberg, Y., Kudryavtseva, E., McKee, A. C., Geula, C., Kowall, N. W., and Khrapko, K. (2006) Mitochondrial DNA deletions are abundant and cause functional impairment in aged human substantia nigra neurons. *Nat Genet* **38**, 518-520

161. Cottrell, D. A., Blakely, E. L., Johnson, M. A., Ince, P. G., Borthwick, G. M., and Turnbull, D. M. (2001) Cytochrome c oxidase deficient cells accumulate in the hippocampus and choroid plexus with age. *Neurobiol Aging* **22**, 265-272

162. Dubessay, P., Garreau-Balandier, I., Jarrousse, A. S., Fleuriet, A., Sion, B., Debise, R., and Alziari, S. (2007) Aging impact on biochemical activities and gene expression of Drosophila melanogaster mitochondria. *Biochimie*

163. Ferguson, M., Mockett, R. J., Shen, Y., Orr, W. C., and Sohal, R. S. (2005) Age-associated decline in mitochondrial respiration and electron transport in Drosophila melanogaster. *Biochem J* **390**, 501-511

164. Marcinek, D. J., Schenkman, K. A., Ciesielski, W. A., Lee, D., and Conley, K. E. (2005) Reduced mitochondrial coupling in vivo alters cellular energetics in aged mouse skeletal muscle. *J Physiol* **569**, 467-473

165. Mansouri, A., Muller, F. L., Liu, Y., Ng, R., Faulkner, J., Hamilton, M., Richardson, A., Huang, T. T., Epstein, C. J., and Van Remmen, H. (2006) Alterations in mitochondrial function, hydrogen peroxide release and oxidative damage in mouse hind-limb skeletal muscle during aging. *Mech Ageing Dev* **127**, 298-306

166. Battisti, C., Formichi, P., Cardaioli, E., Bianchi, S., Mangiavacchi, P., Tripodi, S. A., Tosi, P., and Federico, A. (2004) Cell response to oxidative stress induced apoptosis in patients with Leber's hereditary optic neuropathy. *J Neurol Neurosurg Psychiatry* **75**, 1731-1736

167. von Kleist-Retzow, J. C., Hornig-Do, H. T., Schauen, M., Eckertz, S., Dinh, T. A., Stassen, F., Lottmann, N., Bust, M., Galunska, B., Wielckens, K., Hein, W., Beuth, J., Braun, J. M., Fischer, J. H., Ganitkevich, V. Y., Maniura-Weber, K., and Wiesner, R. J. (2007) Impaired mitochondrial Ca(2+) homeostasis in respiratory chain-deficient cells but efficient compensation of energetic disadvantage by enhanced anaerobic glycolysis due to low ATP steady state levels. *Exp Cell Res*

168. Hagen, T. M., Yowe, D. L., Bartholomew, J. C., Wehr, C. M., Do, K. L., Park, J. Y., and Ames, B. N. (1997) Mitochondrial decay in hepatocytes from old rats: membrane potential declines, heterogeneity and oxidants increase. *Proc Natl Acad Sci U S A* **94**, 3064-3069

169. Pieri, C., Recchioni, R., and Moroni, F. (1993) Age-dependent modifications of mitochondrial trans-membrane potential and mass in rat splenic lymphocytes during proliferation. *Mech Ageing Dev* **70**, 201-212

170. Miyoshi, N., Oubrahim, H., Chock, P. B., and Stadtman, E. R. (2006) Age-dependent cell death and the role of ATP in hydrogen peroxide-induced apoptosis and necrosis. *Proc Natl Acad Sci U S A* **103**, 1727-1731

171. Harper, M. E., Monemdjou, S., Ramsey, J. J., and Weindruch, R. (1998) Age-related increase in mitochondrial proton leak and decrease in ATP turnover reactions in mouse hepatocytes. *Am J Physiol* **275**, E197-206

172. Ozawa, T. (1995) Mechanism of somatic mitochondrial DNA mutations associated with age and diseases. *Biochim Biophys Acta* **1271**, 177-189

173. Lee, H. C., and Wei, Y. H. (2007) Oxidative stress, mitochondrial DNA mutation, and apoptosis in aging. *Exp Biol Med (Maywood)* **232**, 592-606

174. Pamplona, R., Portero-Otin, M., Requena, J. R., Thorpe, S. R., Herrero, A., and Barja, G. (1999) A low degree of fatty acid unsaturation leads to lower lipid peroxidation and lipoxidation-derived protein modification in heart mitochondria of the longevous pigeon than in the short-lived rat. *Mech Ageing Dev* **106**, 283-296

175. Pamplona, R., Barja, G., and Portero-Otin, M. (2002) Membrane fatty acid unsaturation, protection against oxidative stress, and maximum life span: a homeoviscous-longevity adaptation? *Ann N Y Acad Sci* **959**, 475-490

176. Barja, G., and Herrero, A. (2000) Oxidative damage to mitochondrial DNA is inversely related to maximum life span in the heart and brain of mammals. *Faseb J* **14**, 312-318

177. Barja, G. (2004) Free radicals and aging. *Trends Neurosci* **27**, 595-600

178. Schriner, S. E., Linford, N. J., Martin, G. M., Treuting, P., Ogburn, C. E., Emond, M., Coskun, P. E., Ladiges, W., Wolf, N., Van Remmen, H., Wallace, D. C., and Rabinovitch, P. S. (2005) Extension of murine life span by overexpression of catalase targeted to mitochondria. *Science* **308**, 1909-1911

179. Geromel, V., Kadhom, N., Cebalos-Picot, I., Ouari, O., Polidori, A., Munnich, A., Rotig, A., and Rustin, P. (2001) Superoxide-induced massive apoptosis in cultured skin fibroblasts harboring the neurogenic ataxia retinitis pigmentosa (NARP) mutation in the ATPase-6 gene of the mitochondrial DNA. *Hum Mol Genet* **10**, 1221-1228

180. Nijtmans, L. G., Henderson, N. S., Attardi, G., and Holt, I. J. (2001) Impaired ATP synthase assembly associated with a mutation in the human ATP synthase subunit 6 gene. *J Biol Chem* **276**, 6755-6762

181. Korshunov, S. S., Skulachev, V. P., and Starkov, A. A. (1997) High protonic potential actuates a mechanism of production of reactive oxygen species in mitochondria. *FEBS Lett* **416**, 15-18

182. Boveris, A. (1977) Mitochondrial production of superoxide radical and hydrogen peroxide. *Adv Exp Med Biol* **78**, 67-82

183. Pitkanen, S., and Robinson, B. H. (1996) Mitochondrial complex I deficiency leads to increased production of superoxide radicals and induction of superoxide dismutase. *J Clin Invest* **98**, 345-351

184. Chance, B., Sies, H., and Boveris, A. (1979) Hydroperoxide metabolism in mammalian organs. *Physiol Rev* **59**, 527-605

185. Boveris, A., and Chance, B. (1973) The mitochondrial generation of hydrogen peroxide. General properties and effect of hyperbaric oxygen. *Biochem J* **134**, 707-716

186. Skulachev, V. P. (1996) Role of uncoupled and non-coupled oxidations in maintenance of safely low levels of oxygen and its one-electron reductants. *Q Rev Biophys* **29**, 169-202

187. Van Remmen, H., Ikeno, Y., Hamilton, M., Pahlavani, M., Wolf, N., Thorpe, S. R., Alderson, N. L., Baynes, J. W., Epstein, C. J., Huang, T. T., Nelson, J., Strong, R., and Richardson, A. (2003) Life-long reduction in MnSOD activity results in increased DNA damage and higher incidence of cancer but does not accelerate aging. *Physiol Genomics* **16**, 29-37

188. Tsuzuki, T., Egashira, A., Igarashi, H., Iwakuma, T., Nakatsuru, Y., Tominaga, Y., Kawate, H., Nakao, K., Nakamura, K., Ide, F., Kura, S., Nakabeppu, Y., Katsuki, M., Ishikawa, T., and Sekiguchi, M. (2001) Spontaneous tumorigenesis in mice defective in the MTH1 gene encoding 8-oxo-dGTPase. *Proc Natl Acad Sci U S A* **98**, 11456-11461

189. Klungland, A., Rosewell, I., Hollenbach, S., Larsen, E., Daly, G., Epe, B., Seeberg, E., Lindahl, T., and Barnes, D. E. (1999) Accumulation of premutagenic DNA lesions in mice defective in removal of oxidative base damage. *Proc Natl Acad Sci U S A* **96**, 13300-13305

190. de Souza-Pinto, N. C., Eide, L., Hogue, B. A., Thybo, T., Stevnsner, T., Seeberg, E., Klungland, A., and Bohr, V. A. (2001) Repair of 8-oxodeoxyguanosine lesions in mitochondrial dna depends on the oxoguanine dna glycosylase (OGG1) gene and 8-oxoguanine accumulates in the mitochondrial dna of OGG1-defective mice. *Cancer Res* **61**, 5378-5381

191. Esposito, L. A., Melov, S., Panov, A., Cottrell, B. A., and Wallace, D. C. (1999) Mitochondrial disease in mouse results in increased oxidative stress. *Proc Natl Acad Sci U S A* **96**, 4820-4825

192. Muller, F. L., Liu, Y., and Van Remmen, H. (2004) Complex III releases superoxide to both sides of the inner mitochondrial membrane. *J Biol Chem* **279**, 49064-49073

193. Kujoth, G. C., Bradshaw, P. C., Haroon, S., and Prolla, T. A. (2007) The role of mitochondrial DNA mutations in mammalian aging. *PLoS Genet* **3**, e24

194. Yarian, C. S., Rebrin, I., and Sohal, R. S. (2005) Aconitase and ATP synthase are targets of malondialdehyde modification and undergo an age-related decrease in activity in mouse heart mitochondria. *Biochem Biophys Res Commun* **330**, 151-156

195. Yan, L. J., and Sohal, R. S. (1998) Mitochondrial adenine nucleotide translocase is modified oxidatively during aging. *Proc Natl Acad Sci U S A* **95**, 12896-12901

196. Herbst, A., Pak, J. W., McKenzie, D., Bua, E., Bassiouni, M., and Aiken, J. M. (2007) Accumulation of mitochondrial DNA deletion mutations in aged muscle fibers: evidence for a causal role in muscle fiber loss. *J Gerontol A Biol Sci Med Sci* **62**, 235-245

197. Beyer, R. E., Starnes, J. W., Edington, D. W., Lipton, R. J., Compton, R. T., 3rd, and Kwasman, M. A. (1984) Exercise-induced reversal of age-related declines of oxidative reactions, mitochondrial yield, and flavins in skeletal muscle of the rat. *Mech Ageing Dev* **24**, 309-323

198. Kerner, J., Turkaly, P. J., Minkler, P. E., and Hoppel, C. L. (2001) Aging skeletal muscle mitochondria in the rat: decreased uncoupling protein-3 content. *Am J Physiol Endocrinol Metab* **281**, E1054-1062

199. Lee, H. C., Pang, C. Y., Hsu, H. S., and Wei, Y. H. (1994) Differential accumulations of 4,977 bp deletion in mitochondrial DNA of various tissues in human ageing. *Biochim Biophys Acta* **1226**, 37-43

200. Linnane, A. W., Baumer, A., Maxwell, R. J., Preston, H., Zhang, C. F., and Marzuki, S. (1990) Mitochondrial gene mutation: the ageing process and degenerative diseases. *Biochem Int* **22**, 1067-1076

201. Mizushima, N., Yoshimori, T., and Ohsumi, Y. (2003) Role of the Apg12 conjugation system in mammalian autophagy. *Int J Biochem Cell Biol* **35**, 553-561

202. Klionsky, D. J., and Emr, S. D. (2000) Autophagy as a regulated pathway of cellular degradation. *Science* **290**, 1717-1721

203. Darsow, T., Rieder, S. E., and Emr, S. D. (1997) A multispecificity syntaxin homologue, Vam3p, essential for autophagic and biosynthetic protein transport to the vacuole. *J Cell Biol* **138**, 517-529

204. Ishihara, N., Hamasaki, M., Yokota, S., Suzuki, K., Kamada, Y., Kihara, A., Yoshimori, T., Noda, T., and Ohsumi, Y. (2001) Autophagosome requires specific early Sec proteins for its formation and NSF/SNARE for vacuolar fusion. *Mol Biol Cell* **12**, 3690-3702

205. Kerr, J. F., Wyllie, A. H., and Currie, A. R. (1972) Apoptosis: a basic biological phenomenon with wide-ranging implications in tissue kinetics. *Br J Cancer* **26**, 239-257

206. Higami, Y., and Shimokawa, I. (2000) Apoptosis in the aging process. *Cell Tissue Res* **301**, 125-132

207. Dirks, A., and Leeuwenburgh, C. (2002) Apoptosis in skeletal muscle with aging. *Am J Physiol Regul Integr Comp Physiol* **282**, R519-527

208. Kwak, H. B., Song, W., and Lawler, J. M. (2006) Exercise training attenuates age-induced elevation in Bax/Bcl-2 ratio, apoptosis, and remodeling in the rat heart. *Faseb J* **20**, 791-793

209. Kajstura, J., Cheng, W., Sarangarajan, R., Li, P., Li, B., Nitahara, J. A., Chapnick, S., Reiss, K., Olivetti, G., and Anversa, P. (1996) Necrotic and apoptotic myocyte cell death in the aging heart of Fischer 344 rats. *Am J Physiol* **271**, H1215-1228

210. Morrison, J. H., and Hof, P. R. (1997) Life and death of neurons in the aging brain. *Science* **278**, 412-419

211. Lin, M. T., and Beal, M. F. (2006) Mitochondrial dysfunction and oxidative stress in neurodegenerative diseases. *Nature* **443**, 787-795

212. Ott, M., Gogvadze, V., Orrenius, S., and Zhivotovsky, B. (2007) Mitochondria, oxidative stress and cell death. *Apoptosis* **12**, 913-922

213. Orrenius, S., Gogvadze, V., and Zhivotovsky, B. (2007) Mitochondrial oxidative stress: implications for cell death. *Annu Rev Pharmacol Toxicol* **47**, 143-183

214. Kokoszka, J. E., Coskun, P., Esposito, L. A., and Wallace, D. C. (2001) Increased mitochondrial oxidative stress in the Sod2 (+/-) mouse results in the age-related decline of mitochondrial function culminating in increased apoptosis. *Proc Natl Acad Sci U S A* **98**, 2278-2283

215. Lee, C. F., Liu, C. Y., Chen, S. M., Sikorska, M., Lin, C. Y., Chen, T. L., and Wei, Y. H. (2005) Attenuation of UV-induced apoptosis by coenzyme Q10 in human cells harboring large-scale deletion of mitochondrial DNA. *Ann N Y Acad Sci* **1042**, 429-438

216. Liu, C. Y., Lee, C. F., and Wei, Y. H. (2007) Quantitative effect of 4977 bp deletion of mitochondrial DNA on the susceptibility of human cells to UV-induced apoptosis. *Mitochondrion* **7**, 89-95

217. Wang, J., Silva, J. P., Gustafsson, C. M., Rustin, P., and Larsson, N. G. (2001) Increased in vivo apoptosis in cells lacking mitochondrial DNA gene expression. *Proc Natl Acad Sci U S A* **98**, 4038-4043

218. Danielson, S. R., Wong, A., Carelli, V., Martinuzzi, A., Schapira, A. H., and Cortopassi, G. A. (2002) Cells bearing mutations causing Leber's hereditary optic neuropathy are sensitized to Fas-Induced apoptosis. *J Biol Chem* **277**, 5810-5815

219. Mirabella, M., Di Giovanni, S., Silvestri, G., Tonali, P., and Servidei, S. (2000) Apoptosis in mitochondrial encephalomyopathies with mitochondrial DNA mutations: a potential pathogenic mechanism. *Brain* **123 (Pt 1)**, 93-104

220. Mott, J. L., Zhang, D., and Zassenhaus, H. P. (2005) Mitochondrial DNA mutations, apoptosis, and the misfolded protein response. *Rejuvenation Res* **8**, 216-226

221. Gottlieb, E., Armour, S. M., Harris, M. H., and Thompson, C. B. (2003) Mitochondrial membrane potential regulates matrix configuration and cytochrome c release during apoptosis. *Cell Death Differ* **10**, 709-717

222. Cohen, G. M. (1997) Caspases: the executioners of apoptosis. *Biochem J* **326 (Pt 1)**, 1-16

223. Zamzami, N., Marchetti, P., Castedo, M., Zanin, C., Vayssiere, J. L., Petit, P. X., and Kroemer, G. (1995) Reduction in mitochondrial potential constitutes an early irreversible step of programmed lymphocyte death in vivo. *J Exp Med* **181**, 1661-1672

224. Vayssiere, J. L., Petit, P. X., Risler, Y., and Mignotte, B. (1994) Commitment to apoptosis is associated with changes in mitochondrial biogenesis and activity in cell lines conditionally immortalized with simian virus 40. *Proc Natl Acad Sci U S A* **91**, 11752-11756

225. Petit, P. X., Lecoeur, H., Zorn, E., Dauguet, C., Mignotte, B., and Gougeon, M. L. (1995) Alterations in mitochondrial structure and function are early events of dexamethasone-induced thymocyte apoptosis. *J Cell Biol* **130**, 157-167

226. Arnoult, D., Tatischeff, I., Estaquier, J., Girard, M., Sureau, F., Tissier, J. P., Grodet, A., Dellinger, M., Traincard, F., Kahn, A., Ameisen, J. C., and Petit, P. X. (2001) On the evolutionary conservation of the cell death pathway: mitochondrial release of an apoptosis-inducing factor during Dictyostelium discoideum cell death. *Mol Biol Cell* **12**, 3016-3030

227. Marchetti, P., Susin, S. A., Decaudin, D., Gamen, S., Castedo, M., Hirsch, T., Zamzami, N., Naval, J., Senik, A., and Kroemer, G. (1996) Apoptosis-associated derangement of mitochondrial function in cells lacking mitochondrial DNA. *Cancer Res* **56**, 2033-2038

228. Jacobson, M. D., Burne, J. F., King, M. P., Miyashita, T., Reed, J. C., and Raff, M. C. (1993) Bcl-2 blocks apoptosis in cells lacking mitochondrial DNA. *Nature* **361**, 365-369

229. Gamen, S., Anel, A., Montoya, J., Marzo, I., Pineiro, A., and Naval, J. (1995) mtDNA-depleted U937 cells are sensitive to TNF and Fas-mediated cytotoxicity. *FEBS Lett* **376**, 15-18

230. Grubb, D. R., Ly, J. D., Vaillant, F., Johnson, K. L., and Lawen, A. (2001) Mitochondrial cytochrome c release is caspase-dependent and does not involve mitochondrial permeability transition in didemnin B-induced apoptosis. *Oncogene* **20**, 4085-4094

231. Wyllie, A. H., Kerr, J. F., and Currie, A. R. (1980) Cell death: the significance of apoptosis. *Int Rev Cytol* **68**, 251-306

232. Wyllie, A. H., Arends, M. J., Morris, R. G., Walker, S. W., and Evan, G. (1992) The apoptosis endonuclease and its regulation. *Semin Immunol* **4**, 389-397

233. Nagata, S. (2000) Apoptotic DNA fragmentation. *Exp Cell Res* **256**, 12-18

234. Rosl, F. (1992) A simple and rapid method for detection of apoptosis in human cells. *Nucleic Acids Res* **20**, 5243

235. Smith, M. L., and Fornace, A. J., Jr. (1996) Mammalian DNA damage-inducible genes associated with growth arrest and apoptosis. *Mutat Res* **340**, 109-124

236. Sabourin, L. A., Tamai, K., Seale, P., Wagner, J., and Rudnicki, M. A. (2000) Caspase 3 cleavage of the Ste20-related kinase SLK releases and activates an apoptosis-inducing kinase domain and an actin-disassembling region. *Mol Cell Biol* **20**, 684-696

237. Kothakota, S., Azuma, T., Reinhard, C., Klippel, A., Tang, J., Chu, K., McGarry, T. J., Kirschner, M. W., Koths, K., Kwiatkowski, D. J., and Williams, L. T. (1997) Caspase-3-generated fragment of gelsolin: effector of morphological change in apoptosis. *Science* **278**, 294-298

238. Datta, R., Kojima, H., Yoshida, K., and Kufe, D. (1997) Caspase-3-mediated cleavage of protein kinase C theta in induction of apoptosis. *J Biol Chem* **272**, 20317-20320

239. Namura, S., Zhu, J., Fink, K., Endres, M., Srinivasan, A., Tomaselli, K. J., Yuan, J., and Moskowitz, M. A. (1998) Activation and cleavage of caspase-3 in apoptosis induced by experimental cerebral ischemia. *J Neurosci* **18**, 3659-3668

240. Ding, H., Han, C., Zhu, J., Chen, C. S., and D'Ambrosio, S. M. (2005) Celecoxib derivatives induce apoptosis via the disruption of mitochondrial membrane potential and activation of caspase 9. *Int J Cancer* **113**, 803-810

241. Orsini, F., Migliaccio, E., Moroni, M., Contursi, C., Raker, V. A., Piccini, D., Martin-Padura, I., Pelliccia, G., Trinei, M., Bono, M., Puri, C., Tacchetti, C., Ferrini, M., Mannucci, R., Nicoletti, I., Lanfrancone, L., Giorgio, M., and Pelicci, P. G. (2004) The life span determinant p66Shc localizes to mitochondria where it associates with mitochondrial heat shock protein 70 and regulates trans-membrane potential. *J Biol Chem* **279**, 25689-25695

242. Dan, Z., Popov, Y., Patsenker, E., Preimel, D., Liu, C., Wang, X. D., Seitz, H. K., Schuppan, D., and Stickel, F. (2005) Hepatotoxicity of alcohol-induced polar retinol metabolites involves apoptosis via loss of mitochondrial membrane potential. *Faseb J* **19**, 845-847

243. Ikezoe, K., Nakagawa, M., Yan, C., Kira, J., Goto, Y., and Nonaka, I. (2002) Apoptosis is suspended in muscle of mitochondrial encephalomyopathies. *Acta Neuropathol (Berl)* **103**, 531-540

244. Melov, S., Hertz, G. Z., Stormo, G. D., and Johnson, T. E. (1994) Detection of deletions in the mitochondrial genome of Caenorhabditis elegans. *Nucleic Acids Res* **22**, 1075-1078

245. Chung, S. S., Weindruch, R., Schwarze, S. R., McKenzie, D. I., and Aiken, J. M. (1994) Multiple age-associated mitochondrial DNA deletions in skeletal muscle of mice. *Aging (Milano)* **6**, 193-200

246. Edris, W., Burgett, B., Stine, O. C., and Filburn, C. R. (1994) Detection and quantitation by competitive PCR of an age-associated increase in a 4.8-kb deletion in rat mitochondrial DNA. *Mutat Res* **316**, 69-78

247. Simonetti, S., Chen, X., DiMauro, S., and Schon, E. A. (1992) Accumulation of deletions in human mitochondrial DNA during normal aging: analysis by quantitative PCR. *Biochim Biophys Acta* **1180**, 113-122

248. Schwarze, S. R., Lee, C. M., Chung, S. S., Roecker, E. B., Weindruch, R., and Aiken, J. M. (1995) High levels of mitochondrial DNA deletions in skeletal muscle of old rhesus monkeys. *Mech Ageing Dev* **83**, 91-101

249. Lee, C. M., Lopez, M. E., Weindruch, R., and Aiken, J. M. (1998) Association of age-related mitochondrial abnormalities with skeletal muscle fiber atrophy. *Free Radic Biol Med* **25**, 964-972

250. Shoubridge, E. A., Karpati, G., and Hastings, K. E. (1990) Deletion mutants are functionally dominant over wild-type mitochondrial genomes in skeletal muscle fiber segments in mitochondrial disease. *Cell* **62**, 43-49

251. Lopez, M. E., Van Zeeland, N. L., Dahl, D. B., Weindruch, R., and Aiken, J. M. (2000) Cellular phenotypes of age-associated skeletal muscle mitochondrial abnormalities in rhesus monkeys. *Mutat Res* **452**, 123-138

252. Oldfors, A., Larsson, N. G., Holme, E., Tulinius, M., Kadenbach, B., and Droste, M. (1992) Mitochondrial DNA deletions and cytochrome c oxidase deficiency in muscle fibres. *J Neurol Sci* **110**, 169-177

253. Moraes, C. T., Ricci, E., Petruzzella, V., Shanske, S., DiMauro, S., Schon, E. A., and Bonilla, E. (1992) Molecular analysis of the muscle pathology associated with mitochondrial DNA deletions. *Nat Genet* **1**, 359-367

BIOGRAPHICAL SKETCH

Asimina Hiona was born in Ioannina, Greece. She attained her bachelor's degree from Aristotelian University of Thessaloniki with major in exercise physiology. Following graduation, she moved to the US where she obtained a master's degree from Queen College, NY in exercise physiology, with main focus in clinical exercise physiology. While in New York she worked for two years as an exercise physiologist in "Plus One Holding Inc." Finally, deciding to focus her career in basic science, Asimina moved to University of Florida in 2001, to pursue a Ph.D degree. The main focus of her doctoral research is the contribution of mtDNA mutations in skeletal muscle aging, specifically in sarcopenia. Asimina has been a co-author in several peer-reviewed publications. In 2004 she was awarded an American Heart Association Fellowship and in 2005 she was awarded the Leighton E. Cluff award in aging research. She was awarded her Ph.D in summer 2007, with major in biochemistry and molecular biology.